SIS-ECM SSCAFFOLD REMODELS INTO A TMJ DISC ANALOGUE

by

Jesse Lowe

BS, Rowan University, 2010

MS, Rowan University, 2012

Submitted to the Graduate Faculty of

Swanson School of Engineering in partial fulfillment

of the requirements for the degree of

Doctor of Philosophy

University of Pittsburgh

2017

UNIVERSITY OF PITTSBURGH

SWANSON SCHOOL OF ENGINEERING

This dissertation was presented

by

Jesse Lowe

It was defended on

April 3, 2017

and approved by

Stephen Badylak, DVM, PhD, MD, Professor

Department of Surgery

Bryan Brown, PhD, Assistant Professor

Department of Bioengineering

Steven Abramowitch, PhD, Assistant Professor

Department of Bioengineering

Dissertation Advisor: Alejandro Almarza, PhD, Associate Professor

Department of Bioengineering

SIS-ECM SCAFFOLD REMODELS INTO A TMJ DISC ANALOGUE

Jesse Lowe, PhD

University of Pittsburgh, 2017

The temporomandibular joint (TMJ) disc is a fibrocartilaginous tissue located between the condyle of the mandible and glenoid fossa and articular eminence of the temporal bone, forming the TMJ. Damage or derangement of the TMJ disc can require surgical removal, but current autograft replacements will generally resorb within a year, highlighting the need for long term solutions. Extracellular matrix (ECM) scaffolds have shown potential as regenerative medicine graft replacements. Toward this end, the work described in this thesis provides a systematic in vivo approach for the use of small intestine submucosa (SIS) ECM in replacing the porcine disc. Initial studies focused on the effect of growth on the biochemical and biomechanical properties of the porcine TMJ disc and condylar cartilage by characterizing these properties in native pigs at 3, 6, and 9 months. It was determined that growth had no significant effect on the properties of the TMJ disc and condyle. Once baseline native properties were determined, SIS-ECM scaffolds were implanted unilaterally in a porcine TMJ following disc removal and allowed to remodel for 1, 3, and 6 months post implantation. The excised remodeled scaffolds and associated condyles were then characterized and compared against age matched control TMJ discs and condyles. It was determined that the remodeled scaffolds were able to recapitulate native biochemical properties and achieve 50% of the native tensile properties within 3 months

post-implantation. The effect of implantation of the ECM scaffolds on the properties of the condylar cartilage seemed to be the same as no implantation, but both healed. Finally, an in vitro investigation into the effect of ECM and mechanical stimulation on macrophage modulation was performed to provide insight on early ECM scaffold remodeling. It was determined that mechanical stimulation (4 hours of 5% strain at 1 Hz) did not have a significant effect on MO macrophage phenotype towards M1 or M2, while the combination of ECM and mechanical stimulation caused macrophages to display a M2 phenotype. The success of these studies suggest the efficacy of the SIS-ECM scaffold as a potential tissue engineered graft replacement for the damaged TMJ disc.

TABLE OF CONTENTS

LIST OF TABLES

LIST OF FIGURES

PREFACE

I gratefully acknowledge support from the National Institute of Health with grants RO1 DE022055 and 1F31 DE025810, and the National Institute of Biomedical Imaging and Bioengineering's Biomechanics in Regenerative Medicine T32 training grant, T32 EB003392. In addition, I also gratefully acknowledge support from the National Institute of Health Ruth L. Kirschstein National Research grant F31 DE025810.

I would like to thank those who have provided assistance towards this thesis project over the years. To Dr. Heather Szabo-Rodgers, Dr. Elia Beniash, Dr. Hongjiao Ouyang, Dr. Konstantinos Verdelis, Dr. Fatima Syed-Picard, and Dr. Dobrawa Napierala for their constant support and assistance within the Center for Craniofacial Regeneration. I'd like to thank Dr. Charles Sfeir for starting the CCR, and bringing this talented group of researchers together. I'd also like to especially thank Dr. Juan Taboas, who has been incredibly selfless with his time and advice over the course of this thesis, even if that advice went over my head time to time. I would like to thank my thesis committee advisors, Drs. Badylak, Brown, and Abramowitch – for their steadfast support and guidance. Dr. Badylak and Brown's dedication and effort with this thesis is very much appreciated, and Dr. Abramowitch's help and time with all things biomechanics were absolutely essential to the completion of this thesis. I would also like to thank Dr. Mary

Staehle, my Master's thesis advisor. My early years studying with her were incredibly formative and I still have her advice in my head when I am doing my work today.

I would like to give a very special thanks to Dr. Alejandro Almarza, my Ph.D. advisor and mentor over the last 5 years. Not only has Dr. Almarza contributed to the work presented in this dissertation, but has allowed me countless opportunities within the laboratory to grow as a student, scientist, and person. Over this time Dr. Almarza has taught me how to think independently and scientifically, and what it takes to be a strong, encouraging, and passionate scientist. His guidance and support, both my personally and professionally, hass been invaluable, and without him, this dissertation could never have existed.

My fellow lab mates within the Center for Craniofacial Regeneration, Jingming Chen, Amy Chaya, Andrew Brown, Dandan Hong, and George Hung have given the utmost encouragement throughout the years, and their comradery made the last 5 years fly by. In the Almarza lab, I couldn't have accomplished this thesis without help of Adam Chin, Catherine Hagandora, Robert Mortimer, Mauro Tudares, Sarah Henderson, Xinyun Liu and John Li. Their comic relief and many lunch excursions made this thesis much more enjoyable.

On a personal note, I'd like to thank my friends for the perpetual love and support they have given over the course of my life. Thank you for all the friendship, Dustin Ward, Michael Schoch, William Dempsey, James Tramontano, Pavlo Kostetsky, Daniel O'Connell, Michael Muldowney, Peter Gigliotti, Veronica Martinez, and all my friends from Rowan University and here at the University of Pittsburgh. Thank you to all my aunts, uncles, and cousins for their constant love and faith. Thank you to Steve and Lina for the encouragement, talks, and the

several vacations out to Seattle. Thank you to Katie Farraro for being there for me throughout this process, and for making every day better. And finally, thank you to my parents, Karen and Edward, for a lifetime of great advice, inspiration, and love.

INTRODUCTION

The objective of this thesis is a) to characterize the effect of age on the biomechanical and biochemical properties of the temporomandibular joint (TMJ) disc and mandibular condylar cartilage, b) determine the efficacy of a small intestine submucosa extracellular matrix (SIS-ECM) scaffold implanted into a porcine model for 1, 3, and 6 months, and c) investigate the role of mechanical stimulation on early-stage remodeling of the ECM scaffold in vivo. The characterization phase of this project determines the biochemical content of ECM constituents and stress relaxation compressive properties in the TMJ disc and mandibular condylar cartilage at various age points, as well as introduces a novel tensile protocol to reduce overall error observed in tensile properties of the TMJ disc. In the second phase, the efficacy of SIS-ECM scaffolds implanted in a porcine model will be assessed through comparison with the age-matched native values obtained in the first phase. Lastly, the in vitro effect of mechanical stimulation on macrophage phenotype when seeded in ECM will be investigated, to provide insight into the theorized early remodeling process for ECM scaffolds in vivo. The central hypothesis of this thesis is that *with the knowledge of the effect of age on native TMJ tissues, and with established protocols and assays, it will be determined that an SIS-ECM scaffold is a viable TMJ disc analogue within 6 months of implantation in vivo due to constructive remodeling of macrophages*. The following specific aims were used to test this hypothesis:

1) To characterize the effect of age on the TMJ disc and mandibular condylar cartilage. This aim is accomplished by performing biochemical tests for ECM in the TMJ disc and condylar cartilage, validating novel biomechanical testing protocols, and using these protocols to determine the compressive and tensile properties of these tissues. The hypothesis is that *the biochemical content and biomechanical properties will increase with age for both the disc and condylar cartilage*. Total biochemical content is determined for DNA, glycosaminoglycans (GAG) and collagen. The mechanical properties determined are compressive stress relaxation peak stress and modulus; and uniaxial ultimate tensile stress, modulus, and ultimate strain.

2) To determine the efficacy of SIS-ECM scaffolds as a TMJ disc analogue at 1, 3, and 6 months post implantation. This aim is accomplished by performing the biochemical assays and biomechanical protocols established in Aim 1 on the remodeled ECM scaffold explants following implantation in a porcine model, and comparing these values to age-matched tissues to control for the effect of growth. The hypothesis is that *the biochemical content of the remodeled scaffold will be in the same range as the native disc, and that mechanical properties of the remodeled scaffolds will increase over time and reach at least 50% of the magnitude of the native TMJ disc by 6 months of remodeling.* SIS-ECM scaffolds would be considered a success by the parameters of this study if these benchmarks were achieved.

3) To investigate the effect of mechanical stimulation on macrophages seeded on ECM. This aim is meant to elucidate the effect of mechanical stimulation and the presence of ECM on early stage remodeling (Aim 2) of the SIS-ECM scaffolds by performing a 2 day study comparing the phenotype of macrophages seeded on ECM and

mechanically loaded against that of statically cultured macrophages without ECM. The hypothesis is that *mechanical stimulation will increase gene expression of M2 phenotypic macrophages seeded in ECM scaffolds, when compared to static culture.* The macrophages are exposed to 5% strain at 1 Hz for 4 hours, and then allowed to rest for 24 hours before proceeding.

The following chapters provide essential TMJ disc and mandibular condylar cartilage background information and comprehensive descriptions of the experiments performed to fulfill the above specific aims. Chapter 1 summarizes the recent advances in tissue engineering for the TMJ disc, with a focus on in vitro testing to the lack of previous in vivo tissue engineered approaches in this field. It also compares and contrasts the regenerative medicine therapies investigated in the TMJ field with those in the knee meniscus and annulus fibrosus fields, both of which are fibrocartilage tissues like the TMJ disc. The significance of this work is to draw a parallel between the more widely studied knee meniscus and annulus fibrosus fields, and the poorly understood TMJ disc.

Chapter 2 represents specific aim 1. This chapter focuses on determining the total DNA, GAG, and collagen content, as well as the compressive and tensile stresses and moduli of the TMJ disc and the condylar cartilage. It frames these properties as a function of growth, to determine if these properties are significantly different as the pig ages, which would introduce a confounding factor in comparing future tissue engineered devices to control groups of a single age. These values are then related to known biomechanical and biochemical properties of the porcine TMJ disc, to determine the validity of novel protocols developed and presented here.

Chapter 3 represents specific aim 2. The major objective of this aim is to characterize the biochemical and biomechanical properties of SIS-ECM scaffolds that have been implanted in a

porcine model at 3 months of age, and then been allowed to remodel for 1, 3, and 6 months before being explanted. Once the tissues have been characterized, they are compared against age-matched native controls to determine the efficacy of the scaffolds to recapitulate native tissue properties. The condyles of the pigs treated with ECM scaffolds are also characterized and compared to native age-matched control condyles to determine the effect of the presence of these scaffolds in the joint over time, and thus assess the whether the scaffolds protect the condyle from damage.

Chapter 4 represents specific aim 3. The major objective of this aim is to determine if mechanical stimulation, experienced as 5% strain at 1 Hz for 4 hours, combined with the presence of ECM will cause M0 macrophages to express genes of an M2 phenotype. These treated macrophages will be compared against M0 macrophages statically seeded with ECM, mechanically loaded without ECM, and statically seeded with no ECM.

1.0 IN VITRO FIBROCARTILAGE TISSUE ENGINEERED THERAPIES

1.1 INTRODUCTION

Fibrocartilage is the type of cartilage found in temporomandibular joint (TMJ) discs, the annulus fibrosus of intervertebral discs (IVD), and the meniscus of the knee. The clinical necessity of investigating fibrocartilage is highlighted by the large numbers of individuals affected by degeneration of these joints. It is estimated that 10 million Americans are affected by temporomandibular joint disorders, as many as 5 million people are affected by lower back pain attributed to IVD degeneration(Sherman et al., 2010), and 600,000 knee surgeries are performed per year in the United States(Sweigart and Athanasiou, 2001).

Fibrocartilage differs from hyaline and articular cartilage in the ratio of type I collagen to type II collagen (Figure 1). While articular cartilage is predominately collagen type II, fibrocartilage tissues as a group have higher collagen type I content, although the exact ratio can vary by tissue. The TMJ disc, for example, is almost 100% collagen type I(Anderson and Athanasiou, 2009), with trace amounts of collagen type II located in the intermediate zone. The knee meniscus has a heterogeneous distribution of collagen type I and type II, with the lateral head containing almost 100% collagen type I, while the medial head has a collagen I/II ratio of 0.6 (Cheung, 1987). The IVD also has heterogeneous distribution of collagen, with the inner and outer annulus fibrosus having collagen I/II ratios of 0.68 and 0.84, respectively (Eyre and Muir,

1976). These phenotypic differences between the TMJ and both the knee menisci and IVD can necessitate separate treatment modalities for the different tissues.

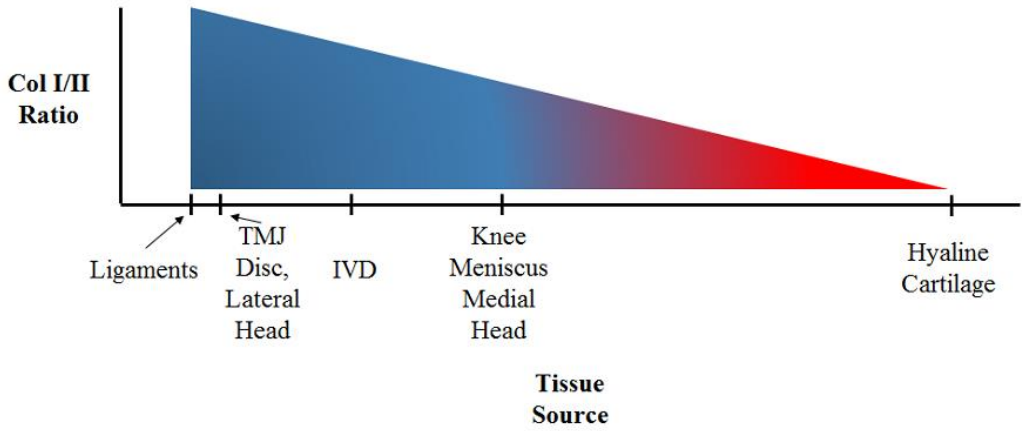

Fig 1

Figure 1. Spectrum of cartilage based on collagen I/II ratio. Fibrocartilage skews towards the higher Col I/II ratio, with the TMJ disc having a Col I/II ratio of almost 1.0. The knee meniscus and IVD have a Col I/II ratio of 0.8. Hyaline and articular cartilage have a Col I/II ratio of near 0.0.

While current treatments exist for these distinct fibrocartilages, they generally rely on surgical methods that do not restore the original tissue. This is because the avascular nature of

these fibrocartilage tissues does not promote healing on its own. As a result, researchers are turning to tissue engineered, cell based therapies as potential grafts for healing and remodeling.

The purpose of this review is to elucidate the progress of in vitro tissue engineering initiatives to treat degenerated fibrocartilage. Only studies that provide biochemical or biomechanical analyses of the tissue engineered therapies will be reviewed, so that the results can be compared appropriately. The first part of this review will focus on tissue engineered strategies for TMJ disc remodeling (Table 1). The second part will focus on advances in knee meniscus (Table 2) and the annulus fibrosus of the IVD tissue engineering (Table 3), and compare them to those of the TMJ disc. The implications of all sets of studies will then be evaluated.

1.2 TEMPOROMANDIBULAR JOINT DISC

The TMJ disc is a fibrocartilage disc (Figure 2) that is positioned between the mandibular condyle and glenoid fossa of the temporal bone. Compared to the knee meniscus and intervertebral disc fields of fibrocartilage research, there are relatively few groups researching the TMJ disc. This has led the field generally behind the other fibrocartilage disciplines with technologies or the study of cell sources, such as stem cells. In the TMJ field, Dr. Athanasiou's group is at the forefront of tissue engineered solutions. The other major players in the field were trained under Dr. Athanasiou, such as Dr. Almarza and Dr. Detamore. To tissue engineer the TMJ disc in vitro, Drs. Athanasiou and Almarza have tested different scaffoldless single cells sources(Almarza and Athanasiou, 2006b), scaffoldless co-cultures(Almarza and Athanasiou, 2006a), and scaffolds (Almarza and Athanasiou, 2005; Bean et al., 2006). The studies below

examine what has transpired in the literature in the last 10 years. For the purposes of this review, we searched in January 2017 the terms ("temporomandibular joint" OR TMJ"), "fibrocartilage", and "in vitro" using the search engine PubMed, and limited the search to the last 10 years. From this, we received 19 results, from which any reviews and papers that didn't report biochemical/biomechanical data were removed, leaving 9 publications (Tables 1 and 2). The studies are presented chronologically, and the values reported are compared against native properties of the human TMJ disc (Kalpakci et al., 2011b).

Figure 2. Rendering of the inferior face of the TMJ. Collagen is aligned anterior-posteriorly in the intermediate zone, and radially around the outer ring of the disc.

Table 1. TMJ in vitro tissue engineered therapy studies, describing cell source, scaffold type, and species. A blank space means no data was available in the study.

Author	Year	Cell Type	Scaffold	Species
Anderson & Athanasiou	2008	TMJ disc cells and costal chondrocytes	None	Goat
Johns & Athanasiou	2008	Costal chondrocytes	None	Goat
Wang et al	2009	Mandibular condylar fibrochondrocytes and articular chondrocytes	PGA	Pig
Anderson & Athanasiou	2009	Articular and costal chondrocytes	None	Goat
Kalpacki et al	2011	Co-cultured articular chondrocytes and meniscus	None	Cow
Hagandora et al	2012	Costal chondrocytes	None	Goat
MacBarb et al	2013	Co-cultured articular chondrocytes and meniscus	None	Cow
MacBarb et al	2013	Co-cultured articular chondrocytes and meniscus	None	Cow
Murphy et al	2015	Costal cartilage	None	Pig
Native Properties (Kalpakci et al., 2011b)	2011			Human

Table 2. TMJ in vitro tissue engineered therapy studies, describing mechanical properties and biochemical properties. A blank space means no data was available in the study.

Author	Year	Compressive Modulus (kPa)	Tensile UTS (MPa)	Tensile Modulus (MPa)	GAG (%/WW)	Collagen (%/WW)	DNA (million cells)
Anderson & Athanasiou	2008	190	1.1	2.3	10	5	
Johns & Athanasiou	2008		0.22	0.54	81	14	2.2
Wang et al	2009				160 ug (total)	2.6 ug (total)	1.75
Anderson & Athanasiou	2009		0.5	0.9	5	0.7	1.5
Kalpacki et al	2011	800		1.9	11	11	
Hagandora et al	2012	450			16 (%/DW)	7 (%/DW)	1
MacBarb et al	2013		2.3	3.4	7	2	
MacBarb et al	2013		2.5		7	4	
Murphy et al	2015	1243	2.3	6.2	7.5	4	
Native Properties(Kalpakci et al., 2011b)	2011	2085	12.8	37.2	0.6	24	.08%/WW

Anderson and Athanasiou in 2008 analyzed the effect of costal chondrocyte passage number on fibrocartilage tissue engineering(Anderson and Athanasiou, 2008). In this study, 2 million goat TMJ disc or costal cartilage cells were allowed to self-assemble in a scaffoldless approach. These constructs were then cultured in Dulbecco's Modified Eagle Medium (DMEM) with 1% Insulin transferring serum (ITS). The cells used in this study were derived from different passage numbers from passage 0 to passage 5. After 6 weeks of culture, it was found that there were no statistical differences in collagen production among costal chondrocyte passages, but passage 5 costal chondrocytes produced significantly more GAG per wet weight than chondrocytes at passages 0, 3, and 5. Mechanically, there were no differences between costal chondrocyte passages in compressive or tensile properties. TMJ disc cell constructs produced 5 times less collagen (5%/WW) than native, which was more than costal chondrocytes at all passages. Also, TMJ disc cell constructs produced 10 times lower compressive (190 kPa compressive modulus) than native, 11 times lower ultimate tensile strength (UTS) (0.5 MPa) than native, and 16 times lower tensile modulus (2.28 MPa) than native (Table 2). All of these values were significantly higher than the other groups. However, these constructs were prohibitively smaller in size than costal chondrocyte constructs. This study is important because it attempted to establish a standard passage number for in vitro experiments, to ensure continuity among experiments and determine effects. This study suggested the efficacy of the costal chondrocytes, while demonstrating that TMJ disc cells would not be an appropriate cell source, even though these constructs produced greater biochemical components and withstood more mechanical forces.

In an effort to determine how growth factors could impact tissue engineered constructs, Johns and Athanasiou in 2008 investigated the effects of growth factors on cells for

fibrocartilage tissue engineering(Johns and Athanasiou, 2008). In this study, 2 million goat costal cartilage cells were allowed to self-assemble in a scaffoldless approach. These constructs were cultured in DMEM with 1% ITS. The effect of transforming growth factor (TGF), insulin growth factor (IGF), fibroblast growth factor (FGF), epidermal growth factor (EGF), and platelet-derived growth factor (PDGF) were investigated individually on the cultured cells, along with a non-growth factor control. After 6 weeks of culture, biochemically, the study found IGF produced the best results, with GAG production being 50 times that of native (81%/WW) and collagen production 2 times less than native (14%/WW). The best mechanical properties are achieved by the non-growth factor control, with tensile strength 20 times less than native (0.22 MPa tensile UTS) and modulus 60 times less than native (0.54 MPa tensile modulus) (Table 2). The paper supports that IGF has the best results based on total amount of biochemical constituents. However, if the percentage of GAGs and collagen per wet weight is used, TGF performs the best of the growth factors. Also, the study uses growth factors at varying concentrations (10 mM to 100 mM) depending on the growth factor, making it difficult to compare the groups.

Wang et al from the Detamore lab in 2009 also investigated cell type for TMJ tissue engineering applications(Wang et al., 2009). In this study, porcine hyaline cartilage and mandibular condylar cartilage cells were seeded at 50 million cells/ml scaffold onto non-woven PGA mesh. The scaffolds were cultured in DMEM with 10% FBS. Each cell type was also exposed to D-glucosamine 6-sulfate and IGF, both individually and in combination. After 6 weeks of culture, the hyaline cartilage cells outperformed the mandibular condylar cartilage cells in total GAG and collagen content. The IGF groups had the highest content of GAG (160 µg) and hydroxyproline (2.6 µg). The authors of this paper did not provide the biochemical values as

percentages of the wet weight though, so a comparison to native properties or other studies is not possible.

Anderson and Athanasiou in 2009 examined the difference between using primary or passaged chondrocytes when compared to costal chondrocytes as a cell source for fibrocartilage tissue engineering(Anderson and Athanasiou, 2009). In this study, 2 million goat primary (P0) and passaged (P3) articular or costal chondrocytes were allowed to self-assemble in agarose wells. Cells were cultured in DMEM with 1% ITS. After culturing for 4 weeks, it was determined that passaged costal chondrocytes performed the best when compared to all the groups in biochemical assessments, producing 40 times the GAG concentration of native (5%/WW) but 35 times less collagen than native (0.7%/WW). Like costal cells, chondrocytes that were passaged also performed better than primary cells in mechanical properties. These constructs, however, had 5 times less ultimate tensile stress (0.5 MPa) and 25 times less tensile modulus (0.9 MPa) than native (Table 2). This is one of the first studies to show that costal cells can produce fibrocartilage constructs more effectively than hyaline articular cartilage cells.

Kalpakci et al from the Athanasiou lab in 2011 studied the effect of TGF β1 and IGF-1 on fibrocartilage tissue engineering constructs(Kalpakci et al., 2011a). In this study, they used scaffoldless co-cultures of bovine femoral chondrocytes and menisci fibrochondrocytes at different ratios (100:0, 75:25, and 50:50 fibrochondrocytes to femoral chondrocytes). To create the constructs, 5.5 million cells were placed into agarose wells. In DMEM, the effect of varying concentrations of TGF- β1 and IGF-1, both individually and in combination, was tested. This study also compared media types, with one set of conditions receiving 10% FBS, and one set receiving no serum treatment. After 4 weeks of culture, the authors performed compressive,

tensile, and biochemical assessments. It was determined that TGF- β1 alone without serum had the largest effect on biochemical production and mechanical properties. These constructs had 20 times the GAG content as the native disc (11%/DW), and two times less collagen content (11%/DW). Also, they were similar to native discs in compressive modulus (0.8 MPa), and were an order of magnitude lower in tensile modulus (1.9 MPa) (Table 2). At the time, this combination produced the highest compressive modulus from in vitro experimentation, as well as the second most collagen from all the studies.

The most recent study to investigate a homogenous cell source in scaffoldless constructs was Hagandora et al from the Almarza lab in 2012, who examined the effect of magnesium ions on potential tissue engineered fibrocartilage constructs(Hagandora et al., 2012). In this study, 2 million goat costal chondrocytes were allowed to self-assemble in agarose wells. Cells were cultured in DMEM/high glucose with 10% FBS. To the media, varying concentrations of $MgCl_2$ and $MgSO_4$ were added and tested. After culturing for 4 weeks, it was determined that low concentrations of magnesium were not different than control in biochemical or biomechanical assays, and higher concentrations of magnesium were significantly lower. The constructs also had a compressive modulus 4 times less than that of native (450 kPa) (Table 2). All groups produced ten times less collagen than native (7%/DW) and 5 times more GAG content than native (16%/DW). A major limitation to this study is the inclusion of media with serum. Since magnesium is a part of signaling pathways, its contributing effect could be masked by the serum. It would be interesting to see what effect magnesium has on cells without serum to determine if magnesium has any effect.

MacBarb et al in 2013 attempted to engineer scaffoldless fibrocartilage constructs resembling the TMJ disc using shape specific negative molds (MacBarb et al., 2013a).

Specifically, they created 50:50 co-cultures of bovine meniscus and hyaline cartilage cells. 12 million cells were placed into agarose wells with a mold that imparted a biconcave shape and were cultured for 5 weeks. During that time, groups were exposed to either biomechanical (passive axial compression) and/or biochemical (Chondroitinase ABC + TGF-β1) stimulation. After culturing, it was found that a combination of biochemical and biomechanical stimulation had the greatest effect on mechanical and biochemical properties. The study was also able to produce construct anisotropy, as there were significant differences between the middle zone and periphery of the construct in mechanical testing. The tensile ultimate stress was 5 times less than native (2.3 MPa), while the tensile modulus was an order of magnitude lower than native (3.4 MPa) and the compressive modulus was half of native (900 kPa). In terms of biochemistry, the constructs contained 12 times less collagen content than native (2%/WW) and 12 times more GAG content than native (7%/WW). The production of a shape-specific construct featuring anisotropy in this study is a significant step forward in in vitro research, since it more closely models what is found in vivo.

Following up on the previous study, MacBarb et al in 2013 studied the effect of Chondroitanase ABC and TGF-β on fibrocartilage tissue engineering constructs(MacBarb et al., 2013b). Specifically, they used co-cultures of bovine articular chondrocytes and meniscus cells at ratios of 50:50 and 75:25 cultured in a scaffoldless technique. In this study 12 million cells were placed into an agarose well and were allowed to self-assemble into a scaffoldless construct. In DMEM with no serum, different combinations of Chondroitanase ABC and TGF-β were tested. After 5 weeks of culture it was found that the combination of Chondroitanase ABC and TGF- β yielded constructs that were 5 times less than native in UTS (2.5 MPa) (Table 2). In

terms of biochemical content, the constructs had five times the GAG content as the native disc (7%/WW), but had 6 times less the collagen content (4%/WW).

Murphy et al. from the Athanasiou lab in 2015 created an ex-vivo defect model that was filled with in vitro neocartilage and determined the effects of biochemical stimulation and enzymatic treatment on neocartilage-TMJ fibrocartilage integration(Murphy et al., 2015). Specifically, they cultured porcine costal cartilage at 750,000 cells/mL in a 48 well plate. After 4 weeks of culture, they implanted the resulting neocartilage into a 5 mm defect in a native TMJ disc, and cultured again for 8 weeks. During this time, the constructs were given either no treatment, biochemical treatment (C-ABC and TGF-β1), or biochemical and enzymatic treatment (media supplemented with lysyl oxidase homologue 2, copper sulfate, and hydroxylysine). After culturing, the authors performed biochemical, compressive, and tensile assessments. It was found that a combination of biochemical stimulation and enzymatic treatment had the greatest effect on mechanical and biochemical properties. The tensile stress (2.3 MPa) was 5 times less than native, and the tensile modulus (6.2 MPa) was 6 times less than native. The compressive modulus (1243 kPa) was half of the native value. For biochemistry, the GAG content (7.5%/WW) was 12 times higher than native, and the collagen content (4%/WW) was 6 times less than native.

Based on the in vitro studies that have been performed, the highest amounts of ECM produced, GAGs and collagen, were obtained when TGF-β1 was used in the culture media. The literature suggests that scaffoldless constructs outperformed seeded-scaffold constructs. However, there has not been a recent direct comparison between the scaffoldless approach and cutting-edge polymer scaffolds. While progress has been shown, current in vitro methods all

produce biomechanical and biochemical properties lower than the native TMJ disc. The largest difference for biomechanical properties comes in the tensile modulus, which is often an order of magnitude lower than native. For biochemical production, studies often do not produce enough collagen and produce too much GAGs content when compared to native TMJ tissues.

Since much of the in vitro literature has tried chemical and mechanical stimulation, as well as scaffolds and scaffoldless constructs, it may be safe to assume that cell sources are the limiting factor. Therefore, moving forward it may be appropriate to investigate the efficacy of stem cells as a cell source for TMJ fibrocartilage tissue engineering. In the other fibrocartilage tissue engineering fields, stem cells have already become the gold standard for achieving closer tissue properties to native.

1.3 OTHER FIBROCARTILAGE: KNEE MENISCUS AND ANNULUS FIBROSUS

1.3.1 Knee Meniscus

The knee meniscus is formed by the medial and lateral fibrocartilage heads in the knee joint (Figure 3). Due to the advanced nature of knee research in comparison to the TMJ field, we decided to highlight stem cell in vitro research, since the field has generally moved beyond native tissue cell sources for tissue engineering purposes. For the purposes of this review, we searched the terms “Knee meniscus”, “fibrocartilage”, “in vitro”, and “stem cells” using the search engine PubMed in January 2017. The search for papers in the knee meniscus area were focused on the 5 most recent in vitro papers that contained biomechanical/biochemical results for comparison (Tables 3 and 4). These papers will be presented chronologically, and compared

against the human native properties of the knee meniscus presented by Sweigart and Athanasiou (Sweigart and Athanasiou, 2001).

Table 3. Knee mensicus in vitro tissue engineered therapy studies, describing cell source, scaffold type and species A blank space means no data was available in the study.

Author	Year	Cell Source	Scaffold	Species
Pabbruwe et al	2010	Bone marrow stem cells	Collagen	Human
Tan et al	2010	Meniscus cells and synovium-derived stem cells	SIS	Porcine
Nerurkar et al	2011	Mesenchymal stem cells	Nanofibrous PCL	Bovine
Cui et al	2012	Mesenchymal stem cells and meniscus cells	None	Human
Mattheis et al	2013	Bone marrow stem cells and meniscus cells	None	Human
Chowdhury et al	2013	Bone marrow stem cells and meniscus cells	None	Human
Croutze et al	2013	Outer and inner meniscus cells	collagen	Human
Fisher et al	2015	Mesenchymcal stem cells	Nanofibrous PCL	Cow
Visser et al	2015	None	Decellularized tissue/hydrogel	Horse
Native Properties(Sweigart and Athanasiou, 2001)	2011			Human

Table 4. Knee mensicus in vitro tissue engineered therapy studies, describing mechanical and biochemical properties. A blank space means no data was available in the study.

Author	Year	Compressive Modulus (kPa)	Tensile UTS (MPa)	Tensile Modulus (MPa)	GAG (ug/DNA)	Collagen (ug/DNA)
Pabbruwe et al	2010		32			
Tan et al	2010	50			75	
Nerurkar et al	2011	22		40	15 (%/DW)	35 (%/DW)
Cui et al	2012				21	180
Mattheis et al	2013				21	
Chowdhury et al	2013				6.3	
Croutze et al	2013				23	
Fisher et al	2015			22		60 µg (total)
Visser et al	2015	66.2				
Native Properties (Sweigart and Athanasiou, 2001)	2011	662	20	24	2 (%/DW)	75 (%/DW)

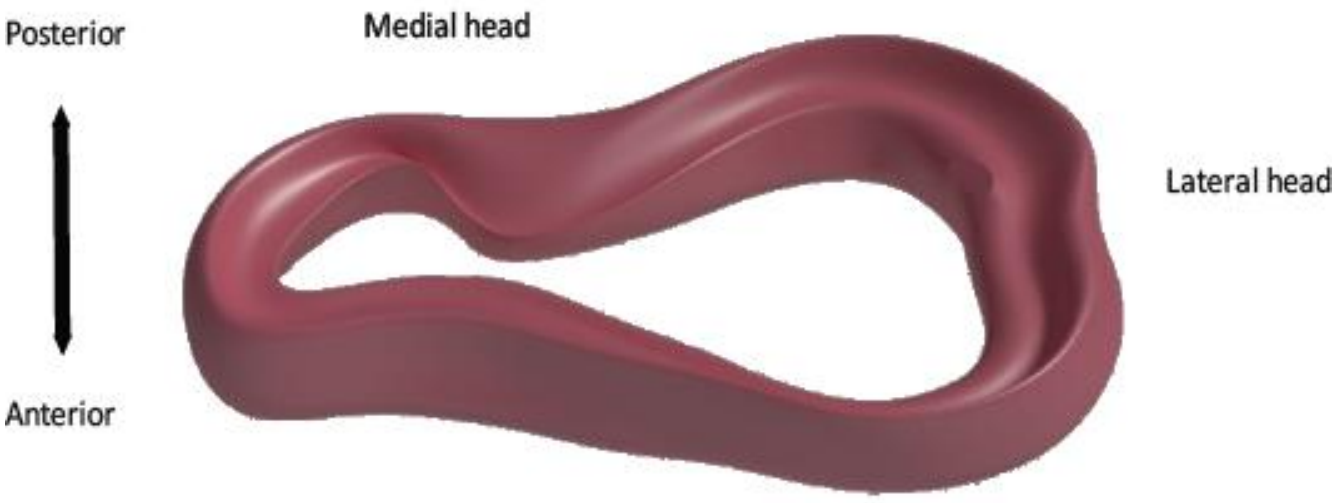

Figure 3. Rendering of the knee meniscus. The meniscus is composed of the medial and lateral heads. The medial head has a collagen I/II ratio of 0.6, while the lateral head has a collagen I/II ratio of almost 1.0.

Matthies et al in 2013 examined the effect of co-culturing stem cells with native cells on matrix formation for fibrocartilage tissue engineering(Matthies et al., 2013). In this study, 250,000 human bone marrow stem cells (BMSCs) and human meniscus cells were allowed to self-assemble in co-cultures of various ratios. Cells were cultured in DMEM with 1% ITS and TGF-β3. The scaffolds were also conditioned with either normal or lowered oxygen tension. After 3 weeks of culture, it was determined that co-cultures of BMSCs and meniscus cells at a ratio of 75:25 performed the best for matrix formation at lowered (3%) oxygen (20 µg GAG/µg DNA) when compared with other co-cultures and pure BMSC and meniscus cultures, but the units prevent comparison to native. While the use of co-cultures proposed in this paper appears

promising, the use of meniscus cells indicate a future requirement of two surgeries to prepare the meniscus, instead of only one.

Chowdhury et al in 2013 investigated the efficacy of chemical treatments on stem cells and meniscus cells(Chowdhury et al., 2013). In this study, 250,000 human meniscus cells and MSCs were allowed to self-assemble, both individually and in co-culture. Cells were cultured in DMEM with 10 ng/mL TGF-β1. The authors also chemically treated some scaffolds from each group with 500 pg/mL interleukin-1β. After 17 days of culture, interleukin-1β had no effect on overall synthesis of GAGs, with no significant differences being seen when comparing similar pellets with or without chemical treatment. Co-culturing BMSCs and meniscus cells produced similar results with BMSCs alone, producing 6.3 µg GAG/µg DNA. Both groups produced GAG significantly more than meniscus cells individually. This paper further advanced the theory that co-cultures of stem cells with meniscus cells provides a potential solution for fibrocartilage tissue engineering.

Croutze et al. in 2013 investigated the effect of oxygen concentration on the biochemistry of inner and outer human meniscus cells on a 3D collagen scaffold(Croutze et al., 2013). In this study, the authors seeded human meniscus cells at 1 million cells/scaffold at passage 3 onto collagen scaffolds. The scaffolds were allowed to culture for 3 weeks in 3% or 21% oxygen. After 3 weeks, it was determined that the 21% oxygen group showed the highest GAG content (23 µg/µg DNA). Also, the authors showed that scaffolds seeded with meniscus cells from the outer meniscus produced higher GAG content (23 µg/µg DNA) than inner meniscus cells (18 µg/µg DNA). The GAG content puts this study on the low end of the studies reviewed here, but also highlights the importance of culture conditions and tissue harvest location on tissue engineering efficacy.

Fisher et al in 2015 investigated the functionality of single and multi-layered MSC-seeded nanofibrous scaffolds(Fisher et al., 2015). Specifically, they engineered PCL nanoscaffolds via electrospinning, and organized the fibers in various angled orientations. Fibers were either arranged in parallel with the direction of the meniscus (0°), perpendicular to the meniscus (90°) or circumferentially. For multilayered scaffolds, combinations of these directions were combined. The scaffolds were then seeded with bovine MSCs at a concentration of 500,000 cells per side of a scaffold and allowed to culture for 6 weeks of culture. In terms of tensile modulus, single layer scaffolds in the 0° direction achieved the highest value (22 MPa), which was roughly the same as native. For collagen content, the multi-layered scaffolds with three sheets in the 0° direction provided the highest collagen content (60 ug). Since the authors only provide total content and no scaffold weights, this cannot be compared to native. This experiment provided an interesting tunable scaffold for tissue engineering, since you can use the directionality and number of nanofibrous layers to achieve higher or lower mechanical and biochemical properties.

Visser et al in 2015, attempted to develop crosslinkable hydrogels for cartilage tissue engineering from cartilage, knee meniscus, and tendon tissue(Visser et al., 2015). Specifically, they harvested femoral condylar cartilage, knee meniscus, and the patellar tendon from horses, and each tissue was decellularized and mixed with gelatin methacryloyl (GelMA) and crosslinked to create hydrogels. It was determined that the cartilage hydrogel achieved the highest compressive modulus (66.2 kPa), which is 10 times less than native. While this scaffold initially displays lower compressive modulus, it would be expected that when seeded with cells, the compressive properties would increase as infiltrating cells began depositing matrix. The

authors seeded equine MSCs and chondrocytes on the scaffolds as well, but only reported normalized biochemical results, making these results incomparable to the other studies presented here.

From the papers reviewed, the lack of mechanical testing performed on the proposed tissue engineered scaffolds makes it difficult to evaluate the efficacy of these therapies. Of the 9 papers, only 1 determined the ultimate compressive strength of the material, and only 3 determined the compressive modulus. A similar problem is observed in the lack of collagen content reported. From the provided GAG data alone, however, it appears that the tissue engineered therapy most suited to producing GAG is the SIS-ECM device seeded with meniscus cells and synovium-derived stem cells, studied by Tan et al. In a broader view of the field, it appears that the trend is moving towards more chemical stimulation of tissue engineered scaffolds in lieu of mechanical stimulation. Moving forward, the opportunity is there to investigate the interaction of chemical and mechanical stimulation on knee meniscus tissue engineered therapies.

In comparison with the TMJ field, the (albeit limited) compressive properties achieved by the knee meniscus field are an order of magnitude lower than those obtained in the TMJ field, despite the fact that the knee meniscus field uses scaffolds for structure at a higher rate. This suggests that the various chondrocytes and fibrochondrocytes used in TMJ tissue engineering are better suited for producing structures with high compressive properties. The opposite is true for the tensile properties reported, although the gap between the TMJ field and the knee meniscus field is much smaller than in compression. For biochemistry, it is harder to compare the fields due to the wide range of units reported, but it appears that in both fields collagen production is substantially lower than native, while GAG production is elevated over native

1.3.2 Annulus Fibrosus of the Intervertebral Disc

The intervertebral disc consists of two separate sections, the annulus fibrosus and the nucleus pulposus (Figure 4). The annulus fibrosus forms an outer ring that surrounds the gel-like nucleus pulposus. The annulus fibrosus is comprised of several laminae of fibrocartilage, and is the focus for this review. Like the knee meniscus field, the research being performed in the knee meniscus field is much more varied than the TMJ. However, similar to knee research, there were limited studies that reported biomechanical or biochemical results. For the purposes of this review, we searched the terms "intervertebral disc", "annulus fibrosus", "fibrocartilage", "in vitro", and "tissue engineering" using the search engine PubMed in January 2017, and limited the results to the last 5 in vitro papers that contained biomechanical/biochemical results for comparison (Tables 5 and 6). These papers will be presented chronologically, and compared against native human annulus fibrosus biochemical properties from Best et al, native compressive properties from Freeman et al, and averaged tensile values from Issac et al and Stemper et al (Best et al., 1994; Freeman et al., 2013; Isaacs et al., 2014; Stemper et al., 2014).

Table 5. Intervertebral disc in vitro tissue engineered therapy studies, describing cell source, scaffold type, and species. A blank space means no data was available in the study.

Author	Year	Cell Source	Scaffold	Species
Park et al	2012	Annulus Fibrosus	Silk scaffolds	Pig
Vadala et al	2012	Annulus Fibrosus	PLLA scaffolds	Cow
Feng et al	2013	Annulus Fibrosus	Nanofibrous PLLA	Human
Cho et al	2013	Annulus Fibrosus		Pig
Turner et al	2013	Annulus Fibrosus	Polycarbonate urethane	Cow
Iu et al	2014	Annulus Fibrosus	Polycarbonate urethane	Cow
Wismer et al	2014	Annulus Fibrosus	Polycaprolactone	Cow
Guillaume et al	2014	Annulus Fibrosus	Porous alginate	Pig
Colombini et al	2015	Annulus Fibrosus	Fibrin gels	Human
Guillaume et al	2015	Annulus Fibrosus	Alginate-collagen	Pig
Native Properties(Colombini et al., 2015; Guillaume et al., 2014; Iu et al., 2014; Wismer et al., 2014)				Human

Table 6. Intervertebral disc in vitro tissue engineered therapy studies, describing mechanical properties and biochemical properties. A blank space means no data was available in the study.

Author	Year	Compressive Modulus (kPa)	Tensile Modulus (MPa)	Ultimate Tensile Stress (MPa)	GAG (%/DW)	Collagen (%/DW)	DNA (ng/scaffold)
Park et al	2012				0.6	0.4	3 (µg/mL scaffold)
Vadala et al	2012				2.5 (µg/µg DNA)	1.4 (µg/µg DNA)	
Feng et al	2013				35 (µg/scaffold)		6 (µg/scaffold)
Cho et al	2013		15		130 (% compared to mature)	90 (% compared to mature)	
Turner et al	2013		8				7.5 (µg)
Iu et al	2014		25	6.5			
Wismer et al	2014		55	7	62 µg	41 (µg/scaffold)	12.5 µg
Guillaume et al	2014	7			60 (µg/µg DNA)	2 (µg/µg DNA)	40 ng/mg
Colombini et al	2015				0.03		
Guillaume et al	2015	6					1900 ng/scaffold
Native Properties (Colombini et al., 2015; Guillaume et al., 2014; Iu et al., 2014; Wismer et al., 2014)		230	35.5	3.2	6	54	

Figure 4. Rendering of the annulus fibrosus. It contains several rings of radially aligned collagen, and has a collagen I/II ratio of 0.8. The center area would contain the nucleus pulposus.

From the same research group as Turner et al, Iu et al in 2014 investigated the use of inner and outer annulus fibrosus cells on a polycarbonate urethane (POU) scaffold(Iu et al., 2014). Specifically, they seeded bovine inner or outer annulus fibrosus at a concentration of 21,000 cells/mm^2 onto PUO scaffolds and allowed for 2 weeks of culture. It was determined that both groups produced tensile moduli of 25 MPa on par with native, and ultimate tensile stresses of 6.5 MPa, which were 2 times native. While ultimately there proved to be no differences in mechanical properties, this was the first study to investigate the idea of comparing annulus fibrosus cell location.

Wismer et al in 2014 explored the use of various scaffold structures and compositions to determine the best option for annulus fibrosus tissue engineered repair(Wismer et al., 2014). Specifically, they seeded cow annulus fibrosus cells at 79,000 cells/cm^2 onto PU or polycaprolactone (PCL) scaffolds. These scaffolds were either processed as oriented or non-oriented electrospun scaffolds. After 3 weeks of culture, it was determined that both unoriented PU and PCL scaffolds produced the same DNA content (12.5 µg) and GAG content (62 µg), higher than the other scaffolds. The oriented PCL scaffolds, however, produced the highest collagen content (41 µg/scaffold), although this was not a significant difference. In biomechanics, the oriented PU scaffold produced the tensile stress (7 MPa) that was 2 times native, while the oriented PCL scaffolds produced the tensile modulus (55 MPa) that was 2 times native. The fact that each scaffold was optimal for different properties allows researchers to tune the scaffold of choice to the design criteria they feel is most important. Orientation of the scaffold fibers appears to be most important for biomechanical properties, while a lack of orientation appears to favor biochemical properties.

Guillaume et al in 2014 investigated the effects of chemical stimulation and oxygen concentration on annulus fibrosus-seeded porous alginate scaffolds(Guillaume et al., 2014). Specifically, they seeded 800,000 porcine annulus fibrosus cells/mL onto a cross-linked porous alginate scaffold and allowed them to culture for 3 weeks. The scaffolds were cultured either with or without TGF-β3 and in either 5% or 20% oxygen. It was determined that scaffolds that were chemically treated with TGF- β3 and 20% oxygen produced the highest DNA (40 ng/mg). The TGF- β3 treated groups in low oxygen conditions produced the highest GAG concentration (60 µg/µg DNA), and collagen content (2 µg/µg DNA). Oxygen had little effect on biomechanical properties, as both low and high oxygen TGF-β3 groups produced a peak

compressive stress of 1 kPa and compressive modulus 7 kPa. These values were compared to native porcine AF tissue at the same testing conditions in the study, and they were 0.7 times native for both values. This varies greatly from the native values listed in Table 3, indicating the viscoelastic nature of this tissue based on the different strain rates used.

Colombini et al in 2015 performed an in vitro characterization of annulus fibrosus cells in collagen-enriched fibrin gels(Colombini et al., 2015). Specifically, they seeded 600,000 human annulus fibrosus cells/scaffold onto either fibrin gels or collagen-enriched fibrin gels. Gels were then cultured for 24 hours and assessed for biochemical content. It was determined that the collagen-enriched fibrin scaffolds produced 3 μg GAG/mg tissue, which corresponds to 0.03%/DW, a value that is 60 times less than native. While this appears to be too low for tissue engineered scaffolds, it should be noted that the in vitro result was a small part of a larger in vivo study, and these collagen-enriched fibrin scaffolds actually produced more GAG than native after in vivo implantation.

In another study by Guillaume et al, this time in 2015, they designed a scaffold construct used to fix defects in the annulus fibrosus in vivo, as opposed to replacing the entire tissue(Guillaume et al., 2015). 425,000 porcine annulus fibrosus cells were seeded onto either alginate or alginate-collagen scaffolds. Each scaffold was treated with either TGF-β3 or phosphate buffered saline (PBS). After 3 weeks of culture, it was determined that TGF-β3 loaded alginate-collagen scaffolds produced the highest DNA content, at 1900 ng/scaffold. The authors also investigated cell migration in these scaffolds, and were able to demonstrate that the TGF-β3 loaded alginate-collagen scaffolds promoted migration of annulus fibrosus cells throughout the scaffold, compared to only migration along the periphery for TGF-β3 loaded

alginate scaffolds. Moving forward, it would be interesting to see if cell-seeded scaffolds outperform the noncellular scaffolds in biomechanical testing.

For in vitro research, the trend appears to be working towards more complex systems that engineer scaffolds incorporating a gel like center and fibrocartilage based outer ring, like the system described in See et al's 2011 study(See et al., 2011). From the studies reviewed here, there is a lack of investigation into the effects of mechanical stimulation. Since intervertebral discs are load bearing joints, mechanical stimulation in vitro might elucidate how the scaffolds would potentially perform in vivo.

It is also clear that the field is heavily focused on the use of electrospun scaffolds. This tendency is understandable due to the layered, laminar nature of the annulus fibrosus in vivo. Also, all 5 studies utilized annulus fibrosus cells as the cell source for their regenerative approaches. It is surprising that there were not more stem cell studies performed, but perhaps that is the future direction of the field. The lack of comparable units for biochemical results also limits the ability to compare between studies.

In comparison with the TMJ field, the compressive properties achieved for tissue engineered annulus fibrosus replacements were the lowest of any fibrocartilage field. A caveat to this is that the compressive strength of the native annulus fibrosus is a full order of magnitude less (230 kPa) than the native TMJ disc (2085 kPa), so the lower compressive properties would be expected. Still, the intervertebral disc community could benefit from trying to incorporate costal and articular chondrocytes as the TMJ field did. In tension, the annulus fibrosus devices reviewed here far outperformed the TMJ community, with values exceeding native and either exceeding (tensile stress) or matching (tensile modulus) the TMJ field. Their improved performance could be based on the use of annulus fibrosus cells, or using different scaffolds than

the knee meniscus community did. It could be of interest to the TMJ community to attempt studies using co-cultures of annulus fibrosus and fibrochondrocytes, or to try some of the scaffolds used in these studies.

In biochemistry, the same difficulties exist in comparing annulus fibrosus regenerative methods to TMJ as with the knee meniscus. The varied use of study-specific units prevents comparison between fields and to native tissues. However, it appears that both fields produce lower collagen concentration than native. In contrast to the TMJ studies, however, the annulus fibrous field produces less GAG than native as well it seems. suited for producing structures with high compressive properties.

1.3.3 Conclusion

The discussed tissue engineered therapies highlight the recent advances in the fibrocartilage regenerative medicine field. In TMJ research, there have been several studies investigating both mechanical and chemical stimulation, but the field needs to introduce stem cells as a potential cell source. For both knee meniscus and IVD research, the fields could integrate more mechanical stimulation to simulate the reaction of the tissue engineered scaffolds to a load bearing environment.

Since the nature of in vitro studies are to experiment with new technologies and determine their potential efficacy in vivo, it could be assumed that fields of research with more in vivo studies are further along than those with less studies. Both knee meniscus and IVD produce more in vivo research. By replacing “in vitro” with “in vivo” in the search term for each field, TMJ yielded only 2 studies, while the knee meniscus and IVD fields had 9 and 8, respectively.

The lack of biomechanical data from testing of tissue engineered scaffolds in the meniscus and IVD field is concerning. While cell seeded scaffolds may perform well in biochemical analysis, this does not correlate to how effective these tissues will be at resisting in vivo biomechanical stresses. This highlights an important advantage that recent in vitro TMJ research possesses, as almost every study reports biomechanical properties of their regenerative technique. This presents a more complete view of the efficacy of the different methods presented, and should be a feature of not only the TMJ field moving forward, but all fibrocartilage in vitro research.

2.0 PROPERTIES OF THE TEMPOROMANDIBULAR JOINT IN GROWING PIGS

2.1 INTRODUCTION

The temporomandibular joint (TMJ) is a bilateral joint formed by the articulation of the mandibular condyle against the glenoid fossa and articular eminence of the temporal bone. A fibrocartilaginous disc known as the TMJ disc is situated between the condyle and fossa in the joint, and works to distribute the compressive and tensile forces in the joint during mandibular movements.(Beek et al., 2000; Donzelli et al., 2004; Tanaka et al., 2004; Tanaka and van Eijden, 2003) It is currently estimated that 5-15% of the population seeks treatment for TMJ disorders, 70% of which are associated with displacement of the TMJ disc.(Farrar and McCarty, 1979; Reston and Turkelson, 2003) The current surgical standard for an irreparable TMJ disc is to perform a discectomy, usually without autograft replacement, due to previous failures of autograft implantation.(Estabrooks et al., 1990; Henry and Wolford, 1993) The resulting absence of an interpositional disc leads to bone on bone contact and remodeling of the mandibular condyle. To prevent this outcome, tissue engineering has emerged as a potential regenerative medicine technique to replace the TMJ disc.

Tissue engineering offers a potential solution to reconstruction of the TMJ disc and/or the articulating surfaces of the TMJ through the development of cell-based and scaffold-based strategies.(Brown et al., 2012a; Brown et al., 2011; Puelacher et al., 1994; Tarafder et al., 2016;

Wu et al., 2014) Clinical translation will require preclinical animal studies across both acute and long-term time points. The pig is generally accepted as an appropriate model for large animal studies of the TMJ, but there is not a consensus on the appropriate age of the pigs for such studies. Pigs are considered skeletally mature at 2 years of age, yet due to size considerations and the limitations of laboratory equipment and facilities, most studies are conducted on pigs between 3-9 months of age. Because of the extremely rapid growth rate (2-3 lbs. /day), TMJ changes may be a confounding factor in the evaluation of efficacy and success of tissue engineered devices and therapies.

While there have been several studies looking into the biochemical and biomechanical properties of the healthy native articulating tissues of the porcine TMJ, there has been no study that examined and compared the effect of age on these properties under the same testing parameters.(Almarza et al., 2006; Beatty et al., 2001; Chladek and Czerwik, 2008; Detamore and Athanasiou, 2003; Detamore et al., 2005; Kalpakci et al., 2011b; Kang et al., 2000; Kim et al., 2003; Koolstra et al., 2007; Kuboki et al., 1997; Lamela et al., 2013; Lumpkins and McFetridge, 2009; Matuska et al., 2016; Murphy et al., 2013; Ruggiero et al., 2015; Singh and Detamore, 2008, 2009; Snider et al., 2008; Tanaka et al., 2003; Tanaka et al., 2006; Willard et al., 2012) To this end, the objective of the present study is to determine the effect of growth on the biochemical and biomechanical properties of porcine TMJ discs and condylar mandibular cartilage at 3, 6, and 9 months of age.

2.2 MATERIALS AND METHODS

2.2.1 Sample procurement

Ten female Yorkshire pig heads at 3, 6, and 9 months of age each were procured from a local abattoir immediately following sacrifice. Within 24 hours of collection, both TMJ discs and mandibular condyles were excised, wrapped in gauze, and soaked in 0.1 M phosphate buffered saline (PBS). All discs and condyles were assessed morphologically and no signs of degeneration were observed. Samples were stored at -20 °C until testing.

2.2.2 Histology

Discs (n = 2 per group) were embedded in the optimal cutting temperature compound (tissue-Tek) for 45 minutes, and then frozen to -80°C. The samples were cryotomed to 10 µm and fixed in cold acetone for 30 minutes. Samples were then stained with hematoxylin and eosin to visualize cellular distribution and content.

2.2.3 Biochemistry

Samples (n = 10 per group) were collected from the intermediate zone of the TMJ disc and the mandibular condylar cartilage using 4 mm biopsy punches (Figure 5). Samples were then digested in 0.1 M Papain at 65 °C overnight. All assays were performed using this digest. The DNA content was measured using a PicoGreen dsDNA quantification kit (Molecular Probes, Inc.). The total hydroxyproline content was assessed using a modified protocol that hydrolyzes

the hydroxyproline group with NaOH, followed by reaction with chloramine T and dimethylaminobenzaldehyde. This allows for a colorimetric output that can be compared against hydroxyproline standards. The total amount of glycosaminoglycans (GAG) was measured using a 1,9-dimethylmethylene blue colorimetric assay, using chondroitin-4-sulfate as a standard.

2.2.4 Compression Testing

Unconfined compression testing and analysis were performed as described previously (n = 10 per group).(Hagandora et al., 2011) Compressive samples of discs and condyles were obtained using 4 mm biopsy punches and allowed to equilibrate in 0.1 M PBS for 1 hour. The sample diameter was measured using calipers. An MTS Insight® was used for testing. Samples were loaded onto a compression platen using a thin film of cyanoacrylate and preloaded to 0.02N before the platen was removed. The water bath was then filled with PBS at 37 °C and maintained with a thermocouple throughout testing. The upper platen was lowered to within 0.1 mm of the cross head position determined previously, and a preload of 0.05 N was applied for 30 min to determine the specimen height. The samples then were subjected to 10 cycles of preconditioning at 9% strain/min to 10% strain. Following preconditioning, the samples underwent 3 stress relaxation strain steps between 10-30% strain at 10% intervals, with 30 minutes of relaxation time between each step.

The peak stress for each strain step was determined using the force obtained and the cross sectional area of the sample. The modulus was determined as the slope of the last 20% of each stress strain curve.

2.2.5 Tensile Testing

Prior to testing, discs were thawed and cut into a dumbbell shape using 8 mm biopsy punches in the intermediate zone of the disc, as shown in Figure 5. The resulting samples were sectioned in a cryotome to approximately 300 µm. This was accomplished by freezing superior surface of the disc to a cryotome platen using optical cutting temperature (OCT) compound, such that the inferior surface of the disc was visible. The cryostat blade cut parallel to the disc surface. Tensile sections were collected in order of their inferior-superior position. This method allowed for multiple sections (n = 3-6 per disc), enabling within disc variance analysis of tensile properties. Following procurement, samples were allowed to equilibrate for one hour at room temperature in 0.1 M PBS.

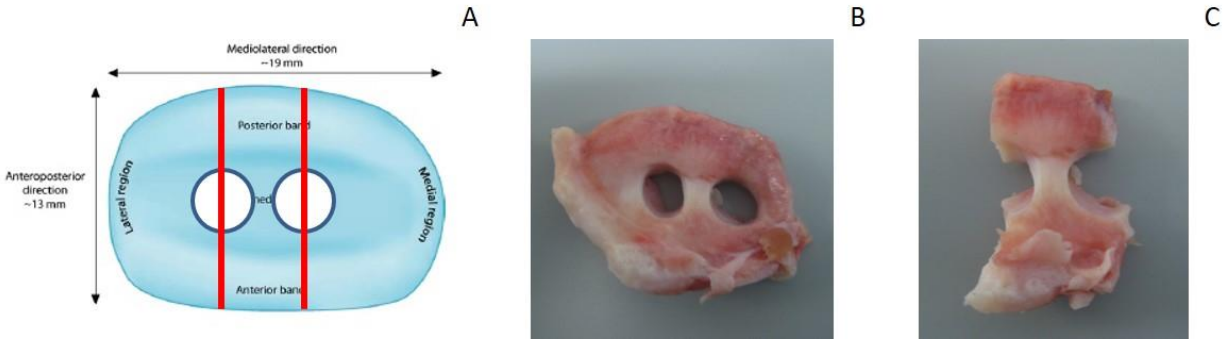

Figure 5. Representation of tensile testing sample preparation. A) Graphical representation of protocol. 8 mm biopsy punches are used to create a dogbone shape in the intermediate zone of the TMJ disc. A razor blade is then used to finish the dogbone shape (red lines). B) TMJ disc after use of biopsy punches. C) Final dogbone shape placed into cryotome for sectioning.

Samples were gripped between 400 grit sandpaper, and placed in pneumatic clamps at 45 PSI, and loaded onto an Instron mechanical testing apparatus (Instron 5566). The grip to grip length was measured using a ruler and varied between 8 mm to 16 mm in the anterior-posterior direction. Specimen thickness was measured using a micrometer (an average of 0.3 ± 0.1 mm), and width was determined using calipers (an average of 2.0 ± 0.3 mm). Samples were preloaded to 0.2 N and the load cell was reset to zero. Twenty cycles of preconditioning were applied at a strain rate of 10 mm/min to 5% strain. For preconditioning, upper bound of 1.1 N and lower bound of 0.45 N for the intensity of the first cycle was applied before continuing on with testing; a range determined from preliminary testing which showed that measured values for stress and strain were outliers (two standard deviation from the mean) if the load did not fall within these bounds. If less than three samples per disc failed to meet this criteria, that disc was not included in analysis. The samples were then pulled to failure at 10 mm/min. The sample data was analyzed for peak stress (maximum stress seen before break), tensile modulus (slope of the stress-strain curve from 4-8% strain), and clamp to clamp strain.

2.2.6 Statistics

A one-way ANOVA was used to determine differences within age groups per disc or condyle for biochemical and biomechanical values, with $p < 0.05$ defined as statistically significant. Tukey's post hoc testing was used to examine any differences between groups. When comparing discs to condyles, a student's t-test was used with significance at $p < 0.05$. All statistical analysis was performed using SPSS. All data are reported as average ± standard deviation.

2.3 RESULTS

2.3.1 Histology

Histological stains of the TMJ discs at 3, 6, and 9 months in the transverse and sagittal plane can be seen in Figure 6. A general decrease in overall cellularity can be seen in the TMJ disc as age increases. There also appears to be minor amounts of adipose tissue incorporated into the 3 month disc, which is not observed in later age groups. Collagen fiber organization becomes more aligned in the anterior posterior direction as age increases.

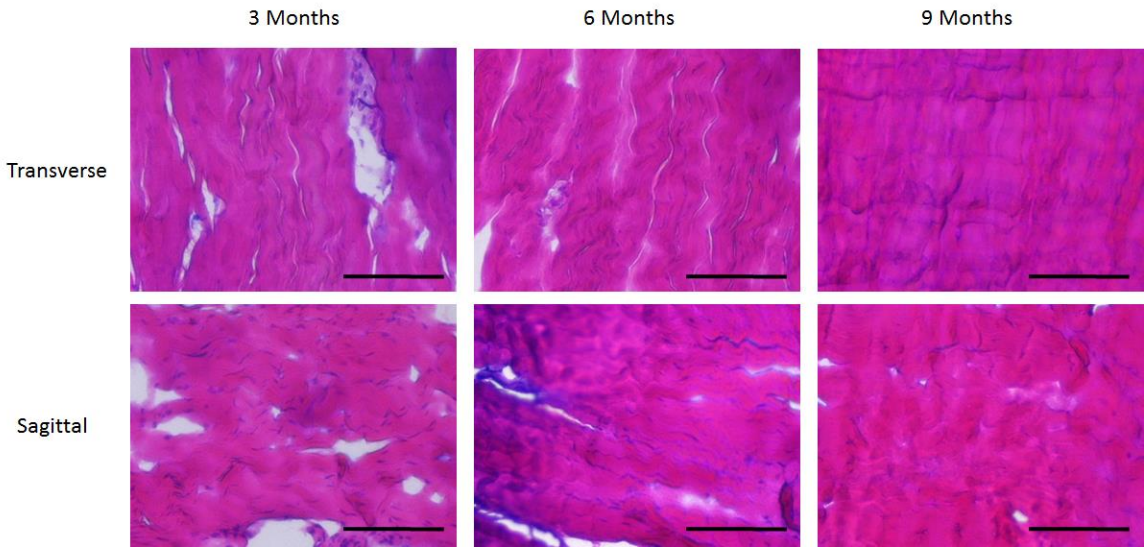

Figure 6. Hematoxylin and Eosin staining of TMJ discs at 3, 6, and 9 months. Row 1: Samples sectioned in the transverse plane. Row 2: Samples sectioned in the sagittal plane. All images were taken from the intermediate zone. Scale bar is 100 µm.

2.3.2 Biochemistry

The DNA content of the discs and condyles are shown in Figure 7. There were no significant differences ($p < 0.05$) in DNA content/dry weight (DW) between TMJ discs at 3, 6, and 9 months of age. There were also no significant differences ($p < 0.05$) in DNA content/DW between condyles at 3, 6, and 9 months of age.

The hydroxyproline content of the discs and condyles are shown in Figure 8. There were no significant differences ($p < 0.05$) in hydroxyproline content/DW between TMJ discs at 3, 6, and 9 months of age. There were also no significant differences ($p < 0.05$) in hydroxyproline content/DW between condyles at 3, 6, and 9 months of age.

The GAG content of the discs and condyles are shown in Figure 9. There were no significant differences ($p < 0.05$) in GAG content/DW between TMJ discs at 3, 6, and 9 months of age. There were also no significant differences ($p < 0.05$) in GAG content between condyles at 3, 6, and 9 months of age.

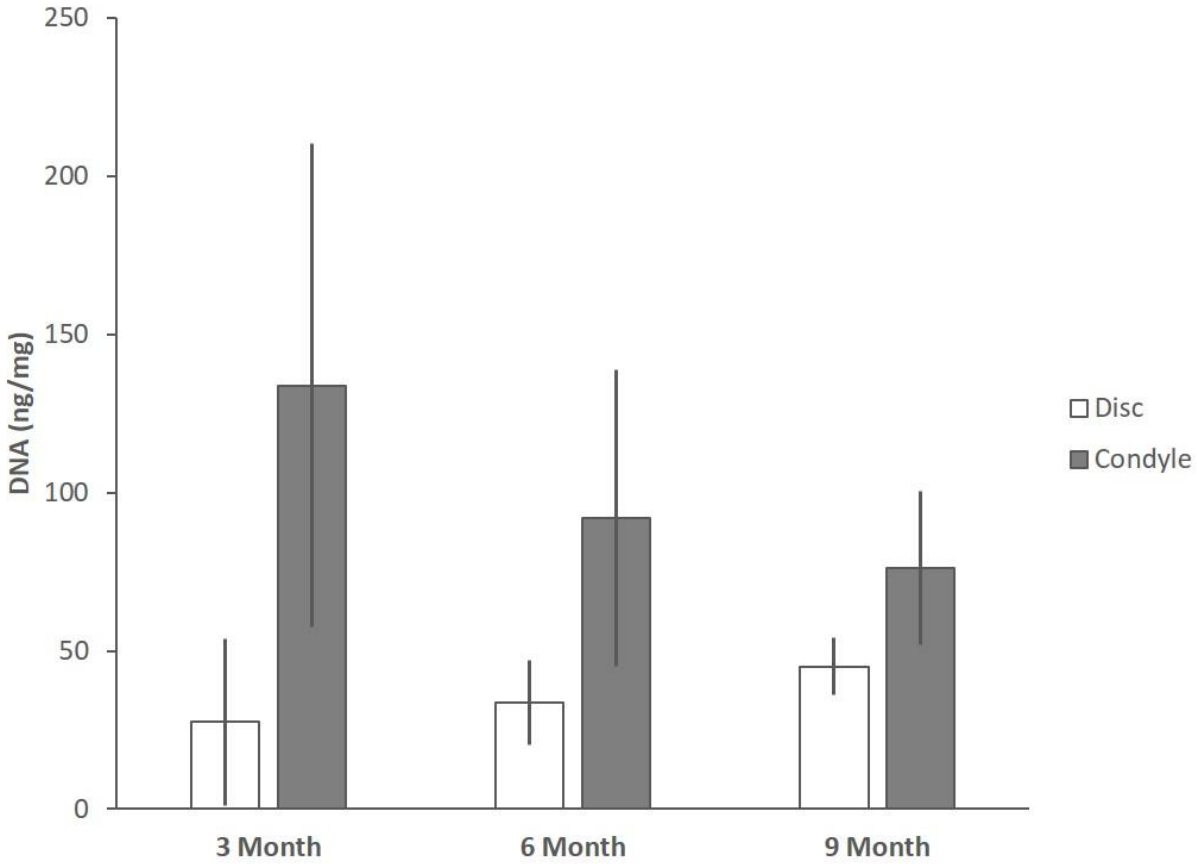

Figure 7. DNA content for TMJ discs (n = 10 per group) and mandibular condyles (n = 10 per group). All error bars represent standard deviation.

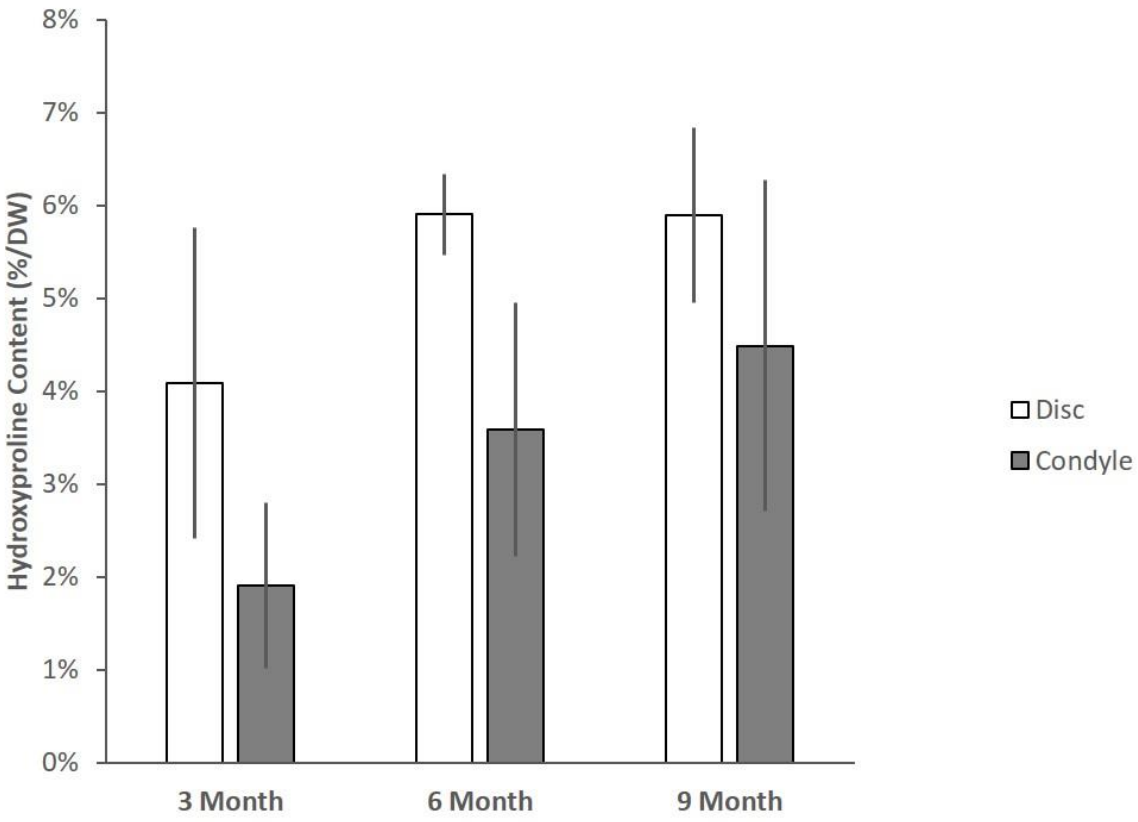

Figure 8. Hydroxyproline content for TMJ discs (n = 10 per group) and mandibular condyles (n = 10 per group). All error bars represent standard deviation.

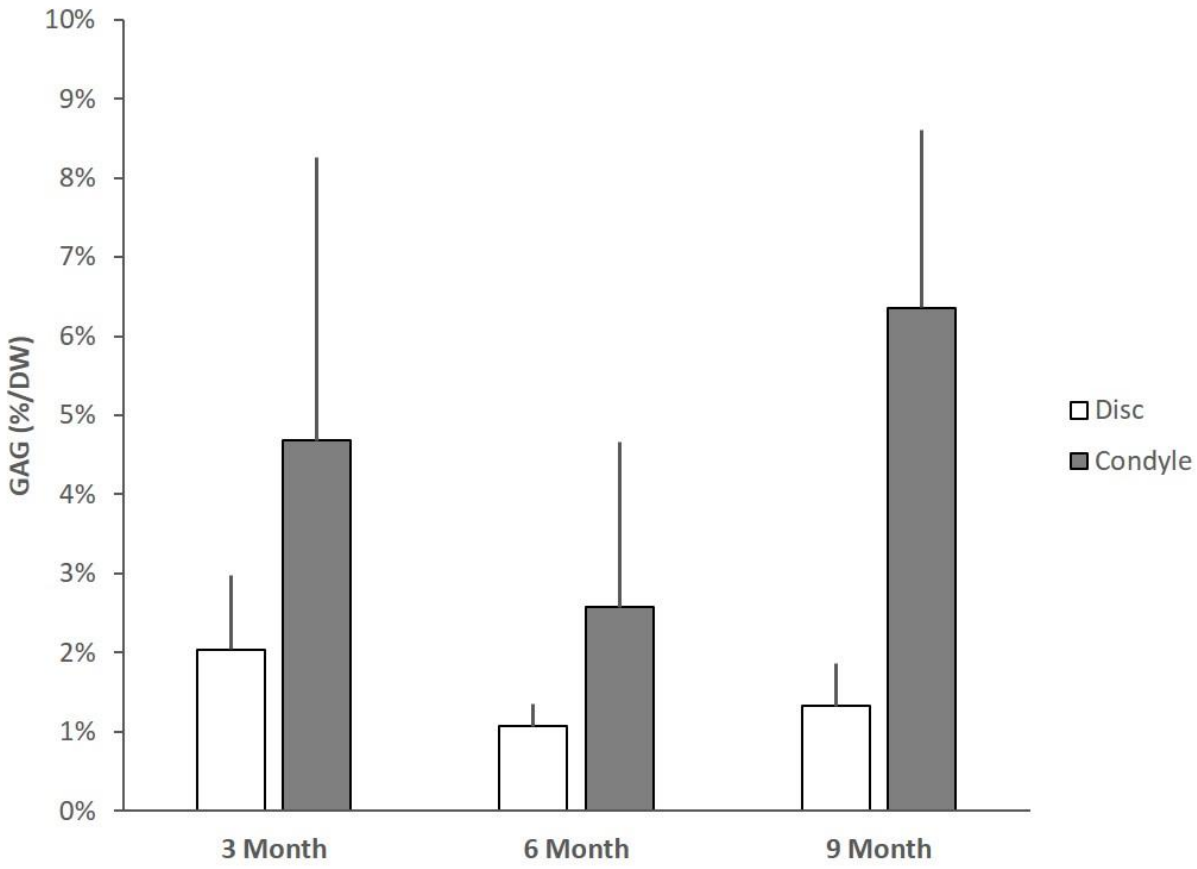

Figure 9. GAG content for TMJ discs (n = 10 per group) and mandibular condyles (n = 10 per group). All error bars represent standard deviation.

2.3.3 Compression Testing

The compressive stresses of the discs and condyles at each strain step are shown in Table 7. There were no significant differences ($p < 0.05$) in compressive stress at 30% strain between TMJ discs at 3, 6, and 9 months of age. There were no significant differences ($p < 0.05$) in compressive stress between condyles at 3, 6, and 9 months of age. The same trend was observed in the 10% and 20% strain steps (Table 7).

The compressive moduli of the discs and condyles at each strain step are shown in Table 7. There were no significant differences ($p < 0.05$) in compressive modulus at 30% strain between TMJ discs at 3, 6, and 9 months of age. There were no significant differences ($p < 0.05$) in compressive modulus between condyles at 3, 6, and 9 months of age. The same trend was observed in the 10% and 20% strain steps (Table 7).

Table 7. Compressive peak stress and modulus results at each strain step for TMJ discs and condyles at each time point (n = 10 per group). All errors represent standard deviation.

Strain Step	Tissue	Age	Peak Stress (kPa)	Compressive Modulus (kPa)
10%	Disc	3 Month	13 ± 11	251 ± 205
		6 Month	7 ± 4	126 ± 75
		9 Month	6 ± 5	127 ± 94
	Condyle	3 Month	6 ± 1	104 ± 23
		6 Month	8 ± 4	135 ± 83
		9 Month	8 ± 6	126 ± 116
20%	Disc	3 Month	61 ± 35	756 ± 366
		6 Month	44 ± 24	656 ± 323
		9 Month	44 ± 35	640 ± 470
	Condyle	3 Month	23 ± 6	263 ± 91
		6 Month	27 ± 15	287 ± 147
		9 Month	27 ± 19	288 ± 197
30%	Disc	3 Month	138 ± 56	1476 ± 487
		6 Month	124 ± 55	1568 ± 588
		9 Month	112 ± 70	1383 ± 689
	Condyle	3 Month	51 ± 16	516 ± 146
		6 Month	61 ± 30	580 ± 240
		9 Month	58 ± 38	607 ± 380

2.3.4 Tensile Testing

To obtain the results for tensile testing, an average stress and modulus was obtained for each individual TMJ disc, consisting of the separate samples obtained for each individual disc. These averaged values for each disc were then aggregated together for each time point, and the average stress and modulus values presented here are the averages of these aggregates. The tensile stress of the discs are shown in Figure 10. There were no significant differences ($p < 0.05$) in tensile stress between TMJ discs at 3, 6, and 9 months of age. There were also no significant differences ($p < 0.05$) in tensile modulus (shown in Figure 11) between discs at 3, 6, and 9 months of age.

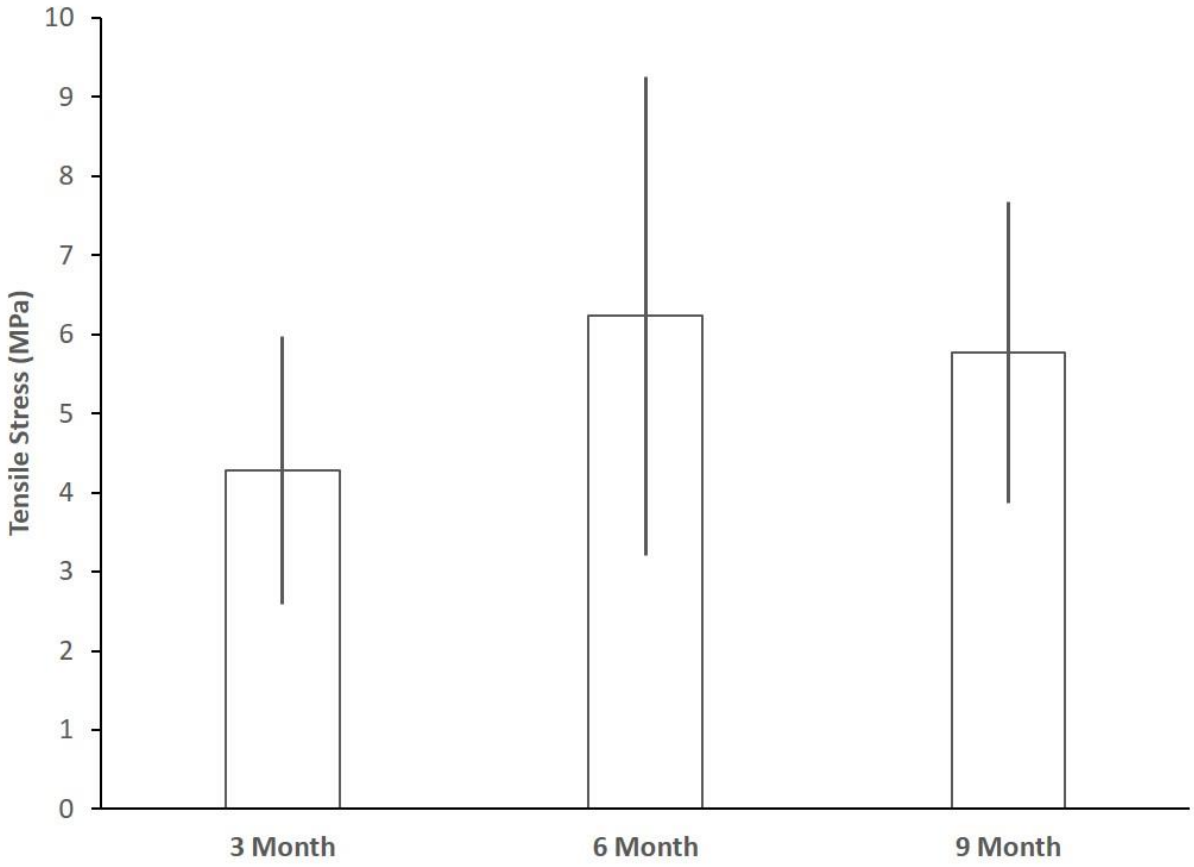

Figure 10. Tensile stress results for TMJ discs (n = 7 per group). All error bars represent standard deviation. There were no significant differences detected.

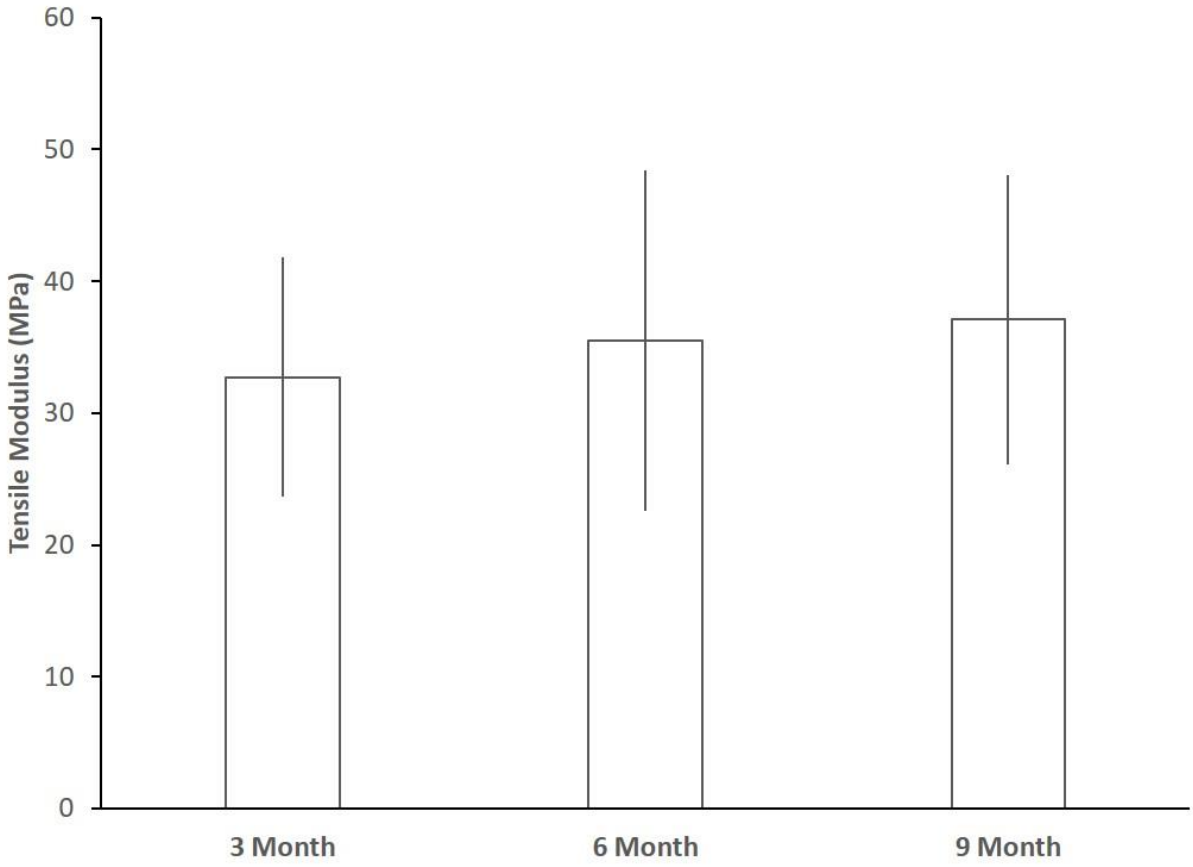

Figure 11. Tensile modulus results for TMJ discs (n = 7 per group). All error bars represent standard deviation. There were no significant differences detected.

2.4 DISCUSSION

The results of this study show that there are no effects of growth on the biochemical or mechanical properties of the porcine TMJ disc or mandibular condylar cartilage. The DNA content of the TMJ discs (0.004%/DW) measured was lower than previously reported (0.14%/DW), while the GAG content (1.5%/DW average) and collagen content (72%/DW average) was in range with previously reported values (0.880%, 68.2% respectively). (Almarza et al., 2006; Willard et al., 2012) The lack of differences in the biochemical content from

different ages correspond to lack of differences in the mechanical properties. Since the extracellular matrix (ECM) remains largely unchanged across time points, it would be expected that the mechanical properties would be similar. The results of mechanical testing also suggest that the collagen deposited by fibrochondrocytes upon formation of the disc are already aligned into a densely packed collagen network by 3 months.

The literature is bereft of studies on the properties of the mandibular condylar cartilage. To our knowledge, this is the first study on the porcine condylar cartilage matrix constituents. Several studies have been performed on the mechanical properties of the mandibular condylar cartilage, but they have either not been stress relaxation studies, or have utilized different strain rates, which does not allow for direct comparisons. (Kuboki et al., 1997; Singh and Detamore, 2008, 2009; Tanaka et al., 2006).

For compression of the TMJ disc, a peak stress at a similar stress relaxation strain rate has not been reported, but a compressive modulus of 2079 ± 581 MPa has been reported at 30% strain, which is in range with the presented values. (Kalpakci et al., 2011b) The tensile peak stress of 5 MPa was in the range of what has been reported for the porcine TMJ disc at 10 mm/min strain rate (5.98 MPa, 4.3 MPa).(Detamore and Athanasiou, 2003; Kalpakci et al., 2011b) The tensile moduli determined here, 35 MPa, was also in range of previously stated values (28.6 MPa, 23.0 MPa).

The utilization of multiple tensile samples per individual disc allowed for average values per disc to be determined, which led to a reduction of overall error observed during testing. For example, if all the samples are used for tensile modulus values, the standard deviation for all samples at 3, 6, and 9 months would be 13.9 MPa, 17.8 MPa, and 17.5 MPa, respectively. However, since samples were averaged first by disc, the standard deviation for tensile modulus

were lower at 3, 6, and 9 months, with values of 9.1 MPa, 12.9 MPa, and 11.0 MPa respectively. The intra-specimen variability in the superior-inferior direction is likely due to the collagen fibers having heterogeneous orientation in the sagittal plane.(Fazaeli et al., 2016) Also, the TMJ's collagen fiber diameter has not been investigated in the intermediate zone in the anterior-posterior direction. This heterogeneity would result in highly variable stress and strain results. The results obtained in this study confirmed this hypothesis, as there was no discernable pattern between the level of stress and modulus observed in that sample's position along the inferior/superior plane at the intermediate zone.

In conclusion, the lack of differences between the 3, 6, and 9 month results for both the porcine TMJ disc and mandibular condylar cartilage indicate that for tissue engineering studies involving multiple time points in skeletally immature porcine models, no age matched controls are necessary from a mechanical and biochemical standpoint. However, it should be noted that changes in the skeletal anatomy due to rapid growth may necessitate the use of animals within a specific age range for surgical studies. The potential for the novel proposed tensile method, the reduction of the variability in tensile modulus, suggest that this method should be used for future biomechanical characterization with TMJ discs.

3.0 REMODELED ECM SCAFFOLD FUNCTIONS AS A TMJ DISC ANALOGUE

3.1 INTRODUCTION

Currently, the surgical standard to treat a patient suffering from severe TMD is to perform a discectomy, resulting in direct bone on bone contact. This is due in part to the failures of implantation of autogenous tissues, such as dermis, temporalis muscle and abdominal adipose tissue(Dimitroulis, 2011; Meyer, 1988; Pogrel and Kaban, 1990). Also, there are no current alloplastic autografts that serve as a potential clinical disc replacement(Estabrooks et al., 1990; Henry and Wolford, 1993). Previous attempts to develop alloplastic materials for implantation have led to increased joint pathology, among other complications(Alonso et al., 2009; Dolwick and Aufdemorte, 1985; Ferreira et al., 2008; Fricton et al., 2002). The outcome of discectomy without graft replacement is bone on bone contact between the mandibular condyle and glenoid fossa of the temporal bone, resulting in remodeling of the joint surfaces. As mentioned in the introduction of chapter 2, tissue engineering has emerged as a potential regenerative medicine technique to replace the TMJ disc to offset these negative outcomes.

One specific material used heavily in tissue engineering is extracellular matrix (ECM), which consists of the secreted proteins, collagens, mucins, elastic fibers, glycosaminoglycans, growth factors, and other molecules that provide structural and signaling functions to a tissue,

and are affected by degradation and synthesis by cells (Hynes and Naba, 2012). ECM has been gaining popularity as an inductive template for tissue engineering due to its ability to prevent shift the healing response from scar tissue to constructive remodeling. The success of this substrate for tissue engineering is attributed to the degradation products of ECM. Specifically, degradation of the ECM by MMPs and metalloproteinases result in the exposure of new recognition sites with potent bioactivity (Davis, 2010; Davis et al., 2000; Maquart et al., 2005). These sites have been shown to influence cell behavior, and can result in a diverse array of bioprocesses, such as angiogenesis and adhesion, among others (Davis, 2010; Davis et al., 2000; Maquart et al., 2005; Ramchandran et al., 1999; Vlodavsky et al., 2002).

ECM based substrates have been used in a wide range of applications due to their ability to promote the process of "constructive remodeling", or the formation of site appropriate, functional tissue(Badylak, 2004). This is expected because the ECM scaffold provides a highly conserved and naturally occurring substrate for tissue reconstruction, cell growth, and viability. There are several aspects about the ECM that allow it to serve as an inductive scaffold, including the mechanical structure of the tissue and its ability to transmit forces and mechanical cues, ECM's modulation of the host response due to the ECM composition, dynamic reciprocity, bioactive degradation products, and an instructive niche for stem cells.

The ECM provides 3-dimensional structural support to the cells, and serves to transmit mechanical forces and as a substrate for cell migration. These properties are attributed to the physical properties of the ECM, which include the rigidity, insolubility, porosity, and topography of the various layers of each ECM tissue(Daley et al., 2008; Lu et al., 2011). The properties of the tissue are highly dependent on the individual layer of the ECM, as each tissue compartment serves a particular purpose within the function of the organ, and the transition between each type

of tissue is accompanied by differences in ECM structure and composition. The myriad physical properties and intricate topography highlight the difficulties in trying to tissue engineer a synthetic ECM replacement, although researchers are still attempting this approach through methods such as electrospinning(Barnes et al., 2007; Kumbar et al., 2008).

The composition is another distinct ECM property to consider. The exact composition of the ECM varies greatly from tissue to tissue, but is composed of collagens, glycoproteins, proteoglycans, mucins elastic fibers, and growth factors. The composition of any specific ECM is highly dependent on the function of that tissue. For example, cartilage ECM is high in collagen and glycosaminoglycans, components specifically designed to provide resistance and recovery to mechanical forces and to allow for high water content. As a result, ECM that is harvested for tissue engineered scaffolds can be selected for compositional functionality in their eventual intended application.

The ECM is also known to have pleiotropic effects upon tissue resident cells, including cell adhesion, proliferation, migration, differentiation, and death(Hynes, 2009; Lu et al., 2011). This is because the ECM is constantly exerting these effects upon cellular behavior and phenotype, and the cells in return remodel the ECM in a process called dynamic reciprocity (Bissell et al., 1982; Boudreau et al., 1995; Ingber, 1991). This dynamic homeostasis is a result of highly regulated cell signaling and patterning processes, and rely heavily upon the expression of matrix metalloproteinases (MMPs), tissue inhibitors if MMPs, fibronectin, laminin, and collagen. The dynamic reciprocity of ECM is a unique feature that has not been reproduced among other tissue engineered biomaterials, as synthetic materials can only be tuned to degrade at specific rates and under specific conditions.

The dynamically reciprocal nature of the ECM requires that the ECM have bioactive biodegradable products. As a result, every component in the ECM is able to degrade and is subject to modification. The main components responsible for degradation of the ECM are the MMPs and metalloproteinases with thrombospondin motif families (ADAMTS)(Cawston and Young, 2010). Degradation from these proteinases can result in the exposure of new recognition sites with potent bioactivity along the surface of the ECM. These byproducts include cryptic sites, which can influence cell behavior, leading to a diverse array of bioprocesses including angiogenesis, antiangiogenesis, chemotaxis, adhesion, and antimicrobial effects (Davis, 2010; Davis et al., 2000; Maquart et al., 2005; Ramchandran et al., 1999; Vlodavsky et al., 2002). One of the most common cryptic site peptides is the Arg-Gly-Asp peptide present within fibronectin, collagen, vitronectin and osteopontin, which is used for cell adhesion and synthetic substrates(Davis, 1992; Davis et al., 2000; Hern and Hubbell, 1998; Hirano et al., 1993; Hsiong et al., 2008; Krammer et al., 1999; LeBaron and Athanasiou, 2000; Seiffert and Smith, 1997; Smith et al., 1996; Ugarova et al., 1995; Vidal et al., 2013).

ECM also serves as an instructive niche for stem cells. The ECM cell niche contributes to the establishment and maintenance of stem cell differentiation through soluble factors and ECM macromolecules(Brizzi et al., 2012; Kazanis and ffrench-Constant, 2011; Reilly and Engler, 2010; Votteler et al., 2010). Within ECM, the degradation and remodeling in the stem cell niche is thought to mediate cell activation and release. The composition, topography, and biomechanics of the ECM regulate stem cell migration and differentiation following stem cell release (Engler et al., 2006; Reilly and Engler, 2010).

The different roles of ECM described above combine to make it highly desirable as an inductive scaffold for tissue engineering. However, for it to not induce an inflammatory host

response, the tissue must be decellularized prior to implantation, while maintaining the ultrastructure and ligand landscape. This process includes physical, ionic, chemical, and enzymatic methods of decellularization, with each method being tuned to the thickness, density, and intended clinical application of the matrix material (Crapo et al., 2011; Gilbert, 2012; Gilbert et al., 2006). When the tissues are not decellularized properly, either through excessive cellular content or significant disruption of the architecture, they induce a pro inflammatory response which adversely affects tissue remodeling. Also, if the decellularization process leads to chemical cross linking of the tissue, it can disrupt the ligand landscape, and prevent the degradation of the ECM in vivo.

ECM supports this constructive remodeling through three major mechanisms, although the exact interactions between these mechanisms are not understood. The three mechanisms are through mechanical forces, the modulation of host responses, and through ECM scaffold degradation. Each of these mechanisms are important to induce an acellular scaffold that is populated by host cells to undergo a remodeling response that deposits site appropriate tissue instead of a pro-inflammatory response. In the absence of any of the following mechanisms, the constructive remodeling desired is not observed and the scaffold produces an unfavorable response.

The use of site appropriate mechanical loading as a mechanism for remodeling ECM into site appropriate tissue has been studied extensively. It has been shown that the absence of mechanical loading can lead to degradation of the ECM scaffold material, dense scar tissue deposition, and an absence of constructive remodeling, even in a case of delayed return to normal mechanical loading (Hodde et al., 1997). It has also been shown that both static and cyclic stretching of cell-seeded ECM in vitro has led to increased collagen deposition, alignment,

and improved mechanical properties(Almarza et al., 2008; Androjna et al., 2007; Gilbert et al., 2007c; Nguyen et al., 2009; Wallis et al., 2008). These effects can potentially attribute to the exposure of cryptic sites leading to remodeling during mechanical stimulation.

The second mechanism is the modulation of the host response, due to their unique surface topologies and ligand landscapes. In general, the host will elicit neutrophil migration to the implantation site in the first two days. This is followed by a prominent macrophage response within 3 days of implantation. These macrophages generally switch from a predominately M1 macrophage response to M2 macrophages by 7-14 days post implantation (Badylak et al., 2008; Brown et al., 2012c; Brown et al., 2009). ECM scaffolds have also shown the ability to evoke a Th2 immune response, generally associated with transplant acceptance (Badylak et al., 2008; Brown et al., 2012b; Brown et al., 2009). It has been shown that crosslinked materials that inhibit macrophage modulation to M2 result in downstream scar tissue formation, suggesting that interactions between host cells and non-crosslinked intact ligands on the surface of the material are necessary for successful remodeling (Badylak et al., 2008; Brown et al., 2012b).

The third mechanism is through ECM scaffold degradation, which as described earlier, leads to the exposure of new recognition sites. It has been shown that carbon-labeled ECM scaffolds were 60% degrade within 30 days post-implantation in the canine Achilles tendon repair (Gilbert et al., 2007a; Gilbert et al., 2007b). The rapid degradation observed can lead to the exposure of these sites, increasing the bioactivity of the implantation. As with the ECM's ability to modulate the host response, cross linked scaffolds produce negative inflammatory outcomes due to their inability to degrade and reveal cryptic sites and bioactive byproducts.

ECM has shown to constructively remodel into site-appropriate tissue in many sites, including esophagus, skeletal muscle, heart, brain, bone, and connective tissue among

others(Badylak et al., 2011; Medberry et al., 2013; Sawkins et al., 2013; Seif-Naraghi et al., 2013; Sicari et al., 2014b; Zantop et al., 2006). More applicable to the TMJ, ECM has already shown promise in two canine studies, remodeling into a site-appropriate tissue that resembles the native TMJ disc 6 months after bilateral implantation(Brown et al., 2012a; Brown et al., 2011).

For the proposed study, we will investigate the use of small intestine submucosa (SIS)-ECM as a graft replacement for the TMJ disc in a porcine model. We have moved from the canine model validated previously to a porcine model due to similarities between porcine TMJ anatomy and function to those of human. These similarities include the size of the articular structures, shape of the disc, and the omnivorous diet(Berg, 1973; Bermejo et al., 1993). Following unilateral implantation of the SIS-ECM scaffolds in a porcine model, we will characterize the resulting ex-vivo remodeled scaffolds at 1, 3, and 6 months post-surgery, and compare against native age-matched controls using protocols established in chapter 2.

3.2 MATERIALS AND METHODS

3.2.1 Specimen Procurement

For control groups, female pigs (n=10 per age group) were obtained from a local abattoir at 3, 6, and 9 months of age. Once obtained, TMJ discs and mandibular condyles from both sides of the head were immediately excised. All discs and condyles were assessed morphologically for signs of degeneration, and none were observed. All specimens were wrapped in gauze, soaked in 0.1 M PBS, and frozen at -20 ^{o}C.

3.2.2 Scaffold Production

Small intestines were obtained from a canine model and washed. The intestinal contents were squeezed from the jejunum down into the Peyer's Patch region, and the intesting was cut just before the Peyer's patch. The intestine was rinsed, and split open using a razor blade and forceps. The intestine was then placed with the luminal side up, and the luminal layer was scraped with an acrylic scraper. The intestine was then flipped and the abluminal side was scraped to remove externam luscle and the underyling mucosal layers. The resulting SIS layer was rinsed and cut into approximately 12-inch lengths.

The tissue was then decellularized as described previously(Brown et al., 2011). Briefly, the tissue was treated in a 0.1% peracetic acid/4% ethanol solution for 2 hours. This was used to decelluarize and disinfect the tissue. The tissue was then washed in PBS and water repeatedly to remove cellular remnants and traces of the peracetic acid and ethanol solution. This also adjusted the pH of the tissue to 7.4. The tissue was then stored as hydrated sheets in water until use.

A portion of this tissue was then frozen and lyophilize, and then cut into smaller pieces and powderized using a Wiley mill with a No. 60 mesh screen. A hard plastic mold was then milled to create an oval depression with the approximate size desired for the ECM graft replacement (10 x 14-mm oval, 2-mm depth). The mold contained a flat surface surrounding this depression to allow for the formation of a pillow-like core. Two hydrated sheets that were stored in water were then cut and pressed into the shape of the depression. 200-300 mg of the particulate ECM created by the mill was then pressed into the depression, and two more hydrated sheets were placed on top to create the pillow shape. The scaffolds were then placed in a

vacuum to dry and seal the construct, and sterilized with ethylene oxide. The final scaffold can be seen in Figure 12.

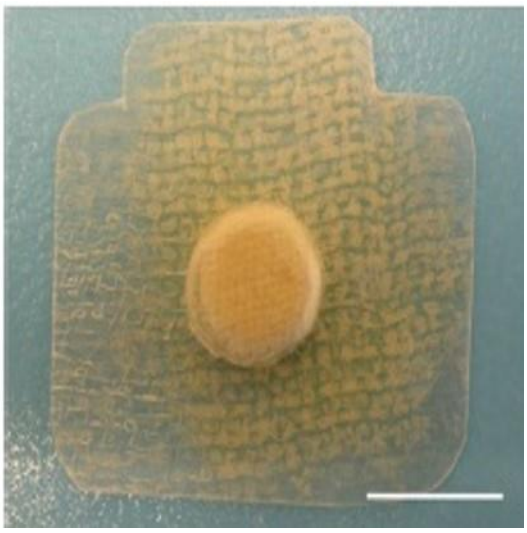

Figure 12. Representation of the SIS-ECM scaffold produced for implantation into the porcine model. Adapted from Brown, et al(Brown et al., 2011).

3.2.3 Surgical Procedure

Pigs are subjected to bilateral compete resection of the TMJ disc, with both sides treated with a scaffold of choice. Anesthesia is induced with Acepromazine (0.1-0.5 mg/kg) and maintained on Isoflurane (1-5%). The surgical approach involves an incision just anterior to the tragus, with soft tissue dissection preserving the local innervation and vasculature (especially the facial nerve) of this portion of the anatomy. The meniscus is isolated, removed from both sides, and replaced by the SIS-ECM scaffold unilaterally. Following the surgical procedure and cessation of inhalation anesthesia, each animal is continually monitored for 24 hours, recording the pulse

rate, strength of pulse, capillary refill time, respiratory rate and ability to maintain an open airway, urinary output, and defecation every 3 hours. Buprenophrine (0.005-0.01 mg/kg IM or IV q12h) is administered for 5 days for pain, and then as needed. Pigs receive Cephalexin (35 mg/kg q12) for 5 days as a prophylactic antibiotic. Due to the nature of the surgical procedure, all pigs are fed a soft diet for 5 days post-surgery and then returned to normal dry feed diet. At the predetermined time of sacrifice, pigs are sedated with Acepromazine (0.1-0.5 mg/kg BW SC) masked with 5% Isoflurane for 5 minutes and then given Pentobarbital Sodium IV (390 mg/4.5 kg BW).

3.2.4 Biochemistry

The collagen and glycosaminoglycan (GAG) content of the remodeled scaffolds, native discs, mandibular condyles, and pre-implantation devices were measured as a percentage of the dry weight of the original samples. Samples were allowed to equilibrate for one hour in 0.1M PBS before wet weights were measured. Specimens were then lyophilized for between 2-4 days in order to determine the dry weight. To determine collagen content, lyophilized tissues were placed in 4 N HCl overnight at 60 ^{o}C to dissolve. Samples were then neutralized with 4 N NaOH, and continued with previously published hydroxyproline assay protocols [1]. The samples were run against hydroxyproline standards, assuming hydroxyproline is 7.4% of collagen, as determined previously [2]. For GAG and DNA content, lyophilized samples were digested in a papain solution (125 µg/mL papain in 50 mmol phosphate buffere containing 5 mmol N-acetyle cysteine overnight at 60 ^{o}C) [3-4]. The total GAG content was measured using a dimethymethylene blue colorimetric assay kit (Biocolor, Newtonabbey, UK), while the DNA

content was measured using a PicoGreen dsDNA Quantitation Kit (Molecular Probes, Inc. Eugene, Oregon).

3.2.5 Tensile Testing

Prior to testing, 8 mm dermal punches were used to create anterior-posterior dogbone shapes of the intermediate zone of the native discs and remodeled ECM scaffolds. These samples were 1-3 mm wide in the thinnest portion of the dogbone. Samples were fixed to a platen using freezing medium and sectioned inferiorly/superiorly to 300-400 micrometers using a cryotome, producing multiple sections per disc, which were all tested. Sections were collected for testing after a single complete section was shaved off the dogbone sample, to ensure uniform thickness for all samples.

For testing, dogbone specimens were then allowed to equilibrate in room temperature 0.1 M PBS for at least 1 hour prior to testing. Specimen width and thicknesses were measured using a micrometer and calipers, respectively. Samples were gripped using 440 grit sandpaper, and placed in pneumatic clamps on a uniaxial mechanical testing apparatus (Instron Model 5566, Canton, MA). Testing occurred in air at room temperature. However, whenever possible, the sample was hydrated with 0.1 M PBS using a felt tip applicator. Samples were then preloaded to 0.2 N to straighten the specimen. The clamp to clamp length was taken as the initial specimen length and used to calculate percent strain. Samples were then preconditioned to 5.5% strain for 20 cycles at a strain rate of 10 mm/min. 5.5% strain was determined to encompass the toe region of the stress strain curve, as determined by initial tensile testing. For preconditioning, an upper (1.1 N) and lower (0.6 N) bound for the first peak of the preconditioning cycle was established as

an acceptable load for native samples, indicating that the sample was not slipping and aligned. These bounds were not applied to remodeled scaffolds. Any samples outside of the established boundary conditions for preconditioning were discarded. Following preconditioning, samples were loaded to failure at a strain rate of 10 mm/min.

The samples were analyzed for the peak tensile stress (tensile stress at failure), tensile modulus (slope of stress-strain behavior between 4-8% strain), and the failure strain (clamp to clamp strain at failure). Each disc or remodeled ECM scaffold yielded 3-7 tensile samples, which were averaged into one value. Remodeled ECM scaffolds were compared to age-matched controls.

3.2.6 Compression Testing

A 4 mm biopsy punch was used to obtain samples from the intermediate zone of the native discs, remodeled scaffolds, and mandibular condyles. Specimens were then allowed to equilibrate in room temperature 0.1 M PBS for at least one hour prior to testing. Specimen diameters were measured using digital calipers, and then the specimen was affixed to a compression platen on a uniaxial testing apparatus (MTS Insight 1-SL) using cyanoacrylate. A 0.02 N preload force was applied to the sample to determine sample height, at which point the crosshead platen was removed. The water bath was then filled with 0.1 M PBS at 37 ^{o}C. A preload of 0.05 N was applied for 30 min. The samples then underwent 10 cycles of preconditioning to 10% strain at a strain rate of 9% strain/min. Immediately following, samples were subjected to stress relaxation compression from 0% to 30% strain in 10% increments, with 30 minutes of relaxation between each strain step. The strain rate for stress relaxation was 9% strain/min. The parameters obtained were the peak stress (maximum stress achieved at each strain step) and peak modulus (slope of the last 20% of the stress-strain curve).

3.2.7 Statistics

A one-way ANOVA was used to determine differences within age groups per disc or condyle for biochemical and biomechanical values, with $p < 0.05$ defined as statistically significant. Tukey's post hoc testing was used to examine any differences between groups. When comparing discs to condyles, a student's t-test was used with significance at $p < 0.05$. All statistical analysis was performed using SPSS. All data are reported as average ± standard deviation.

3.3 RESULTS

3.3.1 Gross Morphology

Representative gross morphology pictures of remodeled ECM scaffolds at 1, 3, and 6 months post-surgery are presented in Figure 13, and compared against a native porcine TMJ disc of approximately 1 year of age. As soon as 1 month post-surgery, the remodeled scaffold has begun to resemble native TMJ disc tissue. By 6 months post-surgery, the remodeled scaffolds begin showing the striations associated with anterior-posteriorly aligned collagen fibers in the intermediate zone. For the study, 11 remodeled scaffolds were obtained from 32 individual pigs, providing a success rate of 34% for scaffold remodeling.

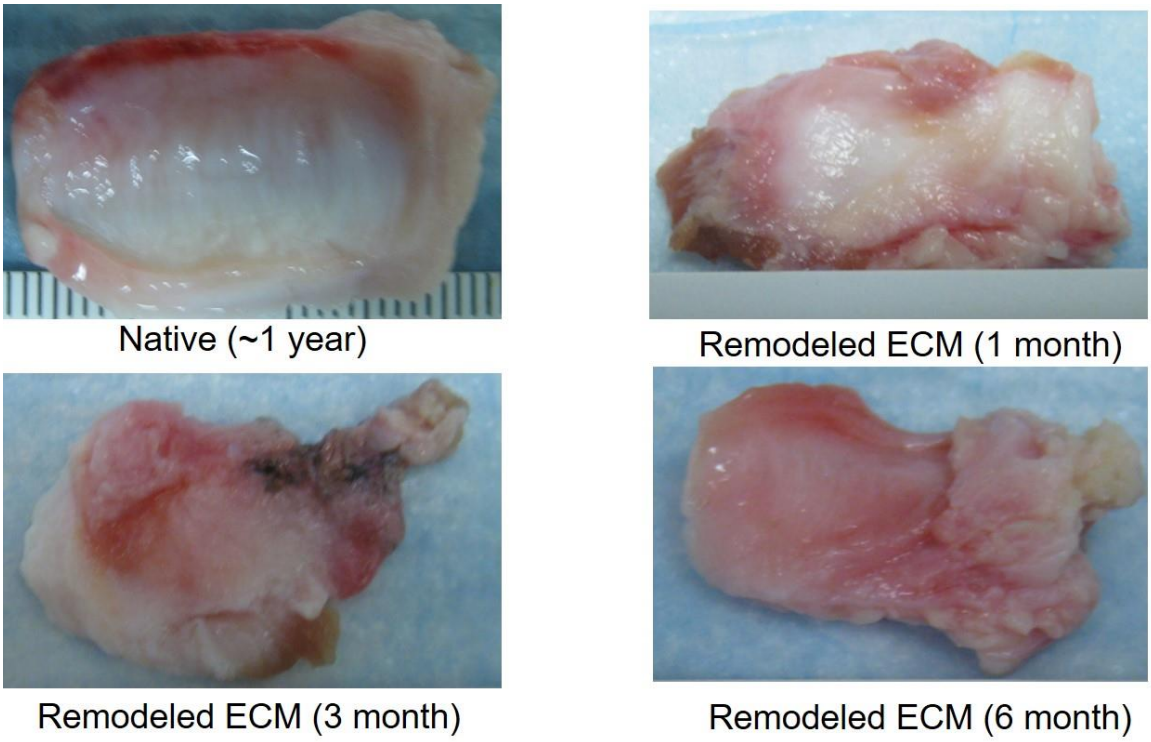

Figure 13. Gross morphology of a native disc at 1 year and remodeled ECM scaffolds at 1, 3, and 6 month post implantation.

3.3.2 Biochemistry

The collagen content of the native discs, remodeled ECM scaffolds, and pre-implantation devices are shown in Figure 14. There was a significant difference ($p < 0.05$) in collagen content (%/dry weight (DW)) between TMJ discs at 1 and 6 months post-surgery (54% ± 2%, 96% ± 2%, respectively), and their age-matched controls at 3 and 9 months (82% ± 9%, 78% ± 13%, respectively). There were no significant differences ($p < 0.05$) in collagen content (%/DW) between TMJ discs at 3 months post-surgery (82% ± 10%), and their age-matched controls at 6

months (83% ± 7%). The preimplantation devices (76% ± 12%) were statistically different from both the 1 and 6 month remodeled devices.

The collagen content of the condyles of the remodeled ECM side and native condyles are shown in Figure 15. There were no significant differences ($p < 0.05$) in collagen content (%/DW) between mandibular condyles at 1, 3, and 6 months post-surgery (38% ± 23%, 43% ± 11%, and 50 ± 25%, respectively), and their age-matched controls at 3, 6, and 9 months (52% ± 23%, 30% ± 13%, and 64% ± 25% respectively).

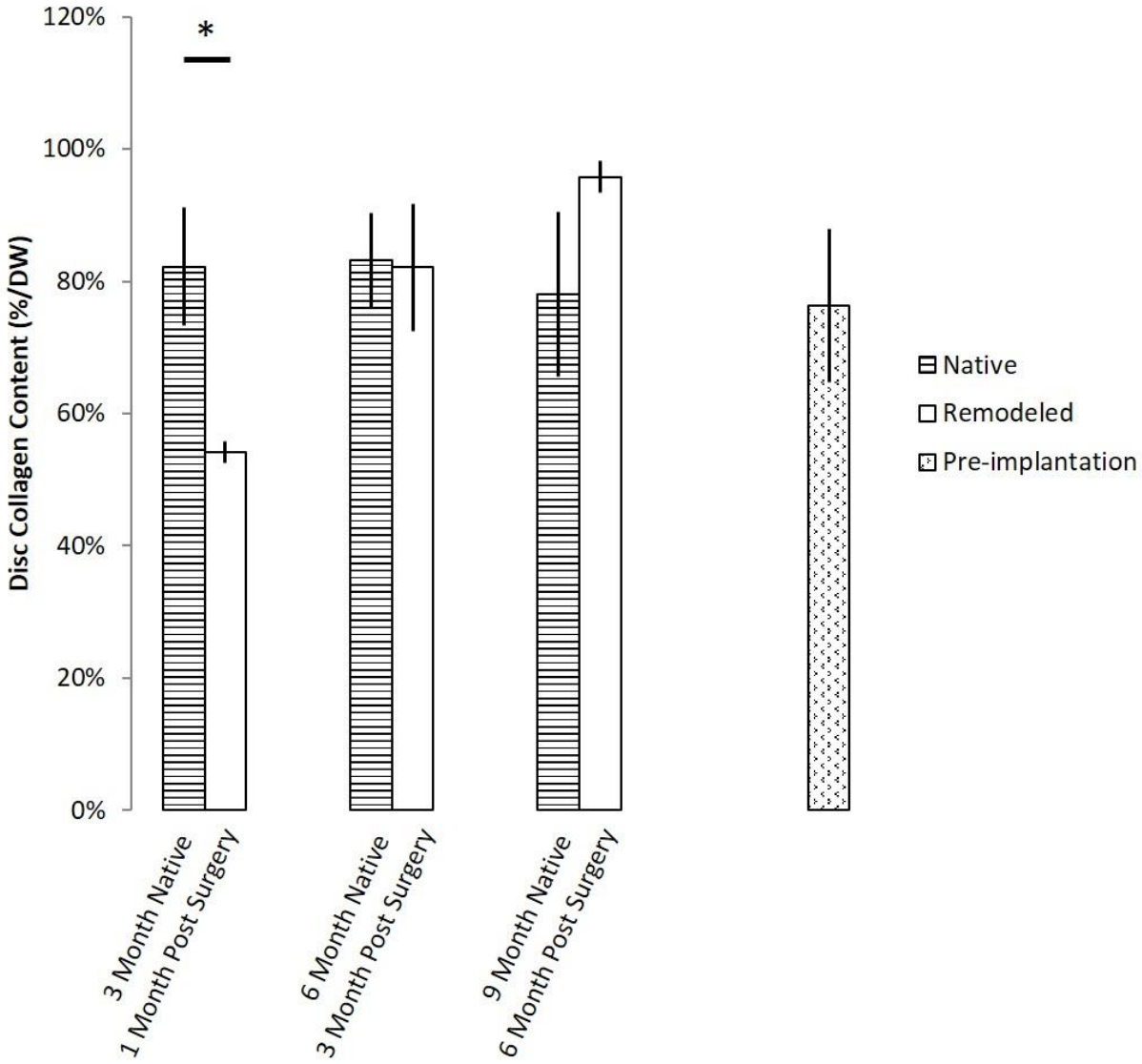

Figure 14. Collagen content for native TMJ discs (n = 9 per group), remodeled scaffolds (n = 3 for 1 month post-surgery, n = 4 for 3 and 6 month post-surgery) and pre-implantation ECM scaffolds (n = 9 per group). All error bars represent standard deviation.

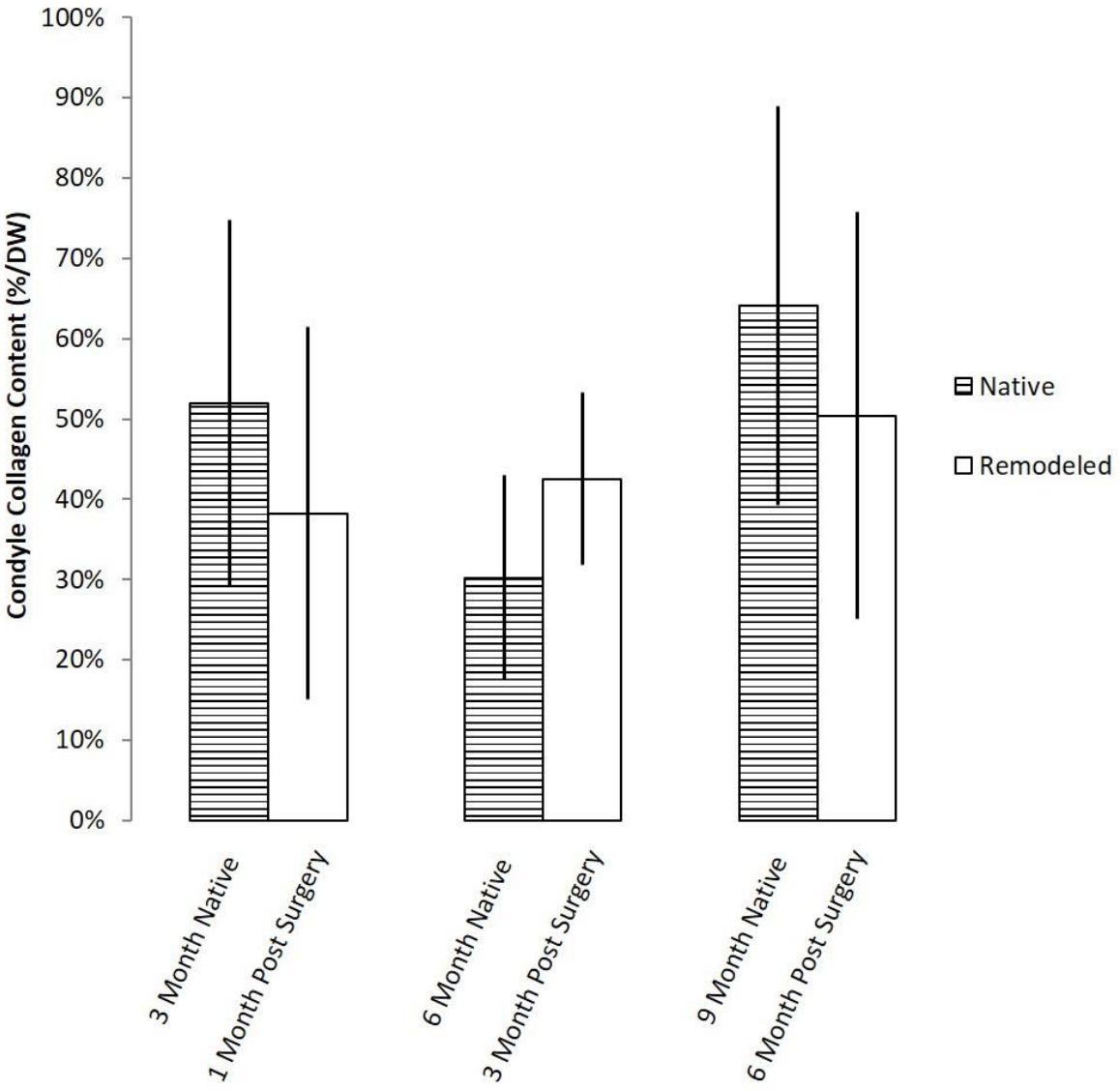

Figure 15. Collagen content for native condyles (n = 10 per group) and treated condyles (n = 13 for 1 month post-surgery, n = 10 for 3 month post-surgery, and n = 8 for 6 month post-surgery). All error bars represent standard deviation.

The GAG content of the native discs, remodeled ECM scaffolds, and pre-implantation devices are shown in Figure 16. There were no significant differences ($p < 0.05$) in GAG content (%/DW) between TMJ discs at 1, 3, and 6 months post-surgery (1.39% ± 0.72%, 1.32% ± 0.35%, 1.30% ± 0.70% respectively), and their age-matched controls at 3, 6, and 9 months (1.13% ± 0.34%, 1.47% ± 0.79%, 1.22% ± 0.51% respectively). The preimplantation devices (1.19% ± 0.30%) were not statistically different from any remodeled scaffold group.

The GAG content of the remodeled ECM condyles and native condyles are shown in Figure 17. There were no significant differences ($p < 0.05$) in collagen content (%/DW) between mandibular condyles at 1, 3, and 6 months post-surgery (5.85% ± 3.96%, 3.41% ± 1.72%, and 2.93% ± 1.93%, respectively), and their age-matched controls at 3, 6, and 9 months (6.35% ± 2.78%, 7.41% ± 3.91%, 6.19% ± 2.57% respectively).

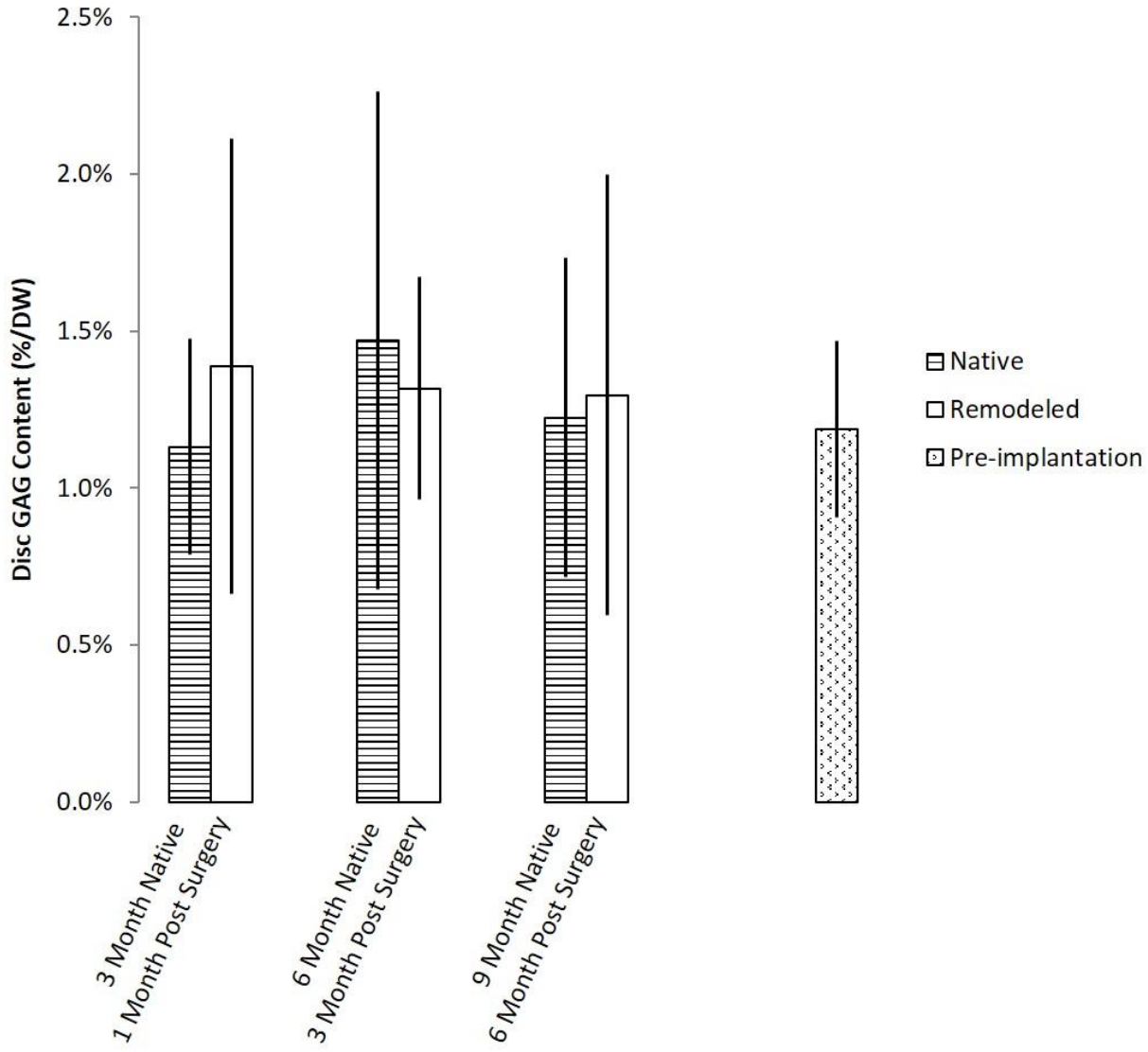

Figure 16. GAG content for native TMJ discs (n = 9 per group), remodeled scaffolds (n = 3 for 1 month post-surgery, n = 4 for 3 and 6 month post-surgery) and pre-implantation ECM scaffolds (n = 9 per group). All error bars represent standard deviation.

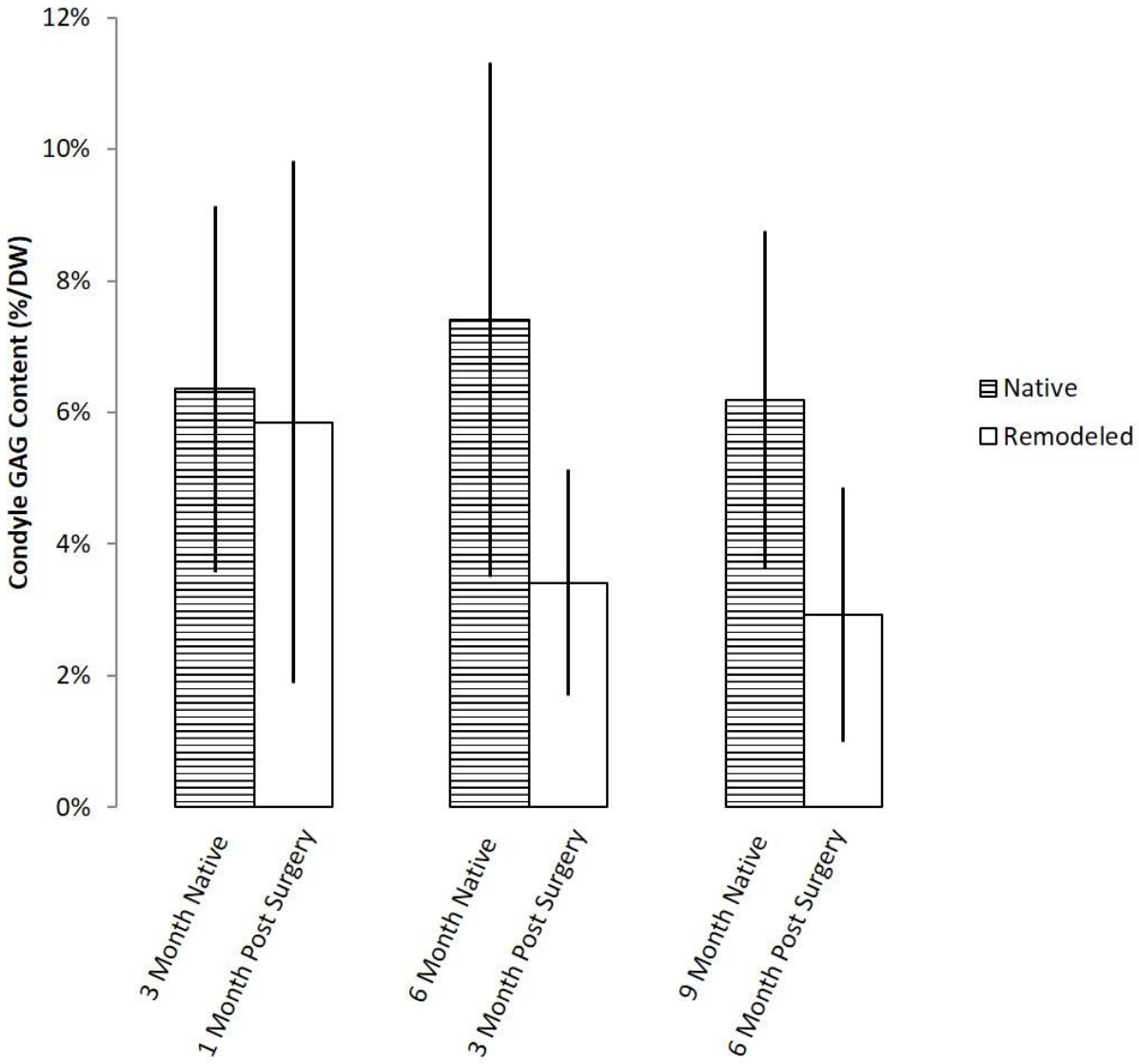

Figure 17. GAG content for native condyles (n = 10 per group) and treated condyles (n = 16 for 1 month post-surgery, n = 11 for 3 month post-surgery, and n = 9 for 6 month post-surgery). All error bars represent standard deviation.

The DNA content of the native discs, remodeled ECM scaffolds, and pre-implantation devices are shown in Figure 18. There were no significant differences ($p < 0.05$) in DNA content (ng/mg) between TMJ discs at 1, 3, and 6 months post-surgery (107 ± 56 ng/mg, 78 ± 43 ng/mg, 78 ± 43 ng/mg respectively), and their age-matched controls at 3, 6, and 9 months (99 ± 19 ng/mg, 51 ± 21 ng/mg, 57 ± 18 ng/mg respectively). The preimplantation devices (112 ± 17 ng/mg) were not statistically different from any remodeled scaffold group.

The DNA content of the remodeled ECM condyles and native condyles are shown in Figure 19. There was a significant difference ($p < 0.05$) in DNA content (ng/mg) between mandibular condyles at 1 month post-surgery (146 ± 63 ng/mg), and their age-matched controls at 3 months (329 ± 112 ng/mg). There were no significant differences ($p < 0.05$) in DNA content (ng/mg) between mandibular condyles at 3 and 6 months post-surgery (130 ± 54 ng/mg, 101 ± 52 ng/mg, respectively), and their age-matched controls at 6 and 9 months (133 ± 62 ng/mg, 60 ± 27 ng/mg, respectively).

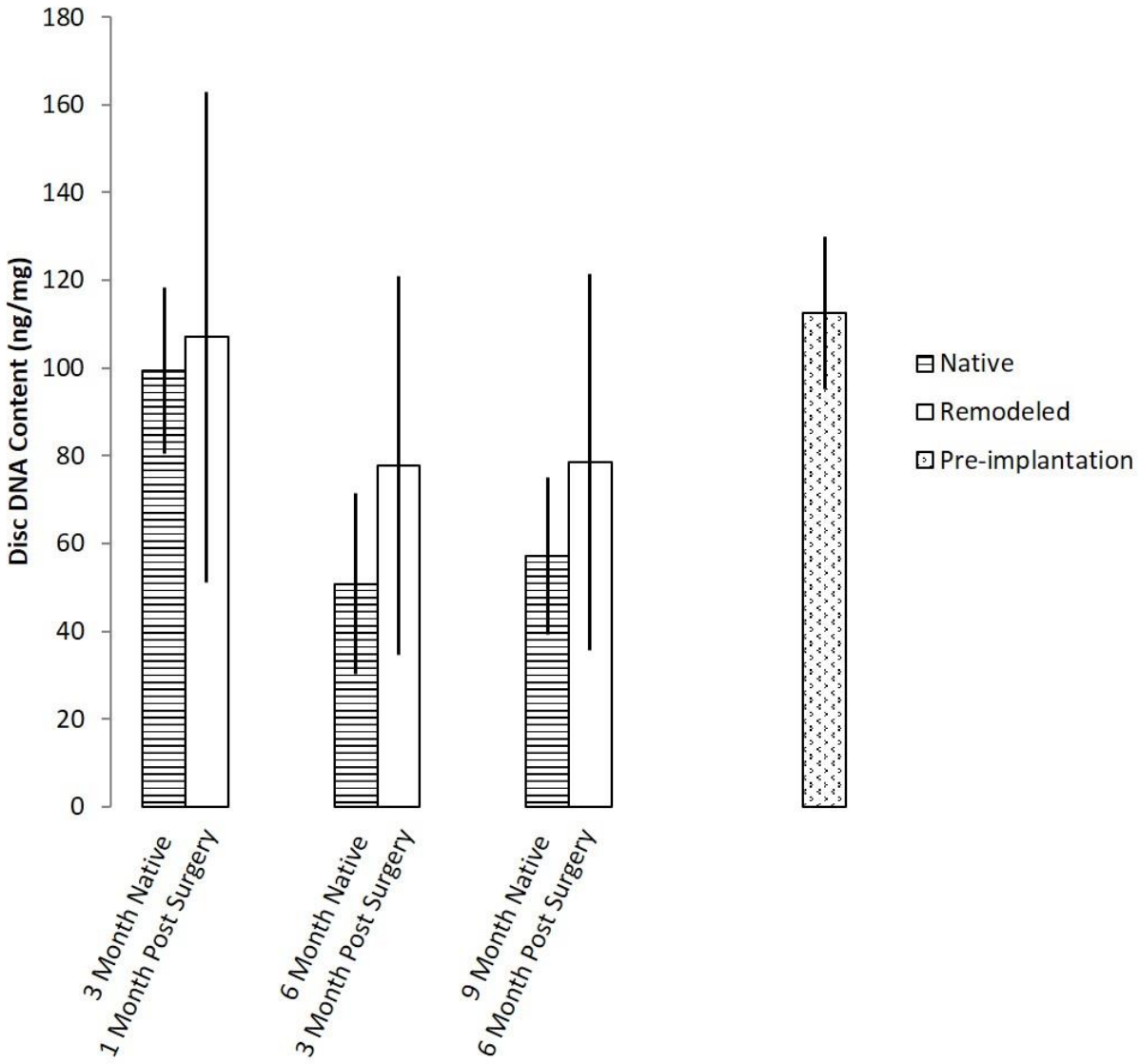

Figure 18. DNA content for native TMJ discs (n = 9 per group), remodeled scaffolds (n = 3 for 1 month post-surgery, n = 4 for 3 and 6 month post-surgery) and pre-implantation ECM scaffolds (n = 9 per group). All error bars represent standard deviation.

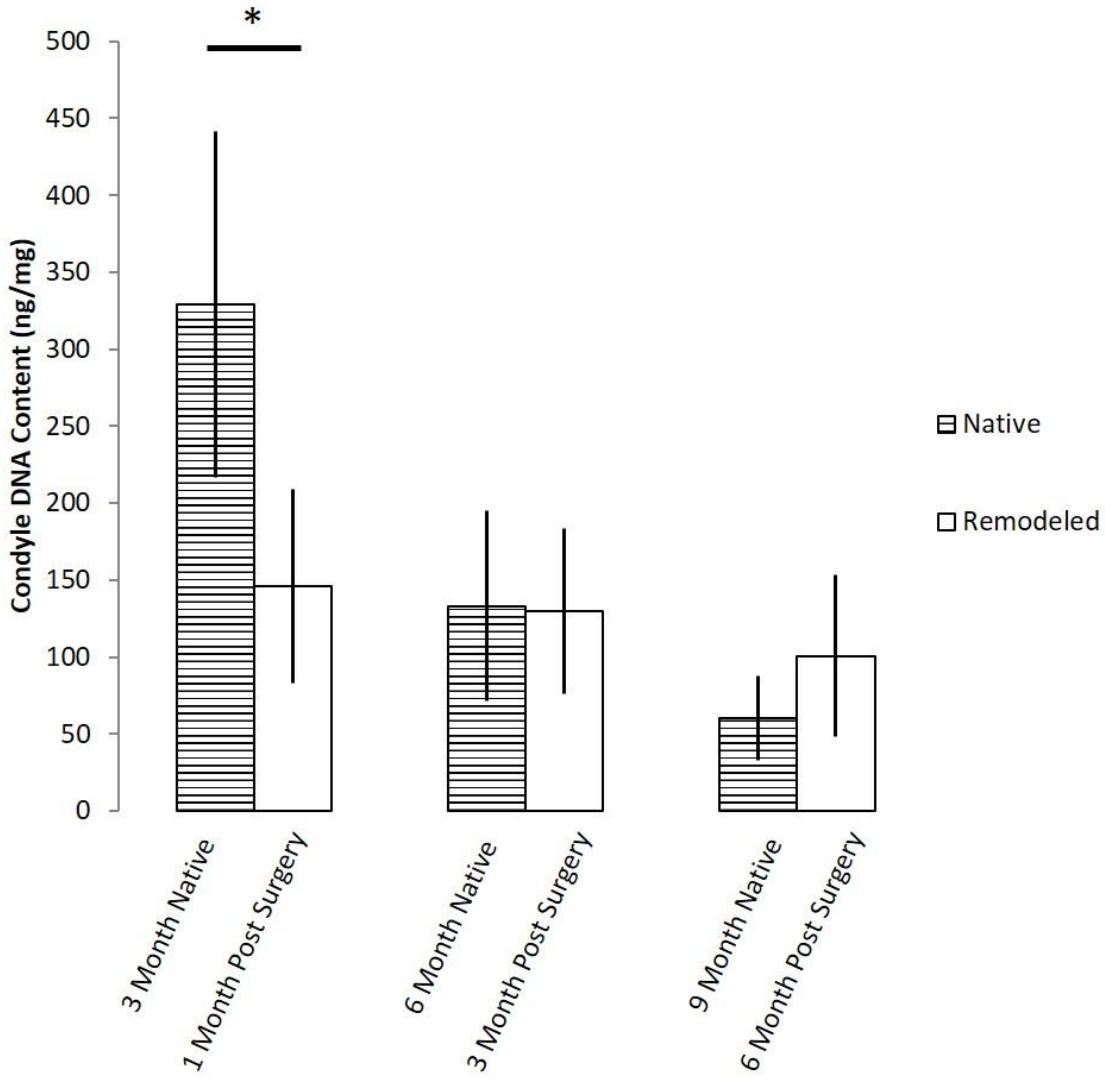

Figure 19. DNA content for native condyles (n = 10 per group) and treated condyles (n = 16 for 1 month post-surgery, n = 11 for 3 month post-surgery, and n = 9 for 6 month post-surgery). All error bars represent standard deviation.

3.3.3 ECM Scaffolds Demonstrate Ability to Remodel Into Viable Scaffold Solution

Comparisons of the tensile peak stress (Figure 20) tensile modulus (Figure 21), and tensile strain (Figure 22) between remodeled scaffolds and native discs at each time point were determined. Ages in this figure are referred to as the age of the pig at sacrifice. At one month post-surgery (4 months of age), there were statistically significant differences between remodeled scaffolds (n = 3) and native (n = 10) in both peak stress (0.64 ± 0.11 MPa and 3.91 ± 1.81 MPa, respectively) and modulus (7.04 ± 2.56 MPa and 28.62 ± 9.16 MPa, respectively), but no statistical differences in strain (19.7% ± 7.7% and 26.2% ± 12.5%, respectively). At 3 months post-surgery (6 months of age), there was no significant difference between remodeled scaffolds (n = 4) and native discs (n = 9) in peak stress (2.73 ± 1.41 MPa and 5.24 ± 1.69 MPa, respectively) or strain (24.8% ± 4.0% and 20.5% ± 4.3%, respectively), but there was a significant difference in modulus (20.04 ± 9.74 MPa and 38.25 ± 10.09 MPa, respectively). There were no significant differences between remodeled scaffolds (n = 4) and native discs (n = 9) at 6 months post-surgery (9 months of age) in stress (1.99 ± 1.66 MPa and 4.57 ± 1.60 MPa, respectively), modulus (15.31 ± 7.60 MPa and 29.84 ± 8.27 MPa, respectively), or strain (23.2% ± 8.3% and 24.2% ± 5.6%, respectively).

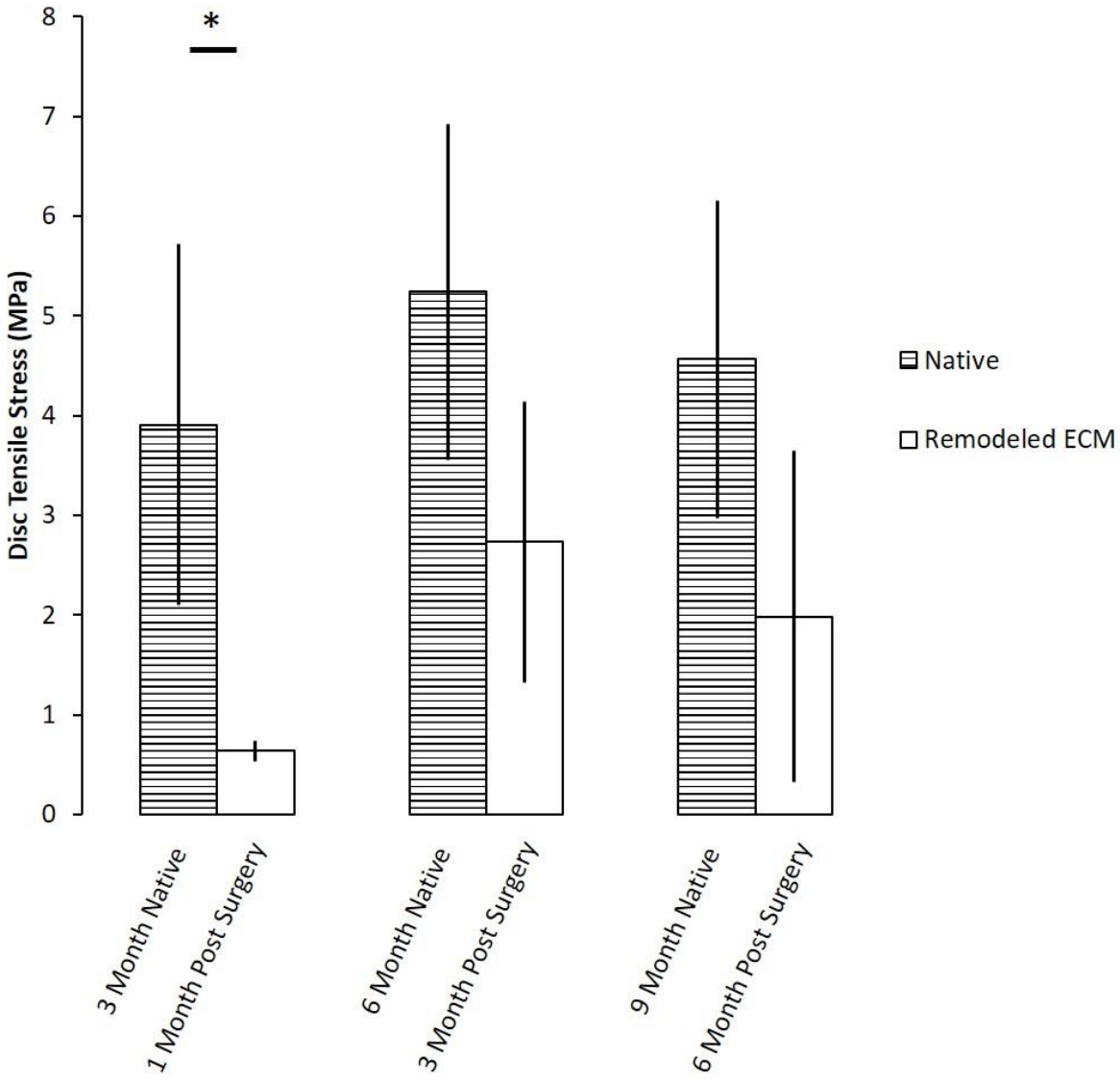

Figure 20. Tensile stress results for the native disc (n = 10) and remodeled scaffolds (n = 3 for 1 month post-surgery, n = 4 for 3 month post-surgery, and n = 3 for 6 month post-surgery). All error bars represent standard deviation.

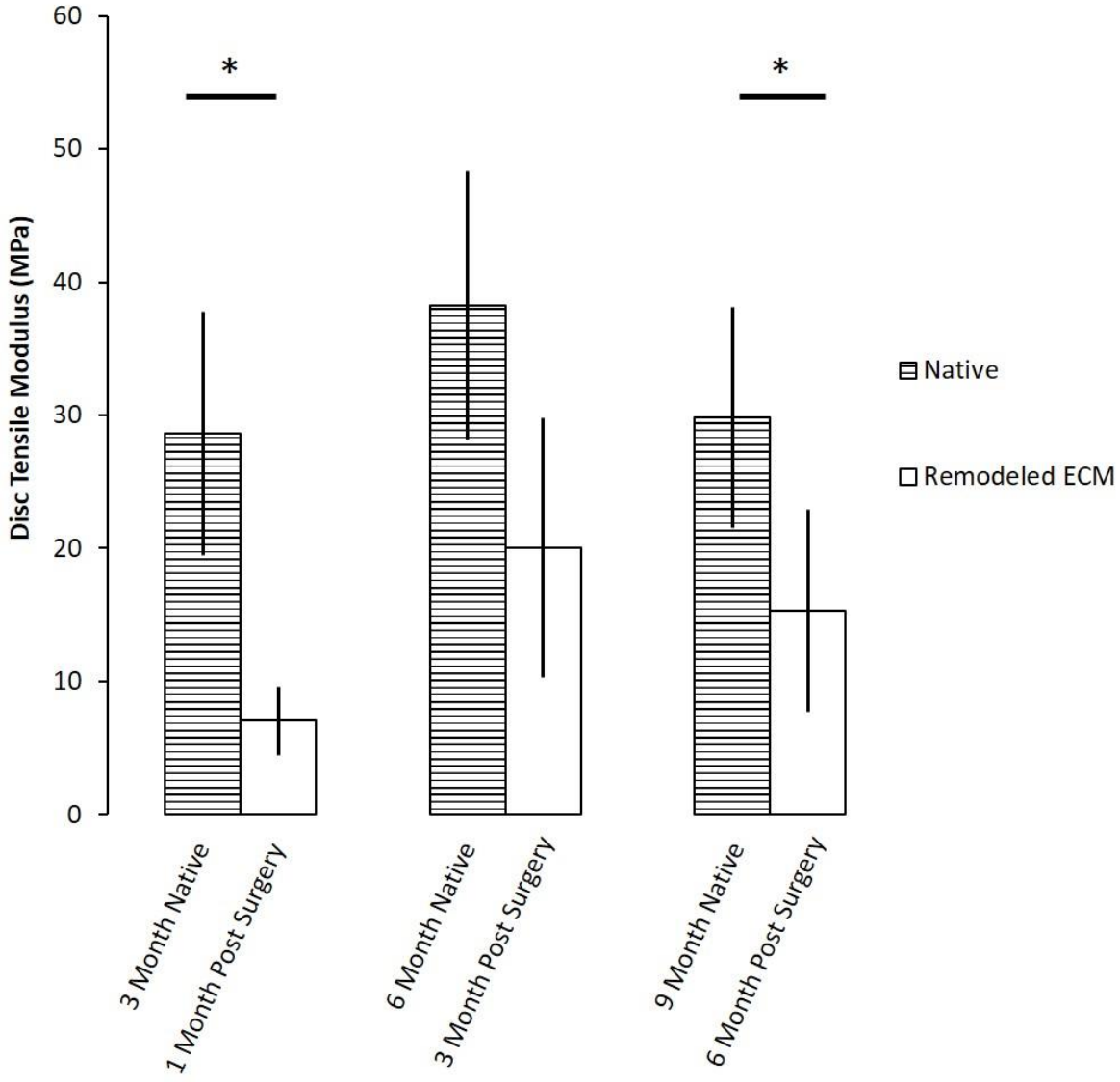

Figure 21 Tensile modulus results for the native disc (n = 10) and remodeled scaffolds (n = 3 for 1 month post-surgery, n = 4 for 3 month post-surgery, and n = 3 for 6 month post-surgery). All error bars represent standard deviation.

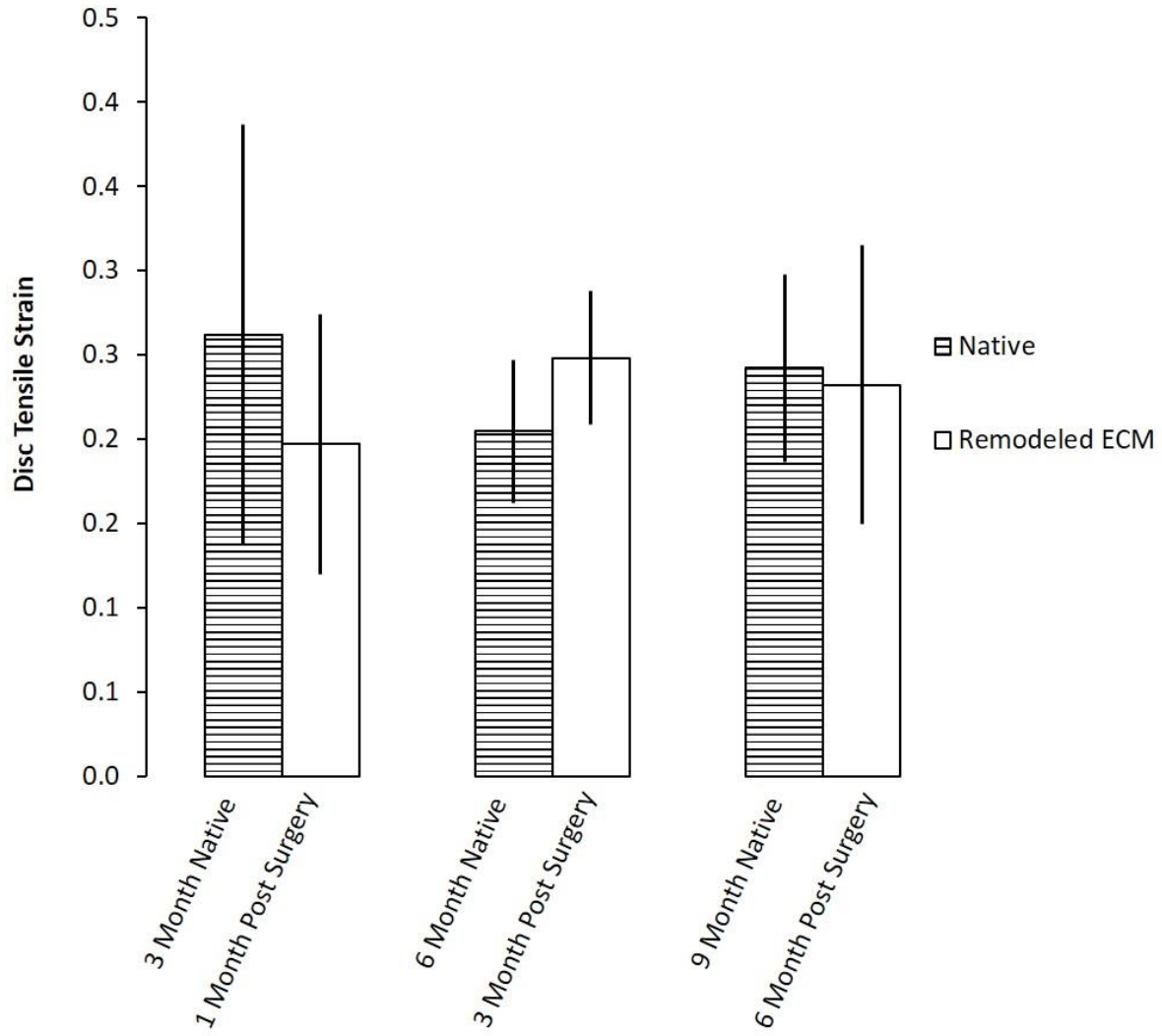

Figure 22. Tensile strain results for the native disc (n = 10) and remodeled scaffolds (n = 3 for 1 month post-surgery, n = 4 for 3 month post-surgery, and n = 3 for 6 month post-surgery). All error bars represent standard deviation.

In compression, the compressive peak stress at 30% strain step (Figure 23) of remodeled scaffolds was 65 ± 50 kPa at 1 month (n=5), 95 ± 39 kPa at 3 months (n=5), and 80 ± 35 kPa at 6 months (n=3) post implantation and was not statistically different ($p > 0.05$) to native (43 ± 35 kPa at 3 month (n=10), 90 ± 22 kPa at 6 months (n=9), and 113 ± 58 kPa at 9 months (n=9)). The compressive modulus at the 30% strain step (Figure 24) of remodeled scaffolds were 710 ± 457 kPa at 1 month, 1108 ± 512 kPa at 3 months, and 893 ± 294 kPa at 6 months post implantation, and were not significantly different ($p < 0.05$) to native (542 ± 430 kPa at 3 month, 1225 ± 261 kPa at 6 months, and 1369 ± 596 kPa at 9 months). It was determined however, that for native samples under peak stress, there were significant differences ($p < 0.05$) between 3 month and 9 month old pigs. 3 month native pigs were also significantly different from 6 month and 9 month pigs in compressive modulus.

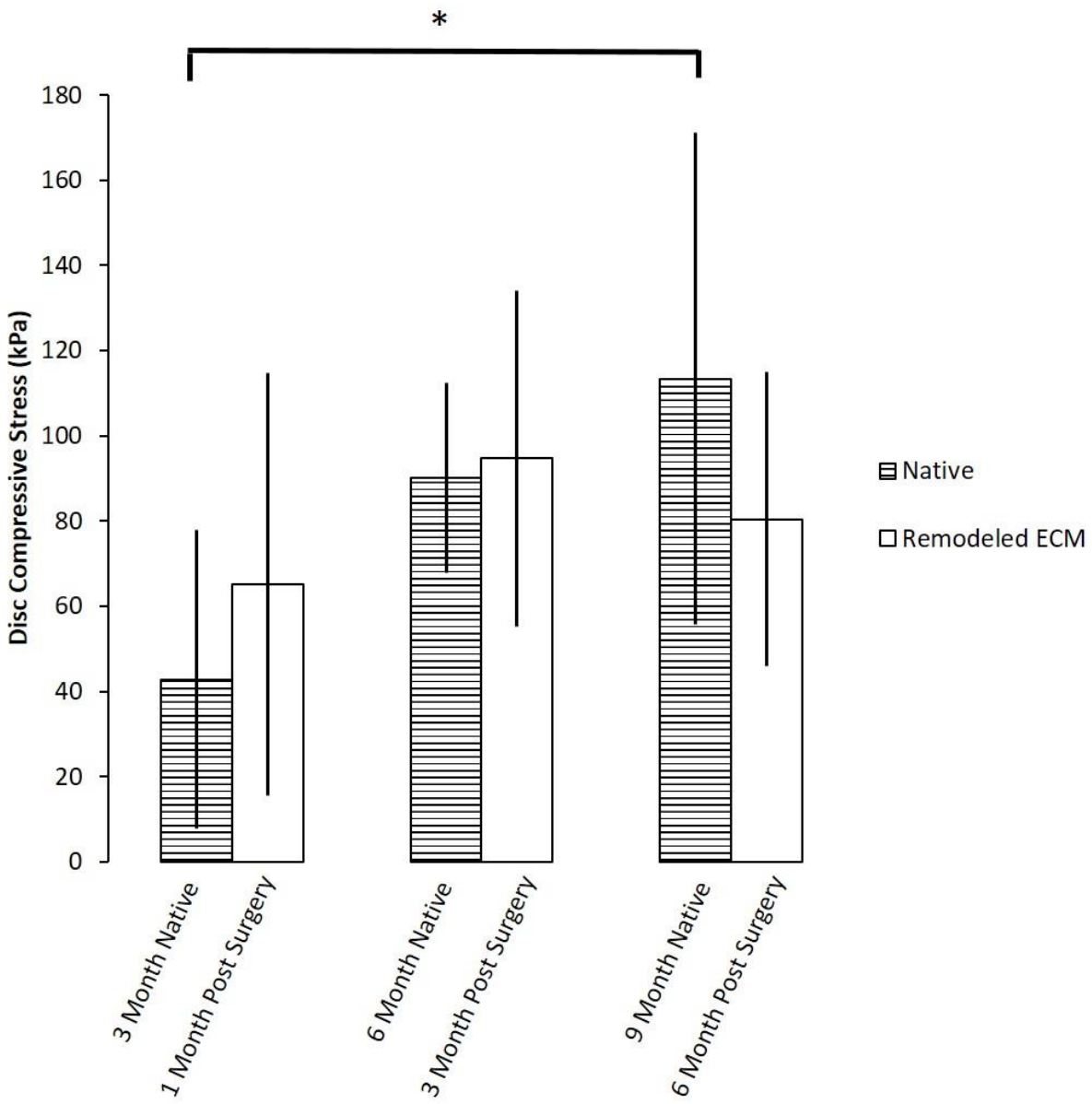

Figure 23. Compressive stress at the 30% strain step results for the native disc (n = 10) and remodeled scaffolds (n = 3 for 1 month post-surgery, n = 4 for 3 month post-surgery, and n = 3 for 6 month post-surgery). All error bars represent standard deviation.

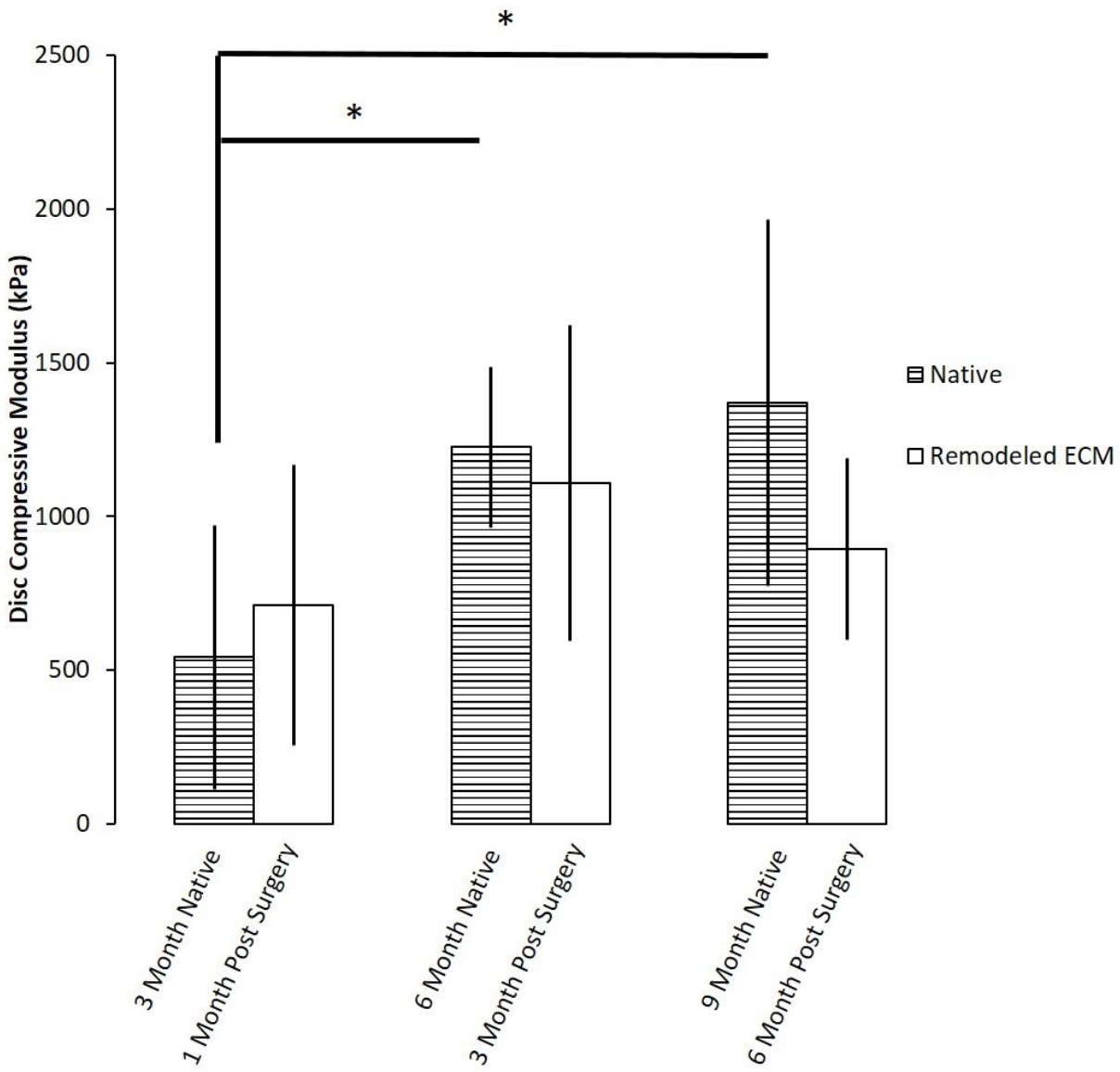

Figure 24. Compressive modulus at the 30% strain step results for the native disc (n = 10) and remodeled scaffolds (n = 3 for 1 month post-surgery, n = 4 for 3 month post-surgery, and n = 3 for 6 month post-surgery). All error bars represent standard deviation.

For the condyles, the compressive properties were determined for both treated condyles, defined as the condyles associated with the joint implanted with an ECM scaffold immediately following discectomy, and contralateral condyles, defined as the condyles on the contralateral side of the head, where no ECM scaffold was implanted following discectomy. The compressive peak stress at the 30% strain step (Figure 25) of the contralateral condylar cartilage at 1 month (29 ± 12 kPa) was statistically different ($p<0.05$) than its age-matched 3 month old control condyle (116 ± 38 kPa), while the treated condyle (42 ± 23 kPa) was not different. The peak stresses of the 3 and 6 month treated (48 ± 19 kPa, 51 ± 9 kPa, respectively) and contralateral (53 ± 35 kPa, 60 ± 36 kPa, respectively) condylar cartilage were no statistically different ($p<0.05$) from their age-matched controls at 6 (67 ± 45 kPa) and 9 (66 ± 44 kPa) months.

The compressive modulus at the 30% strain step (Figure 26) of the contralateral condylar cartilage at 1 month (322 ± 108 kPa) was statistically different ($p<0.05$) than its age-matched 3 month old control condyle (1076 ± 369 kPa), while the treated condyle (451 ± 204 kPa) was not different. The peak stresses of the 3 and 6 month treated (604 ± 511 kPa, 682 ± 142 kPa, respectively) and contralateral (611 ± 411 kPa, 682 ± 394 kPa, respectively) condylar cartilage were no statistically different ($p<0.05$) from their age-matched controls at 6 (689 ± 472 kPa) and 9 (674 ± 437 kPa) months

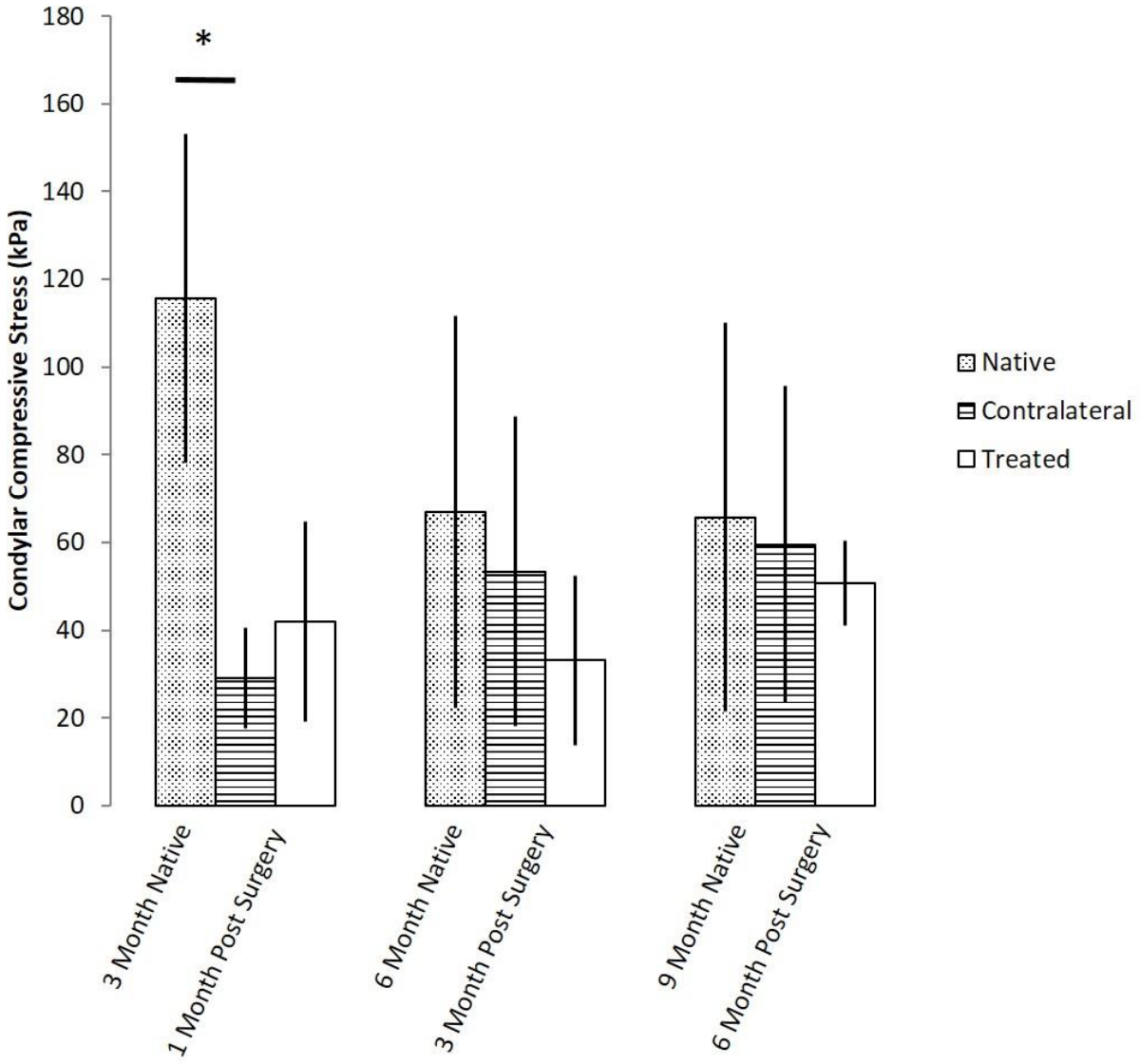

Figure 25. Compressive modulus at the 30% strain step results for the native disc (n = 10), contralateral condyles (n = 9 for one month post-surgery, n = 10 for 3 month post-surgery, and n = 6 for 6 month post-surgery), and treated condyles (n = 11 for 1 month post-surgery, n = 5 for 3 month post-surgery, and n = 4 for 6 month post-surgery). All error bars represent standard deviation.

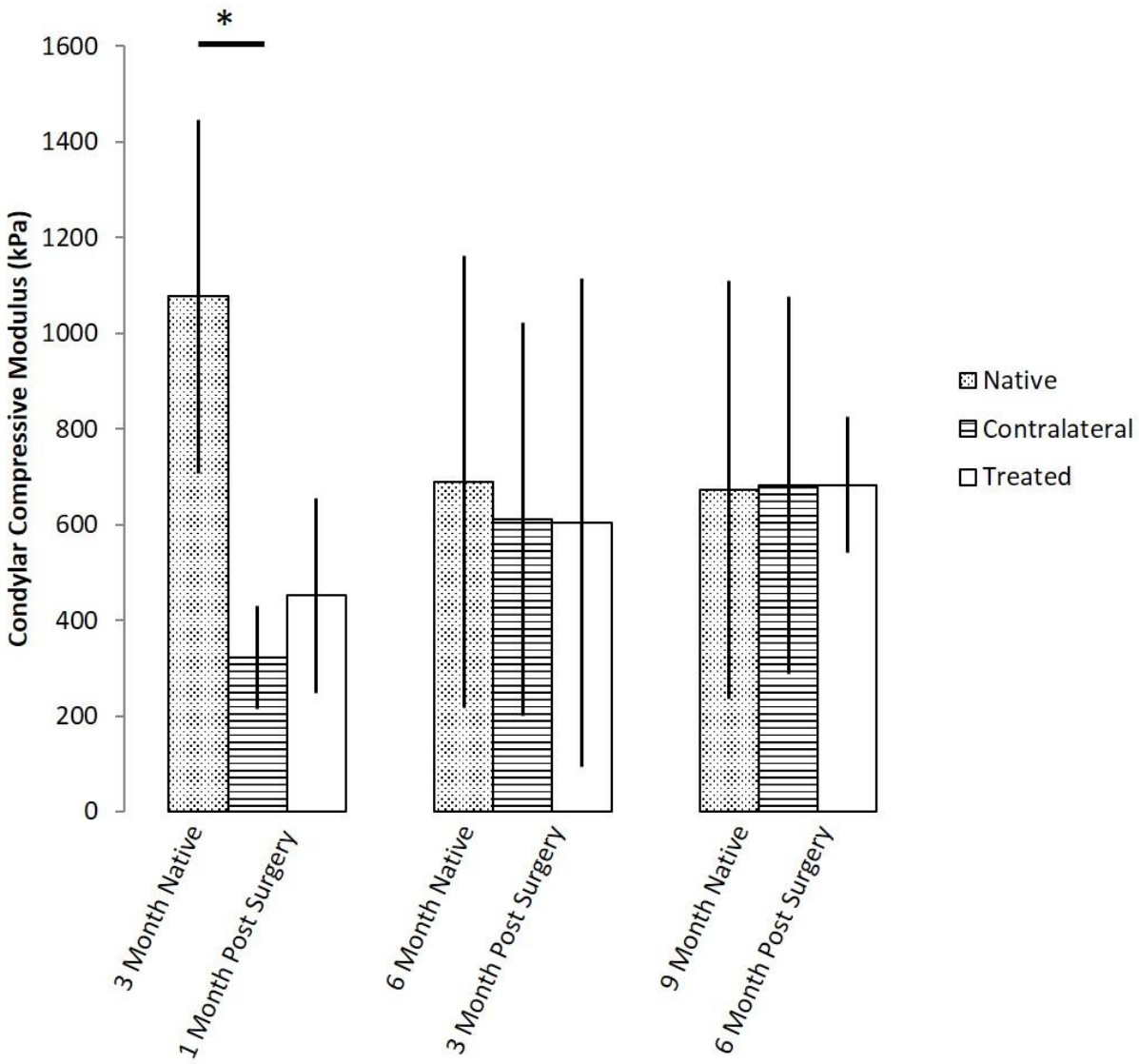

Figure 26. Compressive modulus at the 30% strain step results for the native disc (n = 10), contralateral condyles (n = 9 for one month post-surgery, n = 10 for 3 month post-surgery, and n = 6 for 6 month post-surgery), and treated condyles (n = 11 for 1 month post-surgery, n = 5 for 3 month post-surgery, and n = 4 for 6 month post-surgery). All error bars represent standard deviation.

3.4 DISCUSSION

The results suggest that the ECM scaffold represents a site appropriate graft replacement as soon as 3 months following implantation in a porcine model. Biochemically, the remodeled ECM scaffolds are not statistically different from native discs in GAG or DNA content as soon as 1 month post implantation, and are not different in collagen content by 3 months. Biomechanically, the remodeled ECM scaffolds have achieved at least 50% of the native disc tensile and compressive stress and modulus by 3 months. In gross morphology, the tissues resemble host native tissue as early as 1 month post implantation.

The results also suggest that implantation of an ECM scaffold does not adversely affect condyle remodeling in comparison to an empty contralateral control. While the treated condyles did show significantly decreased compressive stress and modulus at 1 month post implantation when compared to control native condyles where a disc is present, the biomechanical function of the condyles were returned and not different from native by 3 months post-implantation. Also, since the treated condyles were not different from empty contralateral controls, while the ECM scaffold may not prevent initial remodeling, it at least does not inflict negative tissue remodeling beyond what would be expected without a graft replacement. Also, the treated condyle's recapitulation of native compressive properties by 3 months suggests that there were no long term degenerative effects to the condylar cartilage as a result of implantation of ECM scaffolds in the TMJ.

The utilization of the novel tensile protocol developed and introduced in chapter 2 led to more consistent results in this study. Whereas the peak stresses observed from using multiple samples per disc were on par with previously reported values in chapter 2, the standard

deviations reported for native discs in this study for tensile stress (46% for 3 month native, 32% for 6 month native, and 35% for 9 month native) and tensile modulus (32% for 3 month native, 26% for 6 month native, and 28% for 9 month native) were all less than previously reported values (47% for tensile stress, 43% for tensile modulus)(Kalpakci et al., 2011b). This reduction in deviation is attributed to the novel protocol's ability to capture and account for the heterogeneity of collagen organization in the TMJ disc by creating average values over multiple samples throughout the architecture of the intermediate zone of an individual disc.

The differences observed between the native values reported in chapter 2 and in the present study attest could come from a variety of sources of error. For tension, the lack of precision in determining the sample width and thickness can lead to calculation error. Also, the precision of the cryotome to cut even sections of each disc is assumed. In calculating stress, a rectangular shape is assumed for simplification, when the actual shape of the samples is a dogbone. In compression, the native values obtained in chapter 2 only vary from those presented here for 3 month native condyles. Possible sources of error for this discrepancy include differences in age between the two groups of native pigs investigated for each study. If the pigs obtained from the abattoir are several weeks off from each other, this could play a significant role in the potential mechanical properties due to early development of the pigs skeletal and muscular systems. It is also possible that one group of 3 month pigs were stored in a -80 °C freezer for longer than the other group, and the resulting differences in compressive stress and modulus are a result of these altered conditions.

The low percentage of ECM remodeling success is attributed to difficulties in securing the ECM scaffolds into the joint during the surgical procedures because of the presence of the zygomatic arch shielding the TMJ in the porcine anatomy, not from the failure of the ECM to

remodel. Preliminary results of new surgical ECM implantation methods for future in vivo studies has yielded significantly higher success rates in ECM remodeling. This, coincided with the lack of any change to the ECM scaffold itself, suggests that the surgical procedure inhibited ECM remodeling.

There have only been two previous in vivo studies investigating a potential tissue engineering treatment for a damaged TMJ disc(Ahtiainen et al., 2013; Wu et al., 2014). In a study performed by Wu et al, TMJ derived stem cells were seeded on a fibrin scaffold, and were applied to the TMJ disc after perforation for 1 month in a murine model. While the treatment showed positive integration with the surrounding tissue in histology, the discs were not quantified biomechanically or biochemically. Also, this treatment was performed in nude mice, which has many differences to the human TMJ. A limitation of the approach is that it was performed in a perforation model and not to replace the whole disc, which is the clinical standard. In the second study performed by Ahtiainen et al, autologous adipose stem cell (ASC) seeded in polylactic acid (PLA) scaffolds were implanted in a rabbit model following bilateral discectomy for 6 and 12 months. While the PLA scaffold did not cause irritation and allowed normal regeneration of adjacent tissue in the joint, difficulties with the surgical procedure led to the scaffolds being displaced in the joint, causing chronic arthrosis. The resulting remodeled scaffolds were not biochemically or biomechanically characterized either.

In comparison to in vitro tissue engineered studies trying to recapitulate near-native properties, these current results in vivo with ECM scaffolds compare well. MacBarb et al. in 2013 obtained the highest in vitro biomechanical results for a tissue engineered scaffold, with a compressive modulus of 900 kPa at 20% strain at a strain rate of 1% s^{-1}, and in tension with an ultimate tensile strength of 2.3 MPa, and a tensile modulus of 3.4 MPa(MacBarb et al., 2013b).

Our scaffolds achieved lower values of 353 kPa in compressive modulus at 20% strain and 10% min^{-1}, similar 2.0 MPa in ultimate tensile strength, and a higher tensile modulus of 15.3 MPa. The lower compressive values can be attributed to the viscoelastic nature of this tissue and the slower strain rate in this study. Our mechanical results do compare favorably to previously reported TMJ disc native properties of 453 kPa compressive modulus at 20% strain and the same strain rate, 4.3 MPa ultimate tensile strength, and 23.0 MPa tensile modulus(Kalpakci et al., 2011b). Biochemically, our study has reported the highest collagen content currently measured (19%/WW), with the next closest obtained by Johns and Athanasiou in vitro (14%/WW)(Johns and Athanasiou, 2008). Most in vitro studies have also reported GAG contents an order of magnitude higher than the present study. The lowest reported GAG content was 11%/WW, in the study with the highest mechanical properties(Kalpakci et al., 2011a). Again, our biochemical content more closely resembles native, with previously reported values of 27.6%/WW collagen content, and 0.4% GAG/WW(Kalpakci et al., 2011b).

The results presented in this chapter suggest the efficacy of SIS-ECM scaffolds as a long term tissue engineered graft replacement for the TMJ disc following discectomy. As a result, this promising technology should be further explored, and the mechanism of remodeling should be investigated.

4.0 MACROPHAGE RESPONSE TO MECHANICAL STIMULATION AND ECM IN VITRO

4.1 INTRODUCTION

The use of extracellular matrix (ECM) as a scaffold material for in vivo regenerative medicine repair has been studied for a variety of outcomes, ranging from unsatisfactory to satisfactory(Aurora et al., 2015; Sicari et al., 2014b; Turner et al., 2012; Turner et al., 2010; Valentin et al., 2010; Wolf et al., 2015). In terms of the TMJ, as stated before, there have been several studies validating the efficacy of ECM as an inductive template for regenerative medicine therapies in a canine model, but in these models the mechanism for regeneration is poorly understood. It has been suggested that the successful remodeling of the extracellular matrix scaffolds could be attributed to macrophage byproducts of digesting the ECM scaffold (Brown and Badylak, 2013; Gordon and Taylor, 2005; Mantovani et al., 2004; Valentin et al., 2009; Valentin et al., 2010).

Macrophages are a form of white blood cell that exist in all tissues, and can become polarized in response to their surroundings. The two predominant polarizations are M1 macrophages, which encourage inflammation, and M2, which decreases inflammation and encourages tissue repair. Correlation of macrophage polarization with recovery of tissues has been reported in several tissues and organs, and represents a potential area of investigation for

wound healing and tissue repair. The macrophage response is highly regulated, with uncontrolled inflammation proving to be a detrimental process, whereas a controlled and regulated inflammatory response can be a key factor in tissue remodeling following injury.

In skeletal muscle wound repair, the macrophage response has been highly characterized. The capacity for tissue regeneration is highly dependent on the interaction between satellite and inflammatory cells in the wound response (Mauro, 1961; Muir et al., 1965). Following the initial injury, neutrophils will infiltrate the wound site as soon as 2 hours post injury. These neutrophils will reach their maximum numbers between 6 and 24 hours post surgery (Bondesen et al., 2006; Contreras-Shannon et al., 2007; Tidball and Villalta, 2010). The neutrophils that have been recruited will release reactive oxygen species and T-helper 1 cytokines, which serve to recruit monocytes and macrophages. By 3-4 days post injury, the neutrophil response has dissipated, and macrophages become the dominant tissue remodeling participant in the wound (Tidball and Villalta, 2010).

The monocytes that have been recruited by the neutrophils originate in the bone marrow and migrate to the injured tissue site when they differentiate into macrophages (Swirski et al., 2009; Tidball, 2005). Once recruited and differentiated, the macrophages are generally polarized to the M1, pro-inflammatory phenotype through exposure to pro-inflammatory cytokines such as IFN-γ (McLennan, 1996; St Pierre and Tidball, 1994; Tidball, 2005; Tidball and Villalta, 2010). M1 macrophages reach their maximum numbers after 2 days, where they begin showing a transition to the M2 immunoregulatory and anti-inflammatory M2 phenotype (Tidball, 2005). This paradigm shift is not fully understood but has been correlated to increased IL-10 concentrations at 48 hours post-injury, M1 macrphage mediated phagocytosis of apoptotic cells, and exposure of M1 macrophages to the degradation products of ECM (Cohen and Mosser,

2013; Fadok et al., 1998; Liu et al., 2010; Sicari et al., 2014a). Once polarized to the M2 phenotype, macrophages release anti-inflammatory cytokines that promote tissue remodeling and repair (Gordon, 2003; Gordon and Martinez, 2010; Tidball, 2005). The pro-inflammatory products of the M1 population are used to recruit and activate satellite muscle cells within the injury site (Collins and Grounds, 2001; Tidball, 2005; Villalta et al., 2009; Zador et al., 2001). These cells are then aligned, fused, and differentiated in the wound site by paracrine signals from the M2 macrophage population that results after the paradigm shift from M1 to M2.

It has been shown that the delay or elongation of the timeline of neutrophil and macrophage infiltration, polarization, or transition has a significant effect on a tissue's ability to functionally remodel. For example, when macrophages are depleted prior to a toxin induced injury, regeneration and the removal of cellular debris is impaired(Arnold et al., 2007). Depletion of macrophages at the time of injury also restricts tissue regeneration by preventing the M1 response, which in turn prevents recruitment of satellite cells(Arnold et al., 2007; Teixeira et al., 2003). Furthermore, TNF-α knockout animals, a product of M1 macrophages, produce significantly less muscle specific transcription factors, which suggests that TNF-α is necessary for promoting early or proliferative myogenesis (Chen et al., 2005; Warren et al., 2002). When macrophages were removed from the injury site at 2 days, the time period when they would transition to the M2 phenotype, tissue regeneration was impaired (Tidball and Wehling-Henricks, 2007).

A similar response to the skeletal muscle injury response described above can be seen in cutaneous wound healing, as well as healing in the central nervous system (CNS). In both situations, neutrophils immediately infiltrate the wound and recruit macrophages, which start as M1 macrophages before transitioning into a M2 phenotype and inducing tissue regeneration. In

the cutaneous example, however, there is also a granulation tissue formation and wound contraction phase at 7-10 days post injury. In this phase, M2 macrophages release anti-inflammatory and pro-angiogenic factors, which facilitate myofibroblast differentiation and being the deposition of new ECM (Hinz et al., 2012; Sindrilaru and Scharffetter-Kochanek, 2013; Stout, 2010). In the CNS example, the general wound response is more complex due to the presence of the blood-brain barrier. In the early stages of wound healing, microglia, instead of neutrophils, are first recruited to the wound site and create a dense barrier around the lesion (Davalos et al., 2005; Hines et al., 2009). This is followed by the standard neutrophil and monocyte recruitment.

Typically, upon implantation of a foreign body, macrophages will follow a series of stages including injury, protein adsorption, acute inflammation, chronic inflammation, foreign-body reaction, and finally encapsulation(Anderson, 1988; Anderson et al., 2008). Because of this foreign body response (FBR), the tissue engineering field focused on materials that are inert of biocompatible (Brown and Badylak, 2013; Ratner, 2011; Williams, 2008). However, these materials only tend to provide mechanical substitution to the tissue being replaced, and not a full functional remodeled tissue. As a result, the use of bioactive materials such as ECM as inductive templates for tissue regeneration has become prominent. However, due to the strong M1 response to a cellular ECM tissue, these tissues require decellularization treatment prior to implantation.

The macrophage response to a surgical implant is dependent on whether the scaffold implanted is synthetic or biologic. For synthetic materials, strategies to alter the surface chemistry and structural characteristics of the synthetic surface have been examined to better modulate macrophage response and reduce the opportunities for FBRs. One example of this is

the tuning of material pore size. It was found that pore sizes of roughly 30-40 μm produced reduced encapsulation related to FBR and higher vascularity when implanted in cardiac and dermis tissues (Madden et al., 2010; Mills et al., 1992). It has also been observed that in porous synthetic materials, there seems to be a local distribution in macrophage phenotype, with M2 populations on exterior surface of the material and pores, and M1 macrophages distributed throughout the inner porous structure of the scaffold (Sussman et al., 2014). Synthetic materials also utilize growth factors and cytokines to chemically condition the scaffold for improved tissue remodeling (Mokarram et al., 2012).

Researchers are also investigating the macrophage response to biological scaffold materials as well. These materials maintain their natural ligand landscape, which can add complexity to the macrophage host response. It has been shown that their ability to modulate the host macrophage response promotes constructive remodeling (Badylak, 2014; Badylak et al., 2008; Brown et al., 2012c; Brown et al., 2009). It has been shown that ECM based scaffolds facilitate a transition from M1 to M2 phenotype around 7-14 days post implantation(Badylak et al., 2008; Brown et al., 2012c; Brown et al., 2009). As discussed in the previous chapter, these ECM materials have bioactive degradation products that promote tissue remodeling. It has been shown that these byproducts are necessary for the transition to an M2 phenotype. Solubilized ECM has been shown to transition M1 macrophages into a more M2 phenotype, which reduce FBR and encapsulation responses (Wolf et al., 2014). This modulation leads to the ability of ECM to constructively remodel in vivo.

While the success of ECM in the canine TMJ, and as described in Chapter 3, would suggest that these scaffolds follow the general pathway of modulation from M1 phenotypic macrophages to M2 macrophages, it has not been confirmed. Also, the TMJ is constantly

experiencing mechanical forces, both compression and tension, as the TMJ disc articulates between the condyle and fossa. It has been shown previously that mechanical stimulation effects TMJ disc cells in biochemical production, and it has been shown to accelerate proliferation and alter macrophages to a pro-remodeling M2 phenotype in vitro(Almarza and Athanasiou, 2006a; Pongkitwitoon et al., 2016).

In this study, we will be investigating the effect of both mechanical stimulation and the presence of ECM on mouse bone marrow macrophages in vitro. Since tensile forces in the TMJ are an order of magnitude higher in the TMJ than compression forces, tensile mechanical stimulation will be the force investigated. Macrophages will be seeded onto flexible membranes with extracellular matrix and tested in a tension FlexCell mechanical stimulation apparatus to 5% strain at 1 Hz, analyzed for M1 or M2 phenotype by analyzing genes associated with both, and compared against various control groups.

4.2 MATERIALS AND METHODS

4.2.1 Cell Isolation

Male 4 month old mice were euthanized by rapid cervical dislocation, and a shallow incision was made on the hind leg. The distal head of the femur and tibia were then exposed by hip dislocation, and any excess tissue was removed with a scalpel. The bones were then placed in a 50 mL tube in an ice bucket. 50 mL of macrophage complete media (4 mL L929 media (80% DMEM high glucose, 20% FBS, cultured at confluence with L929 cells for 2 weeks and then collected), 40.3 mL Dulbecco's modified eagle media (DMEM) high glucose media, 4 mL fetal

bovine serum (FBS), 0.4 mL HEPES, 0.4 mL Penicillin/Streptomycin, 0.8 mL non-essential amino acids (NEAA), 60 µL β-mercaptoethanol) was placed in a sterile dish, and 5 separate 10 mL syringes were filled with this media with a 30-gauge needle. The long bones were then carefully severed at each end, and a syringe was inserted into the bone marrow cavity of each femur or tibia. The bone cavity was then flushed with media until the bone appeared white, collecting the bone marrow into a sterile 50 mL tube. This process was repeated for all bones.

The 50 mL tube was then spun at 15 RPM for 5 minutes. After centrifuging, the supernatant was aspirated, and the pellet was resuspended in 10 mL of macrophage complete media. The total number of cells were then counted using a hemacytometer. The macrophages were then pipetted equally into 6 well plates and allowed 2 weeks to culture at 37 °C.

4.2.2 Plate Assembly

There were 7 experimental groups for this study to determine the effect of mechanical stimulation (D = dynamic, S = static), and the presence of ECM (E = ECM, N = no ECM). The 4 experimental groups tested were a group that was not mechanically loaded with no ECM (SN), one group that tested the effect of mechanical stimulation only (DN), one group that tested the effect of ECM only (SE), and a final group that tested the effect of mechanical stimulation and the effect of ECM (DE). All groups used 6 well plates with a flexible membrane fit for use in a FlexCell tensile system. ECM was adhered to the flexible membrane using a non-reactive cyanoacrylate adhesive.

These experimental groups were compared against 3 separate control groups of MO phenotype macrophages seeded onto a hard plastic 6 well plate. 2 of the control groups included

a group of MO macrophages pushed towards an M1 phenotype with 20 ng/mL IFN-y and 100 ng/mL LPS in macrophage media, and a group of MO macrophages pushed towards M2 phenotype with 20 ng/mL IL-4 in macrophage media.

After 2 weeks of culture, the macrophages were passaged and counted using a hemacytometer. MØ macrophages were then seeded at 500,000 cells per well into each of the 6 well plates. Due to constraints on the number of cells obtained from the mouse, only 5 wells were used for each experimental plate (n = 5 per experimental group) and 4 wells were used for each control plate (n = 4 per control group). Macrophages were allowed to sit overnight to adhere to the flexible membrane.

4.2.3 Mechanical Loading Regimen

After the cells were allowed to adhere to the plate overnight, the two mechanical loading experimental groups (DN and DE) had plastic platens placed beneath the flexible membrane, leaving the ECM ends overlapping in the DE group (Figure X). The plates and platens were then placed in between two plastic covers to seal and create a vacuum in the 6 well plate, and placed back in the incubator. Hoses were hooked to both sides of the plate, and a pressure sensor was attached to measure the psi applied to the plates. The hoses were attached to a FlexCell system adapted to apply a tensile pressure. With this system, 5% strain at 1 Hz was applied to the mechanically loaded tissue culture plates for 4 hours. The non-mechanically loaded plates were also placed in the incubator to experience the same environmental conditions. After 4 hours of mechanical stimulation, the plates were removed from the apparatus and allowed to sit in the incubator for 24 hours. Concurrently, the control, SN, and SE groups were placed in the incubator but were unloaded during the 4 hours of mechanical stimulation.

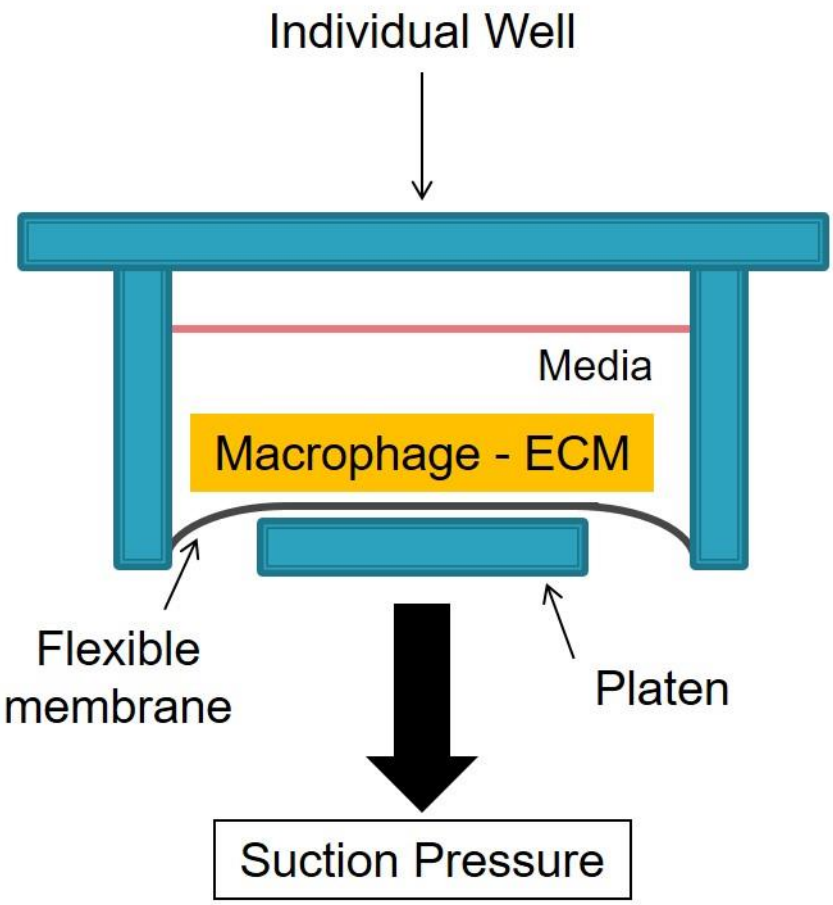

Figure 27. Graphical representation of the DE experimental group in the FlexCell apparatus.

4.2.4 Gene Expression

24 hours after experimental treatment was applied, the macrophages from each group were digested in 1 mL of Trizol for 30 minutes. Cellular material was lifted from the flexible membrane using a cell scraper, and placed in a 1.5 mL tube on ice. 200 mL chloroform per mL of Trizol was added to each tube, and shook vigorously for 15 seconds. The tubes were then placed in a refrigerated centrifuge at 9000 g for 15 min at 4 °C. Following centrifugation, the tubes were carefully placed on ice, and the clear supernatant was collected and placed in a new, sterile tube. 70% ethanol was then added to each tube so that the ratio of supernatant to ethanol was 1:1.

Macrophage RNA was then isolated using the Qiagen RNeasy RNA isolation kit and protocol. RNA isolation was quantified using spectroscopy, with a range of 50 ng/µL – 5 ng/µL RNA depending on the sample. Prior to converting the RNA to cDNA, the RNA values were normalized to the lowest RNA total to ensure that each cDNA had the same amount of template. The RNA was then converted to cDNA using the Thermo Scientific cDNA synthesis kit, and placed in the -80 °C freezer for long term storage.

For the determination of gene expression, 7 genes were analyzed. GAPDH was used as a housekeeping gene, iNOS, TNFα, and IL-6 were used as M1 macrophage phenotype markers, and Arginase, Fizz1, and IL-10 were used as M2 macrophage phenotype markers. The forward and reverse primers used can be seen in Table 8.

Table 8. Gene sequences for housekeeping (GAPDH), M1 macrophage phenotype (iNOS, TNFα, IL-6), and M2 macrophage phenotype (Arginase, Fizz1, IL-10) genes.

Gene	*Sequence*
GAPDH Forward	5’ – AGGTCGGTGTGAACGGATTTG – 3’
GADPH Reverse	5’ – TGTAGACCATGTAGTTGAGGTCA – 3’
iNOS Forward	5’ – CAGGGAGAACAGTACATGAACAC – 3’
iNOS Reverse	5’ – TTGGATACACTGCTACAGGGA – 3’
TNFα Forward	5’ – AGGAGGAGTCTGCGAAGAAGA – 3’
TNFα Reverse	5’ – GGCAGTGGACCATCTAACTCG – 3’
IL-6 Forward	5’ – CCCCAATTTCCAATGCTCTCC – 3’
IL-6 Reverse	5’ – CGCACTAGGTTTGCCGAGTA – 3’
Arginase Forward	5’ – CTCCAAGCCAAAGTCCTTAGAG – 3’
Arginase Reverse	5’ – AGGAGCTGTCATTAGGGACATC – 3’
Fizz1 Forward	5’ – GACTGCTACTGGGTGTGCTT – 3’
Fizz1 Reverse	5’ – GCTGGGTTCTCCACCTCTTC – 3’
IL-10 Forward	5’ – CCCTGGGTGAGAAGCTGAAG – 3’
IL-10 Reverse	*5’ – GCTCCACTGCCTTGCTCTTA – 3’*

For real time polymerase chain reactions (RT-PCR), the Thermo Scientific Maxima SYBR Green/ROX qPCR kit was used. Briefly, a master mix was made for a total of 20 µL per well in a 96 well plate. This master mix was composed of 0.5 µM forward primer, 0.5 µM reverse primer, 12.5 mL SYBR Green/ROX qPCR Master Mix (2X), and water to 20 µL. 20 µL was pipetted in triplicate into a 96 well plate for each experimental group. One gene was analyzed per plate. A StepOne system was used to run and analyze the RT-PCR. A three step cycling protocol was used. First, an uracil-DNA glycosylase (UDG) pre-treatment was performed for 2 minutes at 50 °C. This was followed by an initial denaturation for 10 minutes at 95 °C. Finally, 40 cycles of a 15 s denaturation step at 95 °C, 30 s annealing step 60 °C, and 30 s extension step at 72 °C were performed.

4.2.5 Statistical Analysis

All statistical analysis was performed using SPSS statistical analysis software. To determine statistical differences between groups, normally distributed ΔCt data was compared using a one-way independent ANOVA and Tukey's post hoc analysis with an alpha value of 0.05. Error bars were determined using the 95% confidence interval from bootstrapping and T statistics since the fold change data is not normally distributed.

4.3 RESULTS

4.3.1 Gene Expression

Upon isolation of RNA, total RNA content obtained from the SE group was too low for analysis, requiring the removal of the SE experimental group from the data. The control MO, M1, and M2 macrophages produced approximately 180 ng/µL RNA, while the DN and SN experimental groups produced approximately 30 ng/µL RNA and the DE experimental group produced approximately 10 ng/µL RNA. All RNA was diluted to the lowest DE experimental replicate's RNA concentration to standardize the template cDNA produced.

All gene expression data was normalized to GAPDH and MO macrophage expression for each gene. Each experimental group were compared to M1 and M2 macrophage control groups. The DE experimental group was excluded from the iNOS, Il-6, and Fizz1 gene expression results due to a lack of gene expression amplification.

For the pro inflammatory expression (Figures 28-30), the M1 macrophages expressed a iNOS-/TNFα-/IL-6+ phenotype, inconsistent with the expected expression profile. M2 macrophages expressed an iNOS-/TNFα-/IL-6+ phenotype as well, however the IL-6 expression was significantly lower than that of the M1 macrophages. The SN and DN macrophages both expressed an iNOS-/TNFα-/IL-6+ phenotype that was not significantly different from M0 or M2 macrophage phenotype, suggesting that mechanical stimulation does not cause differences in pro inflammatory gene expression independently. The DE macrophages expressed a TNFα- profile that was not significantly different from any group.

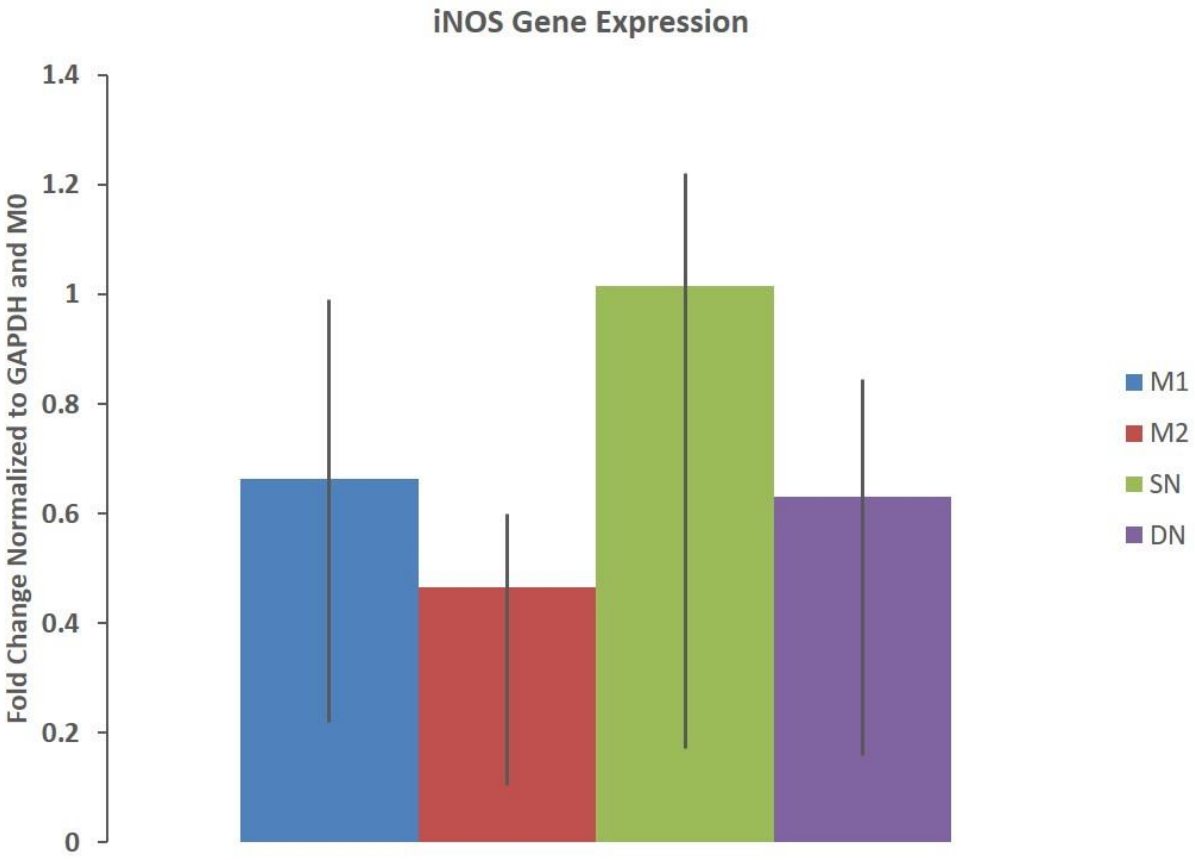

Figure 28. iNOS fold change normalized to GAPDH and MO macrophage gene expression. No differences were observed between groups. Error bars represent 95% confidence interval.

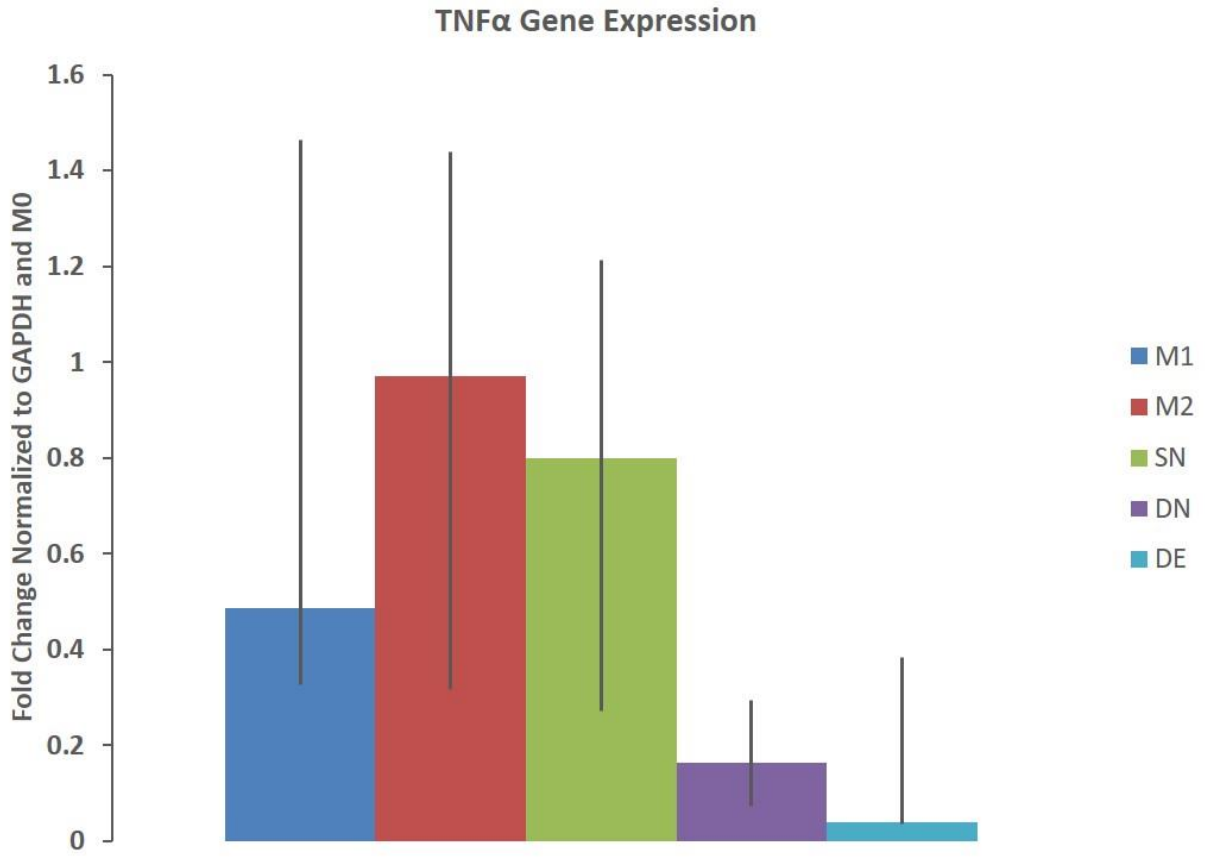

Figure 29. TNFα fold change normalized to GAPDH and MO macrophage gene expression. No differences were observed between groups. Error bars represent 95% confidence interval.

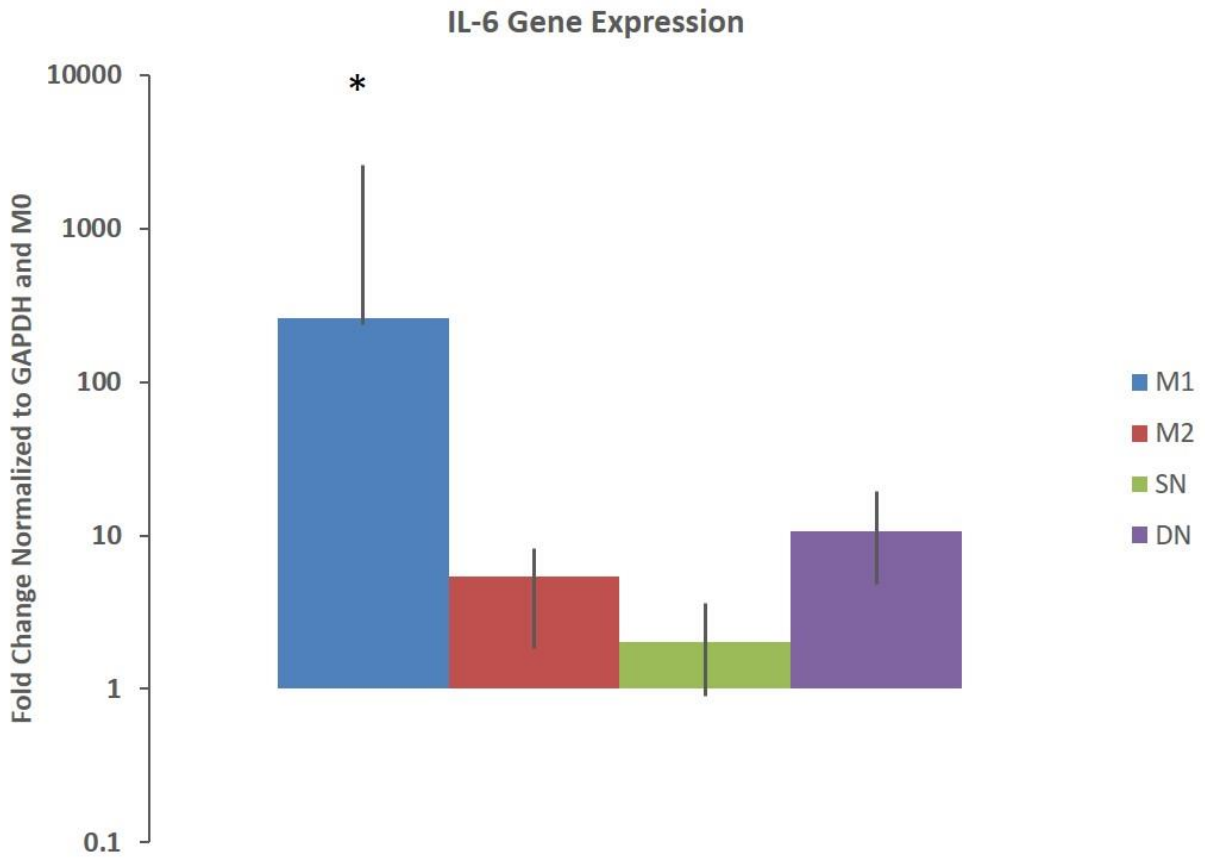

Figure 30. IL-6 fold change normalized to GAPDH and MO macrophage gene expression. M1 control macrophages were significantly higher than all other groups. Error bars represent 95% confidence interval.

For the anti-inflammatory gene expression (Figures 30-32), the M1 macrophages expressed an Arginase+/Fizz+/IL-10- phenotype, however the Fizz1 expression was significantly lower than that of the M2 macrophages. M2 macrophages expressed an Arginase+/Fizz+/IL-10+ phenotype, consistent with the expected expression. This was consistent with the expected expression. The SN macrophages expressed an Arginase+/Fizz+/IL-10+ phenotype, while the DN macrophages expressed an Arginase+/Fizz-/IL-10+. There were no statistical differences in ΔCt values for any gene, however, again suggesting that mechanical stimulation does not cause differences in pro inflammatory gene expression independently. The DE macrophages expressed an Arginase+/ IL-10- phenotype, with Arginase expression significantly higher than the SN and DN experimental groups, while IL-10 expression was significantly lower, suggesting that ECM has a gene-specific pro-inflammatory and anti-inflammatory response.

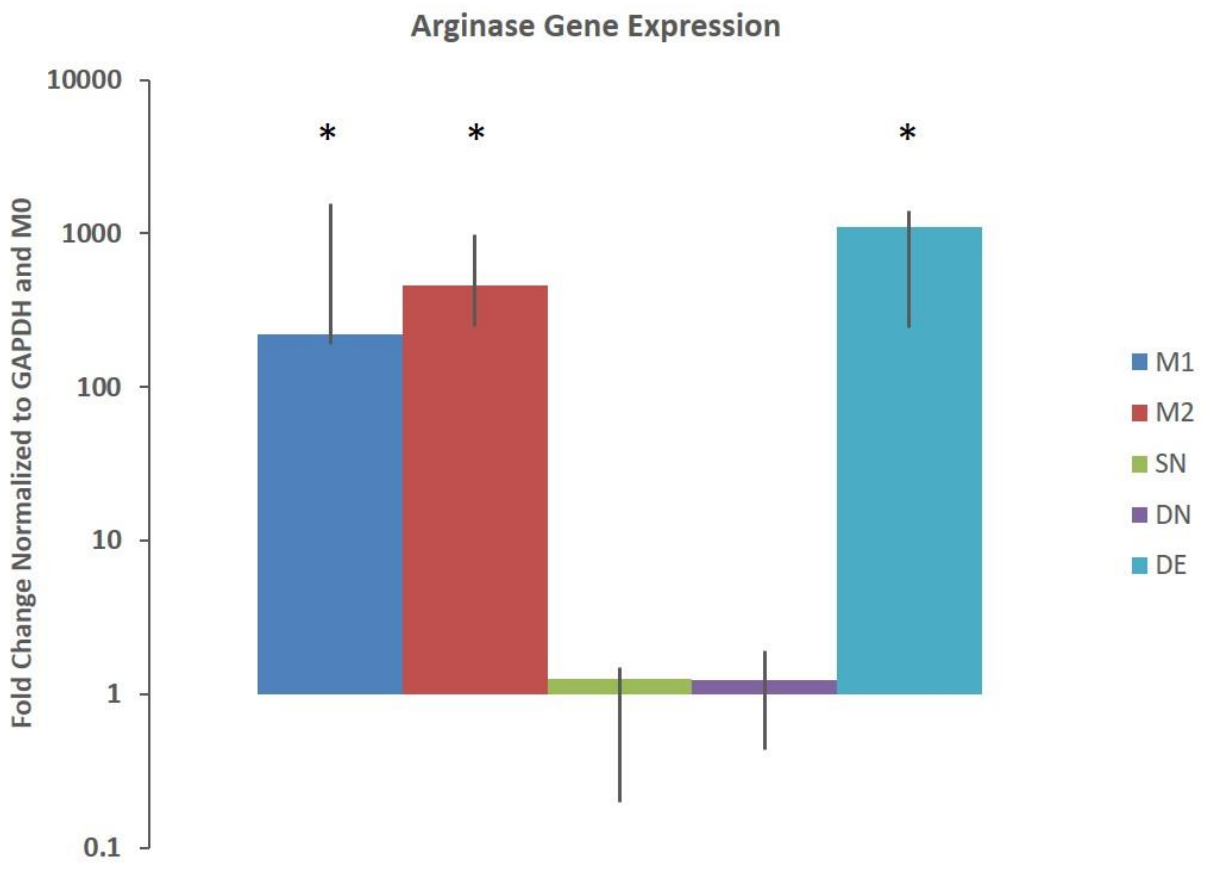

Figure 31. Arginase fold change normalized to GAPDH and MO macrophage gene expression. M1, M2, and DE macrophages were significantly different from the SN and DN experimental groups. Error bars represent 95% confidence interval.

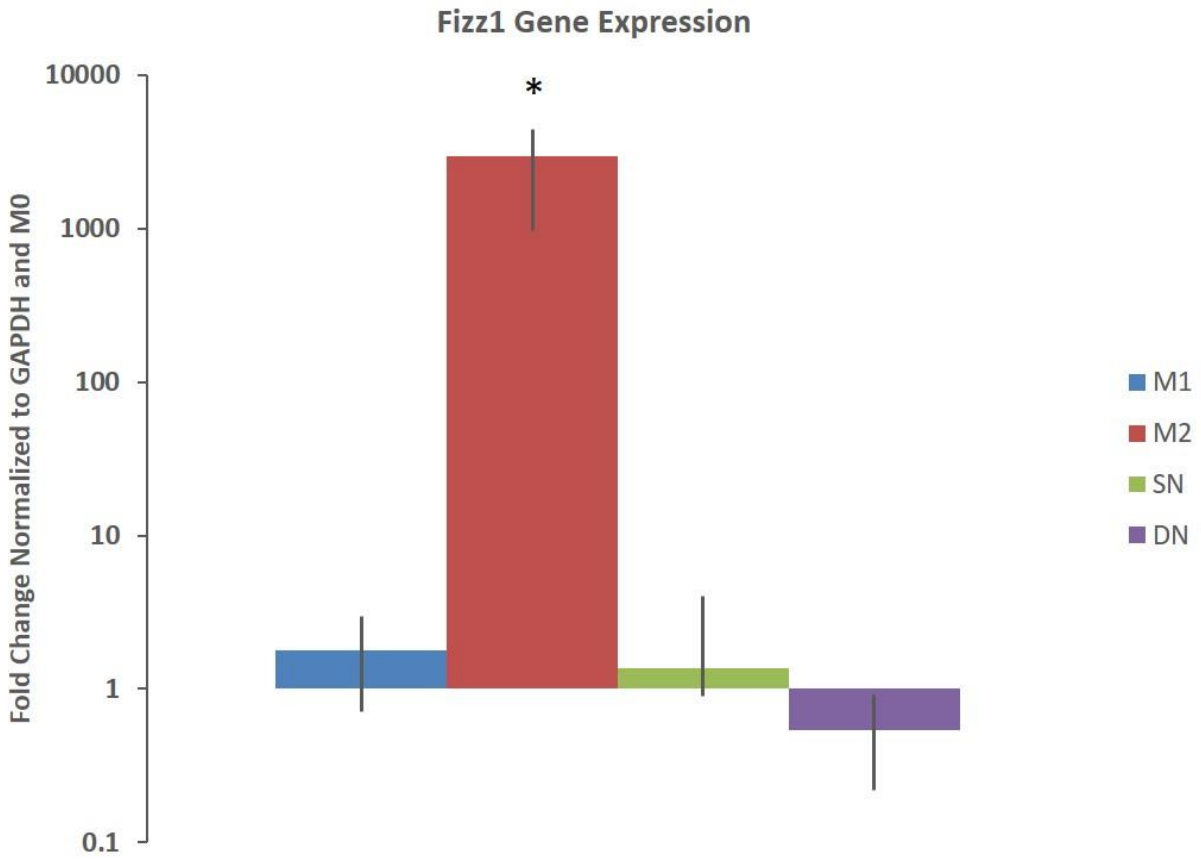

Figure 32. Fizz1 fold change normalized to GAPDH and MO macrophage gene expression. M2 macrophages were significantly different from all other groups. Error bars represent 95% confidence interval.

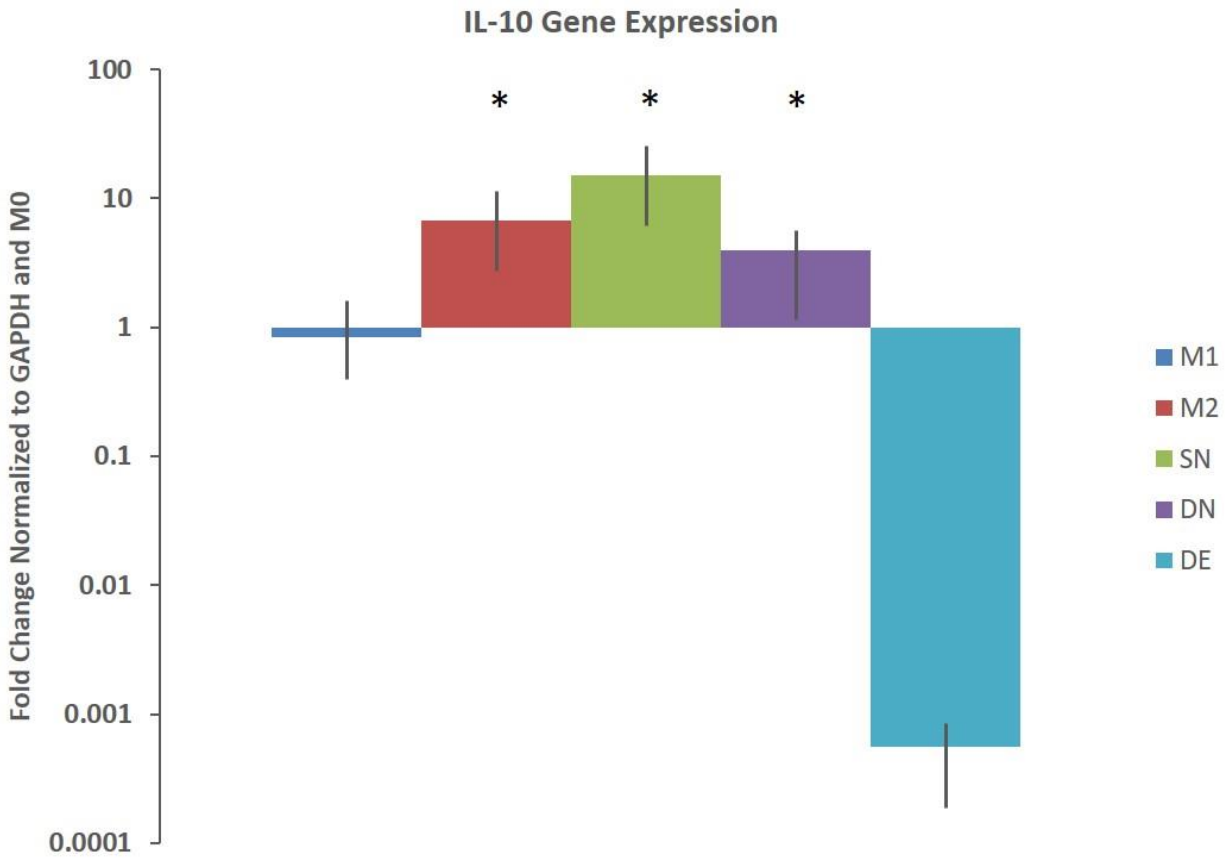

Figure 33. IL-10 fold change normalized to GAPDH and MO macrophage gene expression. M2, SN, and DN macrophages were significantly higher than all M1 and DE macrophages. Error bars represent 95% confidence interval.

4.4 DISCUSSION

The purpose of this pilot study was to elucidate the effect of mechanical stimulation and ECM on macrophage phenotype to investigate a possible explanation for early ECM remodeling in vivo. From the results, no differences were seen in phenotype between macrophages without ECM that were mechanically stimulated or not. Mechanical stimulation only caused significant differentiation from an MO phenotype for the IL-10 gene as well, suggesting that mechanical stimulation at the amplitude and duration in this pilot study do not generally cause any M1 or M2 gene expression. Although the ECM and mechanically stimulated macrophages of the DE group only had detectable amplification for 3 of the analyzed genes, the fold changes obtained for anti-inflammatory Fizz1 were significantly higher than MO macrophages, while also expressing a TNFα-/IL10- profile suggests that the combination of ECM and mechanical stimulation leads to a more M2-comparable phenotype.

There were noticeable difficulties with obtaining RNA during this pilot study. Macrophages attached to the hard plastic 6 well plates produced significantly more RNA than macrophages seeded at the same cell density on the experimental flexible membrane flat plates. This is despite macrophages on both the flexible membrane and plastic 6 well plates appearing at 100% confluency by the time of isolation. This implies that the RNA isolation procedure for the flexible membrane plates needs refinement, and that the use of cell scrapers and Trizol alone are not sufficient. It is also possible that the experimental conditions are leading to cell death, reducing the total amount of RNA upon isolation. Furthermore, experimental groups with ECM strips produced the least RNA of any group, with the SE group producing no RNA for any

experimental replicate, despite no cells observed embedded upon the ECM under microscopic magnification. If the ECM were to be digested to capture any RNA from macrophages that adhered, it was thought that residual RNA from the ECM decellularization process would interfere and mask the RNA of the macrophages, since the RNA concentrations from the macrophages were low already.

It was expected that the M1 control group, consisting of MO macrophages exposed to TNFy and LPS, would display significantly higher fold changes in pro-inflammatory M1 markers iNOS, TNFα, and IL-6 than MO macrophages or M2 macrophages. This was not observed during experimentation, with IL-6 being the only gene that showed significantly higher M1 control group expression. The M2 control group, consisting of MO macrophages exposed to IL-4, performed closer to expectations, with significant increases in anti-inflammatory M2 markers Arginase, Fizz1, and IL-10 expression over MO and M1 macrophages. This suggests that the gene expression profiles of the experimental groups are more reliable for the M2 genes, since these were confirmed with the control groups. It is possible that the primer sequences in Table 2 were not optimal for the cell line, and new primers should be obtained and tested to see if the primer sequences were the cause of the M1 control group's gene expression response.

Mechanical stimulation's lack of impact on the macrophages in the SN and DN groups was surprising, as it has been shown previously that mechanical stimulation can cause modulation of macrophages to an M2 phenotype(Ballotta et al., 2014; Pongkitwitoon et al., 2016). While the study by Pongkitwitoon et al. did not perform tensile mechanical stimulation, Ballotta et al used a FlexCell tensile system as well and saw decreases in M1 macrophage phenotypic genes as well as increased IL-10 expression. However, this study applied higher strains (7% and 12%) at 0.8 Hz continuously for 7 days. The decreases in anti-inflammatory M1

marker expression occurred in day 2 as well, suggesting that the current pilot study may not have extended long enough to observe changes in macrophage phenotype away from an MO phenotype. Also, the study performed by Ballotta et al. analyzed macrophages seeded on a poly-ε-caprolactone bisurea scaffold. In this pilot study, for the limited data of macrophages seeded with ECM, their expression profiles more closely match those of an M2 phenotype. Therefore, the presence of a scaffold may be integral for the modulation of macrophages to an M2 phenotype.

The results of this pilot study provide limited insight into the potential reasons for ECM scaffold remodeling upon implantation in the TMJ. The lack of major differences between the SN and DN experimental groups suggests that the mechanically loaded nature of the TMJ itself may not be the driving force behind ECM remodeling itself. The limited results from the mechanically loaded ECM macrophage group DE suggest that the interplay between these factors may offer a better explanation for the remodeling behavior. As mentioned before, the duration of the pilot study may be a complication, as it has been shown previously that M1 modulation to M2 in ECM may not occur immediately and therefore may not be detected by the pilot study(Brown et al., 2012d). However, the results suggest expanding this pilot study to a more in depth study may be appropriate.

For future iterations of this experiment, new primers sequences for iNOS and TNFα should be obtained and validated. Also, improved RNA isolation methods should be developed, potentially adding more Trizol, increasing exposure time, or freeze-thawing plates to increase cell rupture for RNA release. Finally, the strain during mechanical stimulation should either be increased in amplitude or duration, or a combination of both, to ensure more dynamic results. With this in mind, the current pilot study provided an important first step into examining the

effect of mechanical stimulation and ECM on macrophage expression, and provides potential insight into modulation of macrophages in the TMJ upon implantation of an ECM scaffold.

5.0 DISCUSSION - CONCLUSIONS

The work set forth in this thesis strongly supports the central hypothesis that an SIS-ECM scaffold will remodel into a TMJ disc analogue in the porcine model in vivo within 6 months of implantation. Once the biochemical and biomechanical properties of the TMJ disc mandibular cartilage were characterized, the remodeled scaffolds were statistically in range with their age-matched controls in every parameter by 3 months post implantation. Additionally, the possible mechanism for this remodeling was investigated by analyzing the gene expression and phenotype of mechanically loaded macrophages and comparing them to control.

Characterization of the biochemical and biomechanical properties of the TMJ disc and mandibular condylar cartilage at 3, 6, and 9 months yielded no differences across age groups (Chapter 2). Histological results, however, did highlight differences in cellularity and general collagen orientation across time points, providing insight into how the ECM constituents of the TMJ disc form over time. Novel tensile protocols developed for the determination of tensile properties throughout the thickness of the TMJ disc also led to decreased variability in tensile modulus, as well as emphasized the heterogeneity of collagen fiber organization in the intermediate zone of the TMJ disc. Also, although the condylar cartilage and TMJ disc were not compared to each other at each time point, distinct differences could be seen in the formation and mechanical properties between the TMJ (fibrocartilage) and condylar cartilage (articular cartilage) at each time point in terms of DNA, collagen, and GAG content, as well as

compressive stress and modulus. This reinforces the idea that distinct tissue engineering methodologies are required for fibrocartilage, as the design parameters differ from hyaline cartilage.

The native properties across age groups could then be used as a benchmark for in vivo tissue engineering studies featuring regenerative medicine therapies at various time points. To investigate the potential for tissue engineered therapies in the TMJ, SIS-ECM scaffolds were implanted in a porcine TMJ following discectomy and allowed to remodel for 1, 3, and 6 months (Chapter 3). At this point, the remodeled scaffolds and corresponding condyles were excised and compared against a new set of native controls following the protocols established in Chapter 2. It was determined that the ECM scaffolds were able to remodel into a tissue resembling the TMJ disc within 1-month post-implantation. Also, by 3 months post implantation, the remodeled scaffolds were not statistically different from native age matched controls in DNA content, collagen content, or GAG content. The mechanical properties of the remodeled scaffold were also at least 50% of native within 3 months. The lack of mechanical properties to reach those of native by 6 months suggest that while the biochemical properties of the remodeled scaffolds might reach those of native, the organization and deposition patterns of the ECM constituents don't recapitulate those of the native tissue. This highlights a potential goal for future experiments, where implanted scaffolds can force collagen fibril organization into a framework similar to native discs. Still, the biochemical and biomechanical properties obtained from remodeled ECM scaffolds proved the hypothesis of this study true, and even exceeded the initial design criteria set forth prior to the experiment.

It is also important to consider the effect of the scaffold on the surrounding articulating tissues of the TMJ, namely the condylar cartilage. The excised condyles were not statistically

different from their native age-matched controls in biochemical content, although there was a trend to lower GAG content overall at each progressive time point. Also, while the treated condyles did show significantly decreased compressive stress and modulus at 1 month post implantation when compared to controls, the biomechanical function of the condyles were returned and not different from native by 3 months post-implantation. This suggests that the remodeling of the condyles would have occurred either way, but discectomy and ECM implantation may have accelerated the process, or that the remodeling observed on the treated condyles was able to repair itself. In either event, the treated condyle's recapitulation of native compressive properties by 3 months suggests that there were no long term degenerative effects to the condylar cartilage as a result of implantation of ECM scaffolds in the TMJ.

Once the ECM scaffolds displayed the ability to successfully remodel in the porcine TMJ, a pilot study was performed to try to elucidate the mechanism of remodeling in the early joint environment. To this end, the effects of mechanical stimulation and ECM on macrophage phenotype modulation were investigated. The amplitude for mechanical stimulation chosen was 5% strain, the frequency was 1 Hz, and the duration was 4 hours. A one-time application of the tensile mechanical stimulation was applied in 2D for gene expression analysis, using genes associated with both a pro-inflammatory (M1) and anti-inflammatory (M2) macrophage phenotype, and experimental groups were compared to MO, M1, and M2 control groups. Difficulties with RNA isolation prevented the elucidation of the effect of ECM alone, but it was determined that mechanical stimulation did not have an effect on overall macrophage phenotype modulation. Mechanical stimulation in combination with ECM did lead to an increased expression of the M2 marker IL-6 without any corresponding fold change increases in M1 markers, suggesting that from the limited results the interplay between mechanical stimulation

and ECM may modulate the seeded MO macrophages to an M2 phenotype. While the data is limited, this loosely confirms the core hypothesis behind this pilot study. Several potential limitations to this pilot, however, necessitate further study before any definitive conclusions could be drawn. Future investigations should consider changes in mechanical stimulation amplitude, duration, RNA isolation techniques, and primer sequences for M1 genes.

The results of this thesis are in accordance with the main stated hypothesis that with the knowledge of the effect of age on native TMJ on native TMJ tissues and establishment of novel protocols and assays, it will be determined that SIS-ECM scaffolds are a viable TMJ disc analogue within 6 months of implantation in vivo. The resulting biochemical and biomechanical properties of the remodeled ECM scaffolds actually indicate viability within 3 months, faster than expected in the hypothesis. These properties also exceed the success of previous tissue engineered devices for the TMJ disc in vitro and in vivo, albeit this is the first porcine in vivo tissue engineering TMJ study. The effect of age on native properties in the growing pig has also been elucidated and explored. Finally, the effects of in vitro mechanical stimulation and ECM on macrophages in the early TMJ environment have been investigated. The success of this study strongly suggests the efficacy of the SIS-ECM scaffold as a potential tissue engineered graft replacement for the damaged TMJ disc.

BIBLIOGRAPHY

Ahtiainen, K., Mauno, J., Ella, V., Hagstrom, J., Lindqvist, C., Miettinen, S., Ylikomi, T., Kellomaki, M., Seppanen, R., 2013. Autologous adipose stem cells and polylactide discs in the replacement of the rabbit temporomandibular joint disc. J R Soc Interface 10, 20130287.

Almarza, A.J., Athanasiou, K.A., 2005. Effects of initial cell seeding density for the tissue engineering of the temporomandibular joint disc. Ann Biomed Eng 33, 943-950.

Almarza, A.J., Athanasiou, K.A., 2006a. Effects of hydrostatic pressure on TMJ disc cells. Tissue Eng 12, 1285-1294.

Almarza, A.J., Athanasiou, K.A., 2006b. Evaluation of three growth factors in combinations of two for temporomandibular joint disc tissue engineering. Arch Oral Biol 51, 215-221.

Almarza, A.J., Bean, A.C., Baggett, L.S., Athanasiou, K.A., 2006. Biochemical analysis of the porcine temporomandibular joint disc. Br J Oral Maxillofac Surg 44, 124-128.

Almarza, A.J., Yang, G., Woo, S.L., Nguyen, T., Abramowitch, S.D., 2008. Positive changes in bone marrow-derived cells in response to culture on an aligned bioscaffold. Tissue Eng Part A 14, 1489-1495.

Alonso, A., Kaimal, S., Look, J., Swift, J., Fricton, J., Myers, S., Kehl, L., 2009. A quantitative evaluation of inflammatory cells in human temporomandibular joint tissues from patients with and without implants. J Oral Maxillofac Surg 67, 788-796.

Anderson, D.E., Athanasiou, K.A., 2008. Passaged goat costal chondrocytes provide a feasible cell source for temporomandibular joint tissue engineering. Ann Biomed Eng 36, 1992-2001.

Anderson, D.E., Athanasiou, K.A., 2009. A comparison of primary and passaged chondrocytes for use in engineering the temporomandibular joint. Arch Oral Biol 54, 138-145.

Anderson, J.M., 1988. Inflammatory response to implants. ASAIO Trans 34, 101-107.

Anderson, J.M., Rodriguez, A., Chang, D.T., 2008. Foreign body reaction to biomaterials. Semin Immunol 20, 86-100.

Androjna, C., Spragg, R.K., Derwin, K.A., 2007. Mechanical conditioning of cell-seeded small intestine submucosa: a potential tissue-engineering strategy for tendon repair. Tissue Eng 13, 233-243.

Arnold, L., Henry, A., Poron, F., Baba-Amer, Y., van Rooijen, N., Plonquet, A., Gherardi, R.K., Chazaud, B., 2007. Inflammatory monocytes recruited after skeletal muscle injury switch into antiinflammatory macrophages to support myogenesis. J Exp Med 204, 1057-1069.

Aurora, A., Roe, J.L., Corona, B.T., Walters, T.J., 2015. An acellular biologic scaffold does not regenerate appreciable de novo muscle tissue in rat models of volumetric muscle loss injury. Biomaterials 67, 393-407.

Badylak, S.F., 2004. Xenogeneic extracellular matrix as a scaffold for tissue reconstruction. Transpl Immunol 12, 367-377.

Badylak, S.F., 2014. Decellularized allogeneic and xenogeneic tissue as a bioscaffold for regenerative medicine: factors that influence the host response. Ann Biomed Eng 42, 1517-1527.

Badylak, S.F., Hoppo, T., Nieponice, A., Gilbert, T.W., Davison, J.M., Jobe, B.A., 2011. Esophageal preservation in five male patients after endoscopic inner-layer circumferential resection in the setting of superficial cancer: a regenerative medicine approach with a biologic scaffold. Tissue Eng Part A 17, 1643-1650.

Badylak, S.F., Valentin, J.E., Ravindra, A.K., McCabe, G.P., Stewart-Akers, A.M., 2008. Macrophage Phenotype as a Determinant of Biologic Scaffold Remodeling. Tissue Eng Pt A 14, 1835-1842.

Ballotta, V., Driessen-Mol, A., Bouten, C.V., Baaijens, F.P., 2014. Strain-dependent modulation of macrophage polarization within scaffolds. Biomaterials 35, 4919-4928.

Barnes, C.P., Sell, S.A., Boland, E.D., Simpson, D.G., Bowlin, G.L., 2007. Nanofiber technology: designing the next generation of tissue engineering scaffolds. Adv Drug Deliv Rev 59, 1413-1433.

Bean, A.C., Almarza, A.J., Athanasiou, K.A., 2006. Effects of ascorbic acid concentration on the tissue engineering of the temporomandibular joint disc. Proc Inst Mech Eng H 220, 439-447.

Beatty, M.W., Bruno, M.J., Iwasaki, L.R., Nickel, J.C., 2001. Strain rate dependent orthotropic properties of pristine and impulsively loaded porcine temporomandibular joint disk. J Biomed Mater Res 57, 25-34.

Beek, M., Koolstra, J.H., van Ruijven, L.J., van Eijden, T.M., 2000. Three-dimensional finite element analysis of the human temporomandibular joint disc. J Biomech 33, 307-316.

Berg, R., 1973. Contribution to the applied and topographical anatomy of the temporomandibular joint of some domestic mammals with particular reference to the partial resp. total resection of the articular disc. Folia Morphol (Praha) 21, 202-204.

Bermejo, A., Gonzalez, O., Gonzalez, J.M., 1993. The pig as an animal model for experimentation on the temporomandibular articular complex. Oral Surg Oral Med Oral Pathol 75, 18-23.

Best, B.A., Guilak, F., Setton, L.A., Zhu, W.B., Saednejad, F., Ratcliffe, A., Weidenbaum, M., Mow, V.C., 1994. Compressive Mechanical-Properties of the Human Anulus Fibrosus and Their Relationship to Biochemical-Composition. Spine 19, 212-221.

Bissell, M.J., Hall, H.G., Parry, G., 1982. How does the extracellular matrix direct gene expression? J Theor Biol 99, 31-68.

Bondesen, B.A., Mills, S.T., Pavlath, G.K., 2006. The COX-2 pathway regulates growth of atrophied muscle via multiple mechanisms. Am J Physiol-Cell Ph 290, C1651-C1659.

Boudreau, N., Myers, C., Bissell, M.J., 1995. From laminin to lamin: regulation of tissue-specific gene expression by the ECM. Trends Cell Biol 5, 1-4.

Brizzi, M.F., Tarone, G., Defilippi, P., 2012. Extracellular matrix, integrins, and growth factors as tailors of the stem cell niche. Curr Opin Cell Biol 24, 645-651.

Brown, B.N., Badylak, S.F., 2013. Expanded applications, shifting paradigms and an improved understanding of host-biomaterial interactions. Acta Biomater 9, 4948-4955.

Brown, B.N., Chung, W.L., Almarza, A.J., Pavlick, M.D., Reppas, S.N., Ochs, M.W., Russell, A.J., Badylak, S.F., 2012a. Inductive, scaffold-based, regenerative medicine approach to reconstruction of the temporomandibular joint disk. J Oral Maxillofac Surg 70, 2656-2668.

Brown, B.N., Chung, W.L., Pavlick, M., Reppas, S., Ochs, M.W., Russell, A.J., Badylak, S.F., 2011. Extracellular matrix as an inductive template for temporomandibular joint meniscus reconstruction: a pilot study. J Oral Maxillofac Surg 69, e488-505.

Brown, B.N., Londono, R., Tottey, S., Zhang, L., Kukla, K.A., Wolf, M.T., Daly, K.A., Reing, J.E., Badylak, S.F., 2012b. Macrophage phenotype as a predictor of constructive remodeling following the implantation of biologically derived surgical mesh materials. Acta Biomater 8, 978-987.

Brown, B.N., Londono, R., Tottey, S., Zhang, L., Kukla, K.A., Wolf, M.T., Daly, K.A., Reing, J.E., Badylak, S.F., 2012c. Macrophage phenotype as a predictor of constructive remodeling following the implantation of biologically derived surgical mesh materials (vol 8, pg 978, 2012). Acta Biomater 8, 2871-2871.

Brown, B.N., Ratner, B.D., Goodman, S.B., Amar, S., Badylak, S.F., 2012d. Macrophage polarization: an opportunity for improved outcomes in biomaterials and regenerative medicine. Biomaterials 33, 3792-3802.

Brown, B.N., Valentin, J.E., Stewart-Akers, A.M., McCabe, G.P., Badylak, S.F., 2009. Macrophage phenotype and remodeling outcomes in response to biologic scaffolds with and without a cellular component. Biomaterials 30, 1482-1491.

Cawston, T.E., Young, D.A., 2010. Proteinases involved in matrix turnover during cartilage and bone breakdown. Cell Tissue Res 339, 221-235.

Chen, S.E., Gerken, E., Zhang, Y., Zhan, M., Mohan, R.K., Li, A.S., Reid, M.B., Li, Y.P., 2005. Role of TNF-{alpha} signaling in regeneration of cardiotoxin-injured muscle. Am J Physiol Cell Physiol 289, C1179-1187.

Cheung, H.S., 1987. Distribution of type I, II, III and V in the pepsin solubilized collagens in bovine menisci. Connect Tissue Res 16, 343-356.

Chladek, W., Czerwik, I., 2008. Mechanical properties of temporomandibular joint disc on the basis of porcine preparation investigations. Acta Bioeng Biomech 10, 15-20.

Chowdhury, A., Bezuidenhout, L.W., Mulet-Sierra, A., Jomha, N.M., Adesida, A.B., 2013. Effect of interleukin-1beta treatment on co-cultures of human meniscus cells and bone marrow mesenchymal stromal cells. BMC Musculoskelet Disord 14, 216.

Cohen, H.B., Mosser, D.M., 2013. Extrinsic and intrinsic control of macrophage inflammatory responses. J Leukoc Biol 94, 913-919.

Collins, R.A., Grounds, M.D., 2001. The role of tumor necrosis factor-alpha (TNF-alpha) in skeletal muscle regeneration. Studies in TNF-alpha(-/-) and TNF-alpha(-/-)/LT-alpha(-/-) mice. J Histochem Cytochem 49, 989-1001.

Colombini, A., Lopa, S., Ceriani, C., Lovati, A.B., Croiset, S.J., Di Giancamillo, A., Lombardi, G., Banfi, G., Moretti, M., 2015. In Vitro Characterization and In Vivo Behavior of Human Nucleus Pulposus and Annulus Fibrosus Cells in Clinical-Grade Fibrin and Collagen-Enriched Fibrin Gels. Tissue Eng Pt A 21, 793-802.

Contreras-Shannon, V., Ochoa, O., Reyes-Reyna, S.M., Sun, D.X., Michalek, J.E., Kuziel, W.A., McManus, L.M., Shireman, P.K., 2007. Fat accumulation with altered inflammation and regeneration in skeletal muscle of CCR2-/- mice following ischemic injury. Am J Physiol-Cell Ph 292, C953-C967.

Crapo, P.M., Gilbert, T.W., Badylak, S.F., 2011. An overview of tissue and whole organ decellularization processes. Biomaterials 32, 3233-3243.

Croutze, R., Jomha, N., Uludag, H., Adesida, A., 2013. Matrix forming characteristics of inner and outer human meniscus cells on 3D collagen scaffolds under normal and low oxygen tensions. BMC Musculoskelet Disord 14, 353.

Daley, W.P., Peters, S.B., Larsen, M., 2008. Extracellular matrix dynamics in development and regenerative medicine. J Cell Sci 121, 255-264.

Davalos, D., Grutzendler, J., Yang, G., Kim, J.V., Zuo, Y., Jung, S., Littman, D.R., Dustin, M.L., Gan, W.B., 2005. ATP mediates rapid microglial response to local brain injury in vivo. Nat Neurosci 8, 752-758.

Davis, G.E., 1992. Affinity of integrins for damaged extracellular matrix: alpha v beta 3 binds to denatured collagen type I through RGD sites. Biochem Biophys Res Commun 182, 1025-1031.

Davis, G.E., 2010. Matricryptic sites control tissue injury responses in the cardiovascular system: relationships to pattern recognition receptor regulated events. J Mol Cell Cardiol 48, 454-460.

Davis, G.E., Bayless, K.J., Davis, M.J., Meininger, G.A., 2000. Regulation of tissue injury responses by the exposure of matricryptic sites within extracellular matrix molecules. Am J Pathol 156, 1489-1498.

Detamore, M.S., Athanasiou, K.A., 2003. Tensile properties of the porcine temporomandibular joint disc. J Biomech Eng 125, 558-565.

Detamore, M.S., Orfanos, J.G., Almarza, A.J., French, M.M., Wong, M.E., Athanasiou, K.A., 2005. Quantitative analysis and comparative regional investigation of the extracellular matrix of the porcine temporomandibular joint disc. Matrix Biol 24, 45-57.

Dimitroulis, G., 2011. A critical review of interpositional grafts following temporomandibular joint discectomy with an overview of the dermis-fat graft. Int J Oral Maxillofac Surg 40, 561-568.

Dolwick, M.F., Aufdemorte, T.B., 1985. Silicone-induced foreign body reaction and lymphadenopathy after temporomandibular joint arthroplasty. Oral Surg Oral Med Oral Pathol 59, 449-452.

Donzelli, P.S., Gallo, L.M., Spilker, R.L., Palla, S., 2004. Biphasic finite element simulation of the TMJ disc from in vivo kinematic and geometric measurements. J Biomech 37, 1787-1791.

Engler, A.J., Sen, S., Sweeney, H.L., Discher, D.E., 2006. Matrix elasticity directs stem cell lineage specification. Cell 126, 677-689.

Estabrooks, L.N., Fairbanks, C.E., Collett, R.J., Miller, L., 1990. A retrospective evaluation of 301 TMJ Proplast-Teflon implants. Oral Surg Oral Med Oral Pathol 70, 381-386.

Eyre, D.R., Muir, H., 1976. Types I and II collagens in intervertebral disc. Interchanging radial distributions in annulus fibrosus. Biochem J 157, 267-270.

Fadok, V.A., Bratton, D.L., Konowal, A., Freed, P.W., Westcott, J.Y., Henson, P.M., 1998. Macrophages that have ingested apoptotic cells in vitro inhibit proinflammatory cytokine production through autocrine/paracrine mechanisms involving TGF-beta, PGE2, and PAF. J Clin Invest 101, 890-898.

Farrar, W.B., McCarty, W.L., Jr., 1979. The TMJ dilemma. J Ala Dent Assoc 63, 19-26.
Fazaeli, S., Ghazanfari, S., Everts, V., Smit, T.H., Koolstra, J.H., 2016. The contribution of collagen fibers to the mechanical compressive properties of the temporomandibular joint disc. Osteoarthritis Cartilage 24, 1292-1301.

Ferreira, J.N., Ko, C.C., Myers, S., Swift, J., Fricton, J.R., 2008. Evaluation of surgically retrieved temporomandibular joint alloplastic implants: pilot study. J Oral Maxillofac Surg 66, 1112-1124.

Fisher, M.B., Henning, E.A., Soegaard, N., Bostrom, M., Esterhai, J.L., Mauck, R.L., 2015. Engineering meniscus structure and function via multi-layered mesenchymal stem cell-seeded nanofibrous scaffolds. J Biomech 48, 1412-1419.

Freeman, A.L., Buttermann, G.R., Beaubien, B.P., Rochefort, W.E., 2013. Compressive properties of fibrous repair tissue compared to nucleus and annulus. J Biomech 46, 1714-1721.

Fricton, J.R., Look, J.O., Schiffman, E., Swift, J., 2002. Long-term study of temporomandibular joint surgery with alloplastic implants compared with nonimplant surgery and nonsurgical rehabilitation for painful temporomandibular joint disc displacement. J Oral Maxillofac Surg 60, 1400-1411; discussion 1411-1402.

Gilbert, T.W., 2012. Strategies for tissue and organ decellularization. J Cell Biochem 113, 2217-2222.

Gilbert, T.W., Sellaro, T.L., Badylak, S.F., 2006. Decellularization of tissues and organs. Biomaterials 27, 3675-3683.

Gilbert, T.W., Stewart-Akers, A.M., Badylak, S.F., 2007a. A quantitative method for evaluating the degradation of biologic scaffold materials. Biomaterials 28, 147-150.

Gilbert, T.W., Stewart-Akers, A.M., Simmons-Byrd, A., Badylak, S.F., 2007b. Degradation and remodeling of small intestinal submucosa in canine Achilles tendon repair. J Bone Joint Surg Am 89, 621-630.

Gilbert, T.W., Stewart-Akers, A.M., Sydeski, J., Nguyen, T.D., Badylak, S.F., Woo, S.L., 2007c. Gene expression by fibroblasts seeded on small intestinal submucosa and subjected to cyclic stretching. Tissue Eng 13, 1313-1323.

Gordon, S., 2003. Alternative activation of macrophages. Nature Reviews Immunology 3, 23-35.

Gordon, S., Martinez, F.O., 2010. Alternative Activation of Macrophages: Mechanism and Functions. Immunity 32, 593-604.

Gordon, S., Taylor, P.R., 2005. Monocyte and macrophage heterogeneity. Nat Rev Immunol 5, 953-964.

Guillaume, O., Daly, A., Lennon, K., Gansau, J., Buckley, S.F., Buckley, C.T., 2014. Shape-memory porous alginate scaffolds for regeneration of the annulus fibrosus: Effect of TGF-beta 3 supplementation and oxygen culture conditions. Acta Biomater 10, 1985-1995.

Guillaume, O., Naqvi, S.M., Lennon, K., Buckley, C.T., 2015. Enhancing cell migration in shape-memory alginate-collagen composite scaffolds: In vitro and ex vivo assessment for intervertebral disc repair. J Biomater Appl 29, 1230-1246.

Hagandora, C.K., Chase, T.W., Almarza, A.J., 2011. A comparison of the mechanical properties of the goat temporomandibular joint disc to the mandibular condylar cartilage in unconfined compression. J Dent Biomech 2011, 212385.

Hagandora, C.K., Tudares, M.A., Almarza, A.J., 2012. The effect of magnesium ion concentration on the fibrocartilage regeneration potential of goat costal chondrocytes. Ann Biomed Eng 40, 688-696.

Henry, C.H., Wolford, L.M., 1993. Treatment outcomes for temporomandibular joint reconstruction after Proplast-Teflon implant failure. J Oral Maxillofac Surg 51, 352-358; discussion 359-360.

Hern, D.L., Hubbell, J.A., 1998. Incorporation of adhesion peptides into nonadhesive hydrogels useful for tissue resurfacing. J Biomed Mater Res 39, 266-276.

Hines, D.J., Hines, R.M., Mulligan, S.J., Macvicar, B.A., 2009. Microglia processes block the spread of damage in the brain and require functional chloride channels. Glia 57, 1610-1618.

Hinz, B., Phan, S.H., Thannickal, V.J., Prunotto, M., Desmouliere, A., Varga, J., De Wever, O., Mareel, M., Gabbiani, G., 2012. Recent developments in myofibroblast biology: paradigms for connective tissue remodeling. Am J Pathol 180, 1340-1355.

Hirano, Y., Okuno, M., Hayashi, T., Goto, K., Nakajima, A., 1993. Cell-attachment activities of surface immobilized oligopeptides RGD, RGDS, RGDV, RGDT, and YIGSR toward five cell lines. J Biomater Sci Polym Ed 4, 235-243.

Hodde, J.P., Badylak, S.F., Shelbourne, K.D., 1997. The effect of range of motion on remodeling of small intestinal submucosa (SIS) when used as an Achilles tendon repair material in the rabbit. Tissue Engineering 3, 27-37.

Hsiong, S.X., Huebsch, N., Fischbach, C., Kong, H.J., Mooney, D.J., 2008. Integrin-adhesion ligand bond formation of preosteoblasts and stem cells in three-dimensional RGD presenting matrices. Biomacromolecules 9, 1843-1851.

Hynes, R.O., 2009. The extracellular matrix: not just pretty fibrils. Science 326, 1216-1219.

Hynes, R.O., Naba, A., 2012. Overview of the matrisome--an inventory of extracellular matrix constituents and functions. Cold Spring Harb Perspect Biol 4, a004903.

Ingber, D., 1991. Extracellular matrix and cell shape: potential control points for inhibition of angiogenesis. J Cell Biochem 47, 236-241.

Isaacs, J.L., Vresilovic, E., Sarkar, S., Marcolongo, M., 2014. Role of biomolecules on annulus fibrosus micromechanics: effect of enzymatic digestion on elastic and failure properties. J Mech Behav Biomed Mater 40, 75-84.

Iu, J., Santerre, J.P., Kandel, R.A., 2014. Inner and Outer Annulus Fibrosus Cells Exhibit Differentiated Phenotypes and Yield Changes in Extracellular Matrix Protein Composition In Vitro on a Polycarbonate Urethane Scaffold. Tissue Eng Pt A 20, 3261-3269.

Johns, D.E., Athanasiou, K.A., 2008. Growth factor effects on costal chondrocytes for tissue engineering fibrocartilage. Cell Tissue Res 333, 439-447.

Kalpakci, K.N., Kim, E.J., Athanasiou, K.A., 2011a. Assessment of growth factor treatment on fibrochondrocyte and chondrocyte co-cultures for TMJ fibrocartilage engineering. Acta Biomater 7, 1710-1718.

Kalpakci, K.N., Willard, V.P., Wong, M.E., Athanasiou, K.A., 2011b. An interspecies comparison of the temporomandibular joint disc. J Dent Res 90, 193-198.

Kang, H., Bao, G., Dong, Y., Yi, X., Chao, Y., Chen, M., 2000. [Tensile mechanics of mandibular condylar cartilage]. Hua Xi Kou Qiang Yi Xue Za Zhi 18, 85-87.

Kazanis, I., ffrench-Constant, C., 2011. Extracellular matrix and the neural stem cell niche. Dev Neurobiol 71, 1006-1017.

Kim, K.W., Wong, M.E., Helfrick, J.F., Thomas, J.B., Athanasiou, K.A., 2003. Biomechanical tissue characterization of the superior joint space of the porcine temporomandibular joint. Ann Biomed Eng 31, 924-930.

Koolstra, J.H., Tanaka, E., Van Eijden, T.M., 2007. Viscoelastic material model for the temporomandibular joint disc derived from dynamic shear tests or strain-relaxation tests. J Biomech 40, 2330-2334.

Krammer, A., Lu, H., Isralewitz, B., Schulten, K., Vogel, V., 1999. Forced unfolding of the fibronectin type III module reveals a tensile molecular recognition switch. Proc Natl Acad Sci U S A 96, 1351-1356.

Kuboki, T., Shinoda, M., Orsini, M.G., Yamashita, A., 1997. Viscoelastic properties of the pig temporomandibular joint articular soft tissues of the condyle and disc. J Dent Res 76, 1760-1769.
Kumbar, S.G., James, R., Nukavarapu, S.P., Laurencin, C.T., 2008. Electrospun nanofiber scaffolds: engineering soft tissues. Biomed Mater 3, 034002.

Lamela, M.J., Fernandez, P., Ramos, A., Fernandez-Canteli, A., Tanaka, E., 2013. Dynamic compressive properties of articular cartilages in the porcine temporomandibular joint. J Mech Behav Biomed Mater 23, 62-70.

LeBaron, R.G., Athanasiou, K.A., 2000. Extracellular matrix cell adhesion peptides: functional applications in orthopedic materials. Tissue Eng 6, 85-103.

Liu, D., Sartor, M.A., Nader, G.A., Gutmann, L., Treutelaar, M.K., Pistilli, E.E., Iglayreger, H.B., Burant, C.F., Hoffman, E.P., Gordon, P.M., 2010. Skeletal muscle gene expression in response to resistance exercise: sex specific regulation. BMC Genomics 11, 659.

Lu, P., Takai, K., Weaver, V.M., Werb, Z., 2011. Extracellular matrix degradation and remodeling in development and disease. Cold Spring Harb Perspect Biol 3.

Lumpkins, S.B., McFetridge, P.S., 2009. Regional variations in the viscoelastic compressive properties of the temporomandibular joint disc and implications toward tissue engineering. J Biomed Mater Res A 90, 784-791.

MacBarb, R.F., Chen, A.L., Hu, J.C., Athanasiou, K.A., 2013a. Engineering functional anisotropy in fibrocartilage neotissues. Biomaterials 34, 9980-9989.

MacBarb, R.F., Makris, E.A., Hu, J.C., Athanasiou, K.A., 2013b. A chondroitinase-ABC and TGF-beta1 treatment regimen for enhancing the mechanical properties of tissue-engineered fibrocartilage. Acta Biomater 9, 4626-4634.

Madden, L.R., Mortisen, D.J., Sussman, E.M., Dupras, S.K., Fugate, J.A., Cuy, J.L., Hauch, K.D., Laflamme, M.A., Murry, C.E., Ratner, B.D., 2010. Proangiogenic scaffolds as functional templates for cardiac tissue engineering. Proc Natl Acad Sci U S A 107, 15211-15216.

Mantovani, A., Sica, A., Sozzani, S., Allavena, P., Vecchi, A., Locati, M., 2004. The chemokine system in diverse forms of macrophage activation and polarization. Trends Immunol 25, 677-686.

Maquart, F.X., Bellon, G., Pasco, S., Monboisse, J.C., 2005. Matrikines in the regulation of extracellular matrix degradation. Biochimie 87, 353-360.

Matthies, N.F., Mulet-Sierra, A., Jomha, N.M., Adesida, A.B., 2013. Matrix formation is enhanced in co-cultures of human meniscus cells with bone marrow stromal cells. J Tissue Eng Regen Med 7, 965-973.

Matuska, A.M., Muller, S., Dolwick, M.F., McFetridge, P.S., 2016. Biomechanical and biochemical outcomes of porcine temporomandibular joint disc deformation. Arch Oral Biol 64, 72-79.

Mauro, A., 1961. Satellite cell of skeletal muscle fibers. J Biophys Biochem Cytol 9, 493-495.
McLennan, I.S., 1996. Degenerating and regenerating skeletal muscles contain several subpopulations of macrophages with distinct spatial and temporal distributions. J Anat 188 (Pt 1), 17-28.

Medberry, C.J., Crapo, P.M., Siu, B.F., Carruthers, C.A., Wolf, M.T., Nagarkar, S.P., Agrawal, V., Jones, K.E., Kelly, J., Johnson, S.A., Velankar, S.S., Watkins, S.C., Modo, M., Badylak, S.F., 2013. Hydrogels derived from central nervous system extracellular matrix. Biomaterials 34, 1033-1040.

Meyer, R.A., 1988. The autogenous dermal graft in temporomandibular joint disc surgery. J Oral Maxillofac Surg 46, 948-954.

Mills, C.D., Shearer, J., Evans, R., Caldwell, M.D., 1992. Macrophage arginine metabolism and the inhibition or stimulation of cancer. J Immunol 149, 2709-2714.

Mokarram, N., Merchant, A., Mukhatyar, V., Patel, G., Bellamkonda, R.V., 2012. Effect of modulating macrophage phenotype on peripheral nerve repair. Biomaterials 33, 8793-8801.

Muir, A.R., Kanji, A.H., Allbrook, D., 1965. The structure of the satellite cells in skeletal muscle. J Anat 99, 435-444.

Murphy, M.K., Arzi, B., Hu, J.C., Athanasiou, K.A., 2013. Tensile characterization of porcine temporomandibular joint disc attachments. J Dent Res 92, 753-758.

Murphy, M.K., Arzi, B., Prouty, S.M., Hu, J.C., Athanasiou, K.A., 2015. Neocartilage integration in temporomandibular joint discs: physical and enzymatic methods. J R Soc Interface 12.

Nguyen, T.D., Liang, R., Woo, S.L., Burton, S.D., Wu, C., Almarza, A., Sacks, M.S., Abramowitch, S., 2009. Effects of cell seeding and cyclic stretch on the fiber remodeling in an extracellular matrix-derived bioscaffold. Tissue Eng Part A 15, 957-963.

Pogrel, M.A., Kaban, L.B., 1990. The role of a temporalis fascia and muscle flap in temporomandibular joint surgery. J Oral Maxillofac Surg 48, 14-19.

Pongkitwitoon, S., Weinheimer-Haus, E.M., Koh, T.J., Judex, S., 2016. Low-intensity vibrations accelerate proliferation and alter macrophage phenotype in vitro. J Biomech 49, 793-796.

Puelacher, W.C., Wisser, J., Vacanti, C.A., Ferraro, N.F., Jaramillo, D., Vacanti, J.P., 1994. Temporomandibular joint disc replacement made by tissue-engineered growth of cartilage. J Oral Maxillofac Surg 52, 1172-1177; discussion 1177-1178.

Ramchandran, R., Dhanabal, M., Volk, R., Waterman, M.J., Segal, M., Lu, H., Knebelmann, B., Sukhatme, V.P., 1999. Antiangiogenic activity of restin, NC10 domain of human collagen XV: comparison to endostatin. Biochem Biophys Res Commun 255, 735-739.

Ratner, B.D., 2011. The biocompatibility manifesto: biocompatibility for the twenty-first century. J Cardiovasc Transl Res 4, 523-527.

Reilly, G.C., Engler, A.J., 2010. Intrinsic extracellular matrix properties regulate stem cell differentiation. J Biomech 43, 55-62.

Reston, J.T., Turkelson, C.M., 2003. Meta-analysis of surgical treatments for temporomandibular articular disorders. J Oral Maxillofac Surg 61, 3-10; discussion 10-12.

Ruggiero, L., Zimmerman, B.K., Park, M., Han, L., Wang, L., Burris, D.L., Lu, X.L., 2015. Roles of the Fibrous Superficial Zone in the Mechanical Behavior of TMJ Condylar Cartilage. Ann Biomed Eng 43, 2652-2662.

Sawkins, M.J., Bowen, W., Dhadda, P., Markides, H., Sidney, L.E., Taylor, A.J., Rose, F.R., Badylak, S.F., Shakesheff, K.M., White, L.J., 2013. Hydrogels derived from demineralized and decellularized bone extracellular matrix. Acta Biomater 9, 7865-7873.

See, E.Y., Toh, S.L., Goh, J.C., 2011. Effects of radial compression on a novel simulated intervertebral disc-like assembly using bone marrow-derived mesenchymal stem cell cell-sheets for annulus fibrosus regeneration. Spine (Phila Pa 1976) 36, 1744-1751.

Seif-Naraghi, S.B., Singelyn, J.M., Salvatore, M.A., Osborn, K.G., Wang, J.J., Sampat, U., Kwan, O.L., Strachan, G.M., Wong, J., Schup-Magoffin, P.J., Braden, R.L., Bartels, K., DeQuach, J.A., Preul, M., Kinsey, A.M., DeMaria, A.N., Dib, N., Christman, K.L., 2013. Safety and efficacy of an injectable extracellular matrix hydrogel for treating myocardial infarction. Sci Transl Med 5, 173ra125.

Seiffert, D., Smith, J.W., 1997. The cell adhesion domain in plasma vitronectin is cryptic. J Biol Chem 272, 13705-13710.

Sherman, J., Cauthen, J., Schoenberg, D., Burns, M., Reaven, N.L., Griffith, S.L., 2010. Economic impact of improving outcomes of lumbar discectomy. Spine J 10, 108-116.

Sicari, B.M., Dziki, J.L., Siu, B.F., Medberry, C.J., Dearth, C.L., Badylak, S.F., 2014a. The promotion of a constructive macrophage phenotype by solubilized extracellular matrix. Biomaterials 35, 8605-8612.

Sicari, B.M., Rubin, J.P., Dearth, C.L., Wolf, M.T., Ambrosio, F., Boninger, M., Turner, N.J., Weber, D.J., Simpson, T.W., Wyse, A., Brown, E.H., Dziki, J.L., Fisher, L.E., Brown, S., Badylak, S.F., 2014b. An acellular biologic scaffold promotes skeletal muscle formation in mice and humans with volumetric muscle loss. Sci Transl Med 6, 234ra258.

Sindrilaru, A., Scharffetter-Kochanek, K., 2013. Disclosure of the Culprits: Macrophages-Versatile Regulators of Wound Healing. Adv Wound Care (New Rochelle) 2, 357-368.

Singh, M., Detamore, M.S., 2008. Tensile properties of the mandibular condylar cartilage. J Biomech Eng 130, 011009.

Singh, M., Detamore, M.S., 2009. Stress relaxation behavior of mandibular condylar cartilage under high-strain compression. J Biomech Eng 131, 061008.

Smith, L.L., Cheung, H.K., Ling, L.E., Chen, J., Sheppard, D., Pytela, R., Giachelli, C.M., 1996. Osteopontin N-terminal domain contains a cryptic adhesive sequence recognized by alpha9beta1 integrin. J Biol Chem 271, 28485-28491.

Snider, G.R., Lomakin, J., Singh, M., Gehrke, S.H., Detamore, M.S., 2008. Regional dynamic tensile properties of the TMJ disc. J Dent Res 87, 1053-1057.

St Pierre, B.A., Tidball, J.G., 1994. Differential response of macrophage subpopulations to soleus muscle reloading after rat hindlimb suspension. J Appl Physiol (1985) 77, 290-297.

Stemper, B.D., Baisden, J.L., Yoganandan, N., Shender, B.S., Maiman, D.J., 2014. Mechanical yield of the lumbar annulus: a possible contributor to instability: Laboratory investigation. J Neurosurg Spine 21, 608-613.

Stout, R.D., 2010. Editorial: macrophage functional phenotypes: no alternatives in dermal wound healing? J Leukoc Biol 87, 19-21.

Sussman, E.M., Halpin, M.C., Muster, J., Moon, R.T., Ratner, B.D., 2014. Porous implants modulate healing and induce shifts in local macrophage polarization in the foreign body reaction. Ann Biomed Eng 42, 1508-1516.

Sweigart, M.A., Athanasiou, K.A., 2001. Toward tissue engineering of the knee meniscus. Tissue Eng 7, 111-129.

Swirski, F.K., Nahrendorf, M., Etzrodt, M., Wildgruber, M., Cortez-Retamozo, V., Panizzi, P., Figueiredo, J.L., Kohler, R.H., Chudnovskiy, A., Waterman, P., Aikawa, E., Mempel, T.R., Libby, P., Weissleder, R., Pittet, M.J., 2009. Identification of splenic reservoir monocytes and their deployment to inflammatory sites. Science 325, 612-616.

Tanaka, E., del Pozo, R., Tanaka, M., Asai, D., Hirose, M., Iwabe, T., Tanne, K., 2004. Three-dimensional finite element analysis of human temporomandibular joint with and without disc displacement during jaw opening. Med Eng Phys 26, 503-511.

Tanaka, E., Hanaoka, K., van Eijden, T., Tanaka, M., Watanabe, M., Nishi, M., Kawai, N., Murata, H., Hamada, T., Tanne, K., 2003. Dynamic shear properties of the temporomandibular joint disc. J Dent Res 82, 228-231.

Tanaka, E., van Eijden, T., 2003. Biomechanical behavior of the temporomandibular joint disc. Crit Rev Oral Biol Med 14, 138-150.

Tanaka, E., Yamano, E., Dalla-Bona, D.A., Watanabe, M., Inubushi, T., Shirakura, M., Sano, R., Takahashi, K., van Eijden, T., Tanne, K., 2006. Dynamic compressive properties of the mandibular condylar cartilage. J Dent Res 85, 571-575.

Tarafder, S., Koch, A., Jun, Y., Chou, C., Awadallah, M.R., Lee, C.H., 2016. Micro-precise spatiotemporal delivery system embedded in 3D printing for complex tissue regeneration. Biofabrication 8, 025003.

Teixeira, C.F., Zamuner, S.R., Zuliani, J.P., Fernandes, C.M., Cruz-Hofling, M.A., Fernandes, I., Chaves, F., Gutierrez, J.M., 2003. Neutrophils do not contribute to local tissue damage, but play a key role in skeletal muscle regeneration, in mice injected with Bothrops asper snake venom. Muscle Nerve 28, 449-459.

Tidball, J.G., 2005. Inflammatory processes in muscle injury and repair. Am J Physiol Regul Integr Comp Physiol 288, R345-353.

Tidball, J.G., Villalta, S.A., 2010. Regulatory interactions between muscle and the immune system during muscle regeneration. Am J Physiol-Reg I 298, R1173-R1187.

Tidball, J.G., Wehling-Henricks, M., 2007. Macrophages promote muscle membrane repair and muscle fibre growth and regeneration during modified muscle loading in mice in vivo. J Physiol 578, 327-336.

Turner, N.J., Badylak, J.S., Weber, D.J., Badylak, S.F., 2012. Biologic scaffold remodeling in a dog model of complex musculoskeletal injury. J Surg Res 176, 490-502.

Turner, N.J., Yates, A.J., Jr., Weber, D.J., Qureshi, I.R., Stolz, D.B., Gilbert, T.W., Badylak, S.F., 2010. Xenogeneic extracellular matrix as an inductive scaffold for regeneration of a functioning musculotendinous junction. Tissue Eng Part A 16, 3309-3317.

Ugarova, T.P., Zamarron, C., Veklich, Y., Bowditch, R.D., Ginsberg, M.H., Weisel, J.W., Plow, E.F., 1995. Conformational transitions in the cell binding domain of fibronectin. Biochemistry 34, 4457-4466.

Valentin, J.E., Stewart-Akers, A.M., Gilbert, T.W., Badylak, S.F., 2009. Macrophage participation in the degradation and remodeling of extracellular matrix scaffolds. Tissue Eng Part A 15, 1687-1694.

Valentin, J.E., Turner, N.J., Gilbert, T.W., Badylak, S.F., 2010. Functional skeletal muscle formation with a biologic scaffold. Biomaterials 31, 7475-7484.

Vidal, G., Blanchi, T., Mieszawska, A.J., Calabrese, R., Rossi, C., Vigneron, P., Duval, J.L., Kaplan, D.L., Egles, C., 2013. Enhanced cellular adhesion on titanium by silk functionalized with titanium binding and RGD peptides. Acta Biomater 9, 4935-4943.

Villalta, S.A., Nguyen, H.X., Deng, B., Gotoh, T., Tidball, J.G., 2009. Shifts in macrophage phenotypes and macrophage competition for arginine metabolism affect the severity of muscle pathology in muscular dystrophy. Hum Mol Genet 18, 482-496.

Visser, J., Levett, P.A., te Moller, N.C., Besems, J., Boere, K.W., van Rijen, M.H., de Grauw, J.C., Dhert, W.J., van Weeren, P.R., Malda, J., 2015. Crosslinkable hydrogels derived from cartilage, meniscus, and tendon tissue. Tissue Eng Part A 21, 1195-1206.

Vlodavsky, I., Goldshmidt, O., Zcharia, E., Atzmon, R., Rangini-Guatta, Z., Elkin, M., Peretz, T., Friedmann, Y., 2002. Mammalian heparanase: involvement in cancer metastasis, angiogenesis and normal development. Semin Cancer Biol 12, 121-129.

Votteler, M., Kluger, P.J., Walles, H., Schenke-Layland, K., 2010. Stem cell microenvironments--unveiling the secret of how stem cell fate is defined. Macromol Biosci 10, 1302-1315.

Wallis, M.C., Yeger, H., Cartwright, L., Shou, Z., Radisic, M., Haig, J., Suoub, M., Antoon, R., Farhat, W.A., 2008. Feasibility study of a novel urinary bladder bioreactor. Tissue Eng Part A 14, 339-348.

Wang, L., Lazebnik, M., Detamore, M.S., 2009. Hyaline cartilage cells outperform mandibular condylar cartilage cells in a TMJ fibrocartilage tissue engineering application. Osteoarthritis Cartilage 17, 346-353.

Warren, G.L., Hulderman, T., Jensen, N., McKinstry, M., Mishra, M., Luster, M.I., Simeonova, P.P., 2002. Physiological role of tumor necrosis factor alpha in traumatic muscle injury. FASEB J 16, 1630-1632.

Willard, V.P., Kalpakci, K.N., Reimer, A.J., Athanasiou, K.A., 2012. The regional contribution of glycosaminoglycans to temporomandibular joint disc compressive properties. J Biomech Eng 134, 011011.

Williams, D.F., 2008. On the mechanisms of biocompatibility. Biomaterials 29, 2941-2953.

Wismer, N., Grad, S., Fortunato, G., Ferguson, S.J., Alini, M., Eglin, D., 2014. Biodegradable Electrospun Scaffolds for Annulus Fibrosus Tissue Engineering: Effect of Scaffold Structure and Composition on Annulus Fibrosus Cells In Vitro. Tissue Eng Pt A 20, 672-682.

Wolf, M.T., Carruthers, C.A., Dearth, C.L., Crapo, P.M., Huber, A., Burnsed, O.A., Londono, R., Johnson, S.A., Daly, K.A., Stahl, E.C., Freund, J.M., Medberry, C.J., Carey, L.E., Nieponice,

A., Amoroso, N.J., Badylak, S.F., 2014. Polypropylene surgical mesh coated with extracellular matrix mitigates the host foreign body response. J Biomed Mater Res A 102, 234-246.

Wolf, M.T., Dearth, C.L., Sonnenberg, S.B., Loboa, E.G., Badylak, S.F., 2015. Naturally derived and synthetic scaffolds for skeletal muscle reconstruction. Adv Drug Deliv Rev 84, 208-221.

Wu, Y., Gong, Z., Li, J., Meng, Q., Fang, W., Long, X., 2014. The pilot study of fibrin with temporomandibular joint derived synovial stem cells in repairing TMJ disc perforation. Biomed Res Int 2014, 454021.

Zador, E., Mendler, L., Takacs, V., de Bleecker, J., Wuytack, F., 2001. Regenerating soleus and extensor digitorum longus muscles of the rat show elevated levels of TNF-alpha and its receptors, TNFR-60 and TNFR-80. Muscle Nerve 24, 1058-1067.

Zantop, T., Gilbert, T.W., Yoder, M.C., Badylak, S.F., 2006. Extracellular matrix scaffolds are repopulated by bone marrow-derived cells in a mouse model of achilles tendon reconstruction. J Orthop Res 24, 1299-1309.